COMPUTER VISION FOR AUTONOMOUS NAVIGATION

June 5, 1988

Martial Hebert
Carnegie-Mellon University

Content

Degrees of Autonomy

Direct Operation

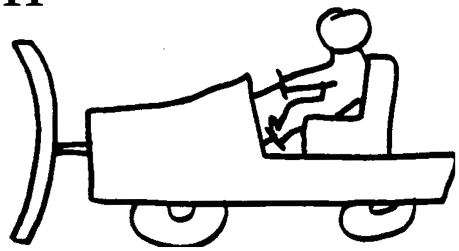

Teleoperation

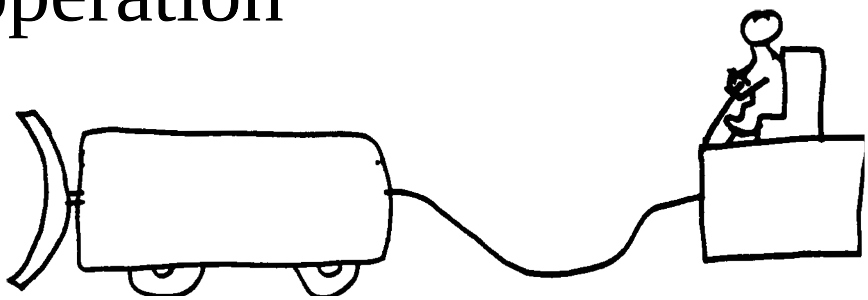

Supervised Operation

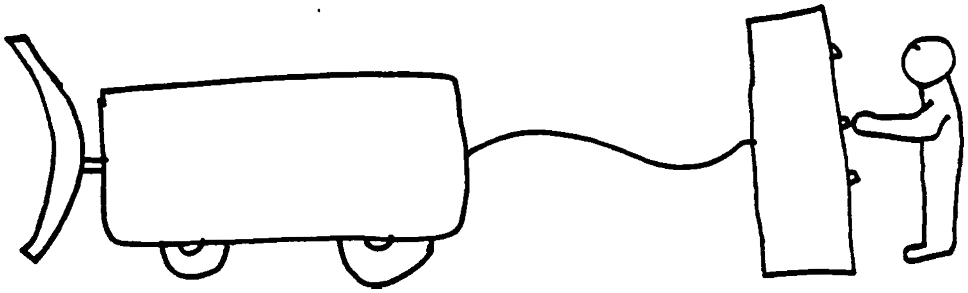

Autonomous System

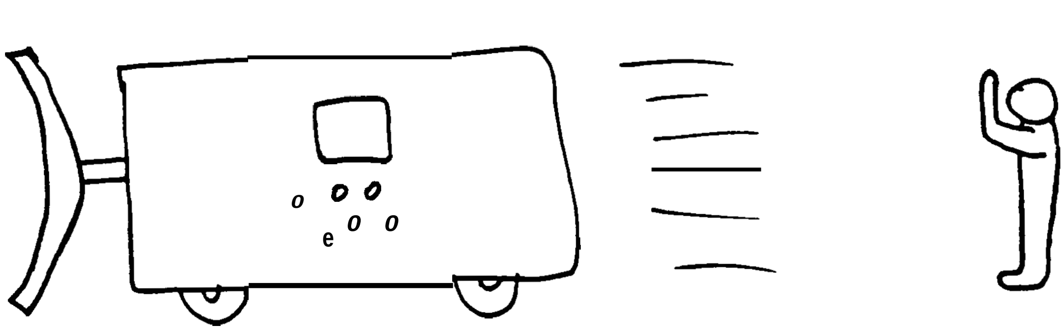

Applications of autonomous mobile robots (incomplete list, in no particular order)

- Indoor navigation **(SRI,** Stanford, INRIA, LAAS, CMU)
- Indoor cleaning (LIFIA, LAAS)
- Construction (Rex Excavator (CMU))
- On-road navigation (ALV project (CMU, Martin Marietta, Maryland Univ.))
- Chauffeur (Munich Univ.)
- Undersea exploration (UNH, Texas A&M, NBS (MAUV))
- Off-road exploration && transportation (Hughes **AI,** CMU, Martin Marietta (ALV), Ohio State walking machine)
- Planetary explorer (CMU, **JPL)**
- Surveillance (CMU/Denning Mobile Robots)

Components of a mobile robot

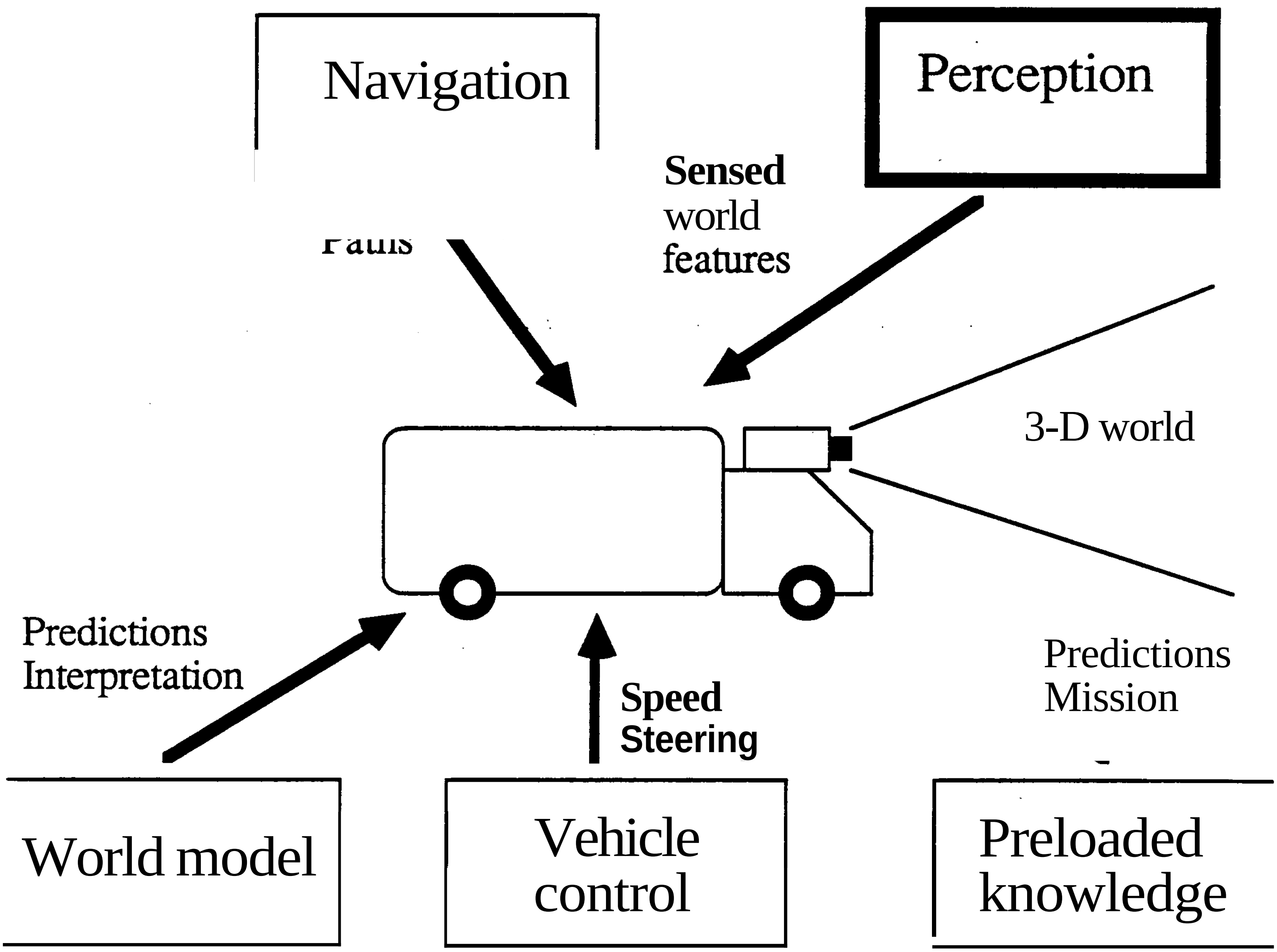

PERCEPTION FOR NAVIGATION

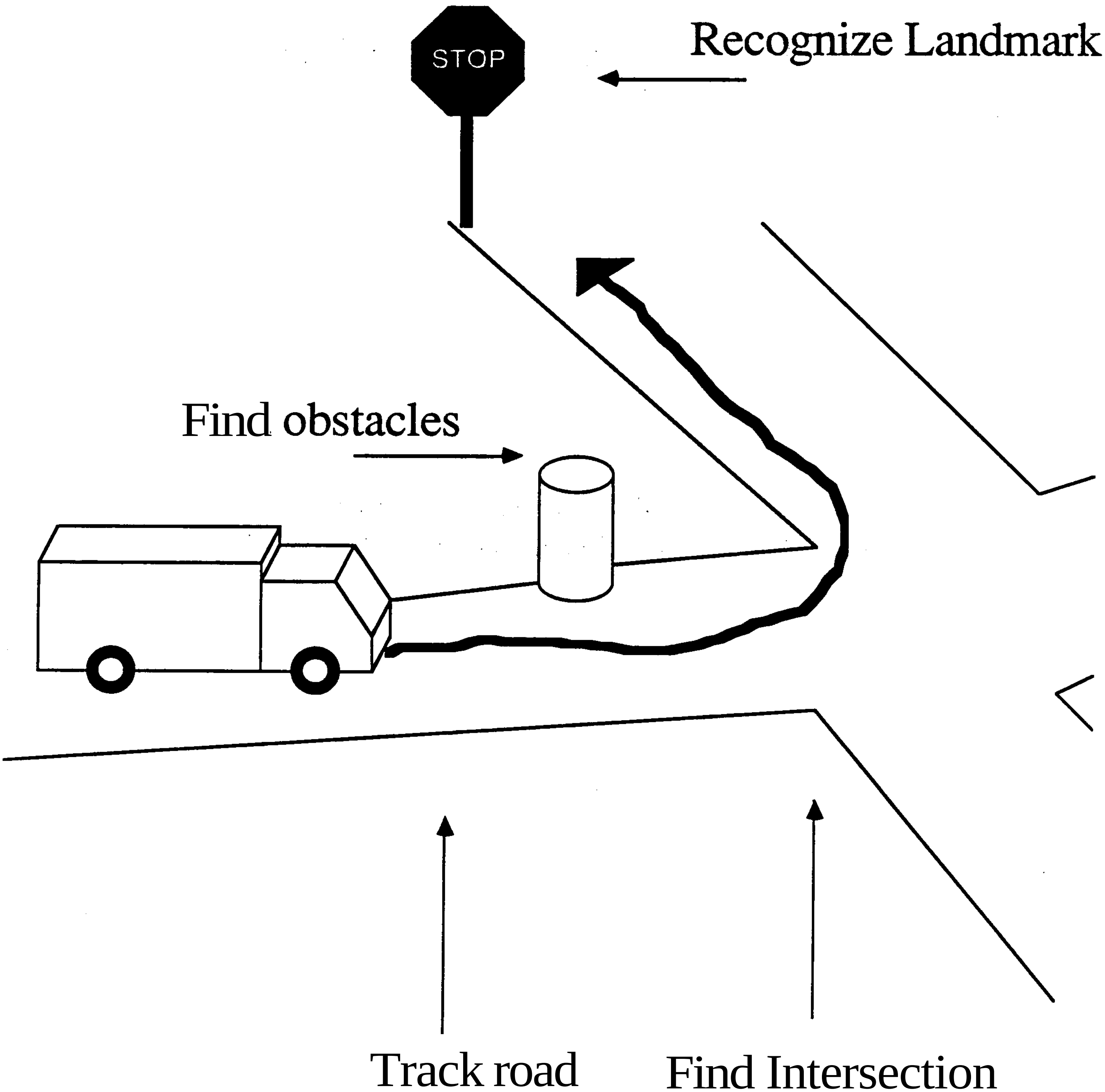

MODELING

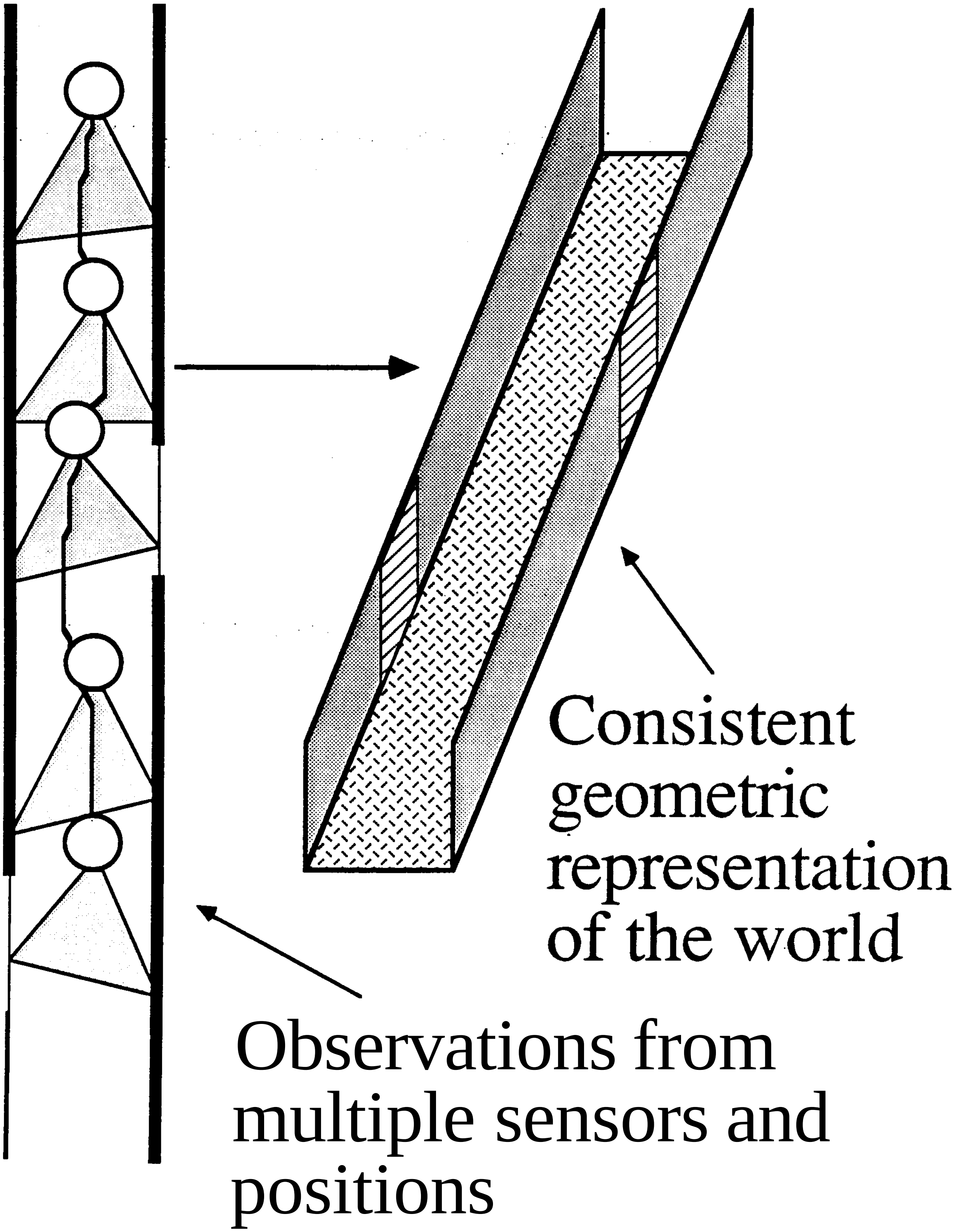
Consistent geometric representation of the world
Observations from multiple sensors and positions

Challenges for perception

- Uncertainty: Errors may accumulate as the vehicle moves if perception uncertainty is not explicitly represented.
- Mobility: Variability between sensor observations.
- 3-D: Obstacles, terrains, ..etc. are **part** of a 3-D world.

Sensors

- Passive:
  - Video camera
  - Passive stereo vision
- Active:
  - Sonar
  - Laser range finder

Video cameras

Context:

- Object tracking: Blob or edge extraction, vehicle tracking from image to image through feedback to vehicle controller.
- Indoor navigation: Edge detection, interpretation in highly constraint environment (e.g. Vertical and horizontal edges of walls and furniture).
- Road following:
  - Road **edges** extraction and tracking.
  - Road **region** extraction for color data.

Main problem:

Calibration ⇒ A camera provides only 2-D information whereas the vehicle moves in a 3-D world.

Calibration problem

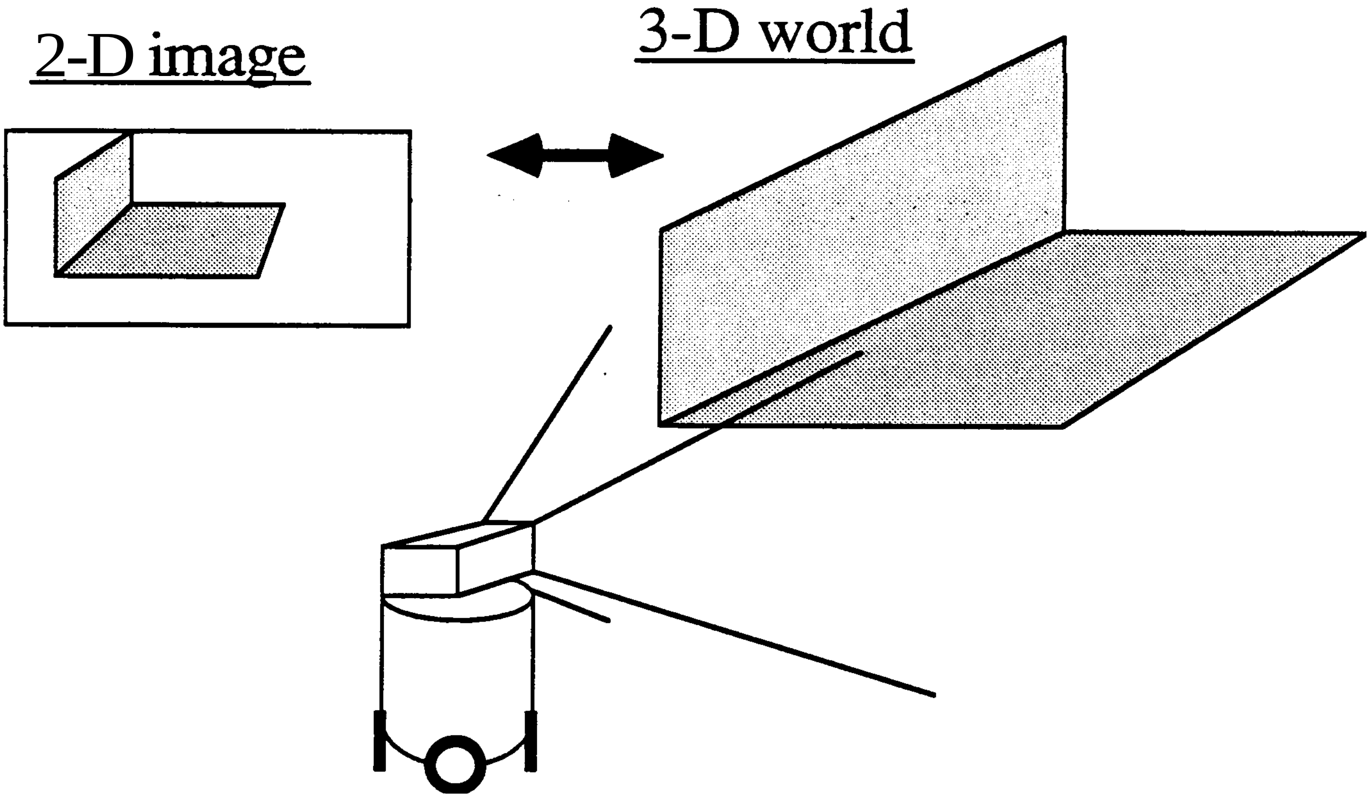

Possible solution:

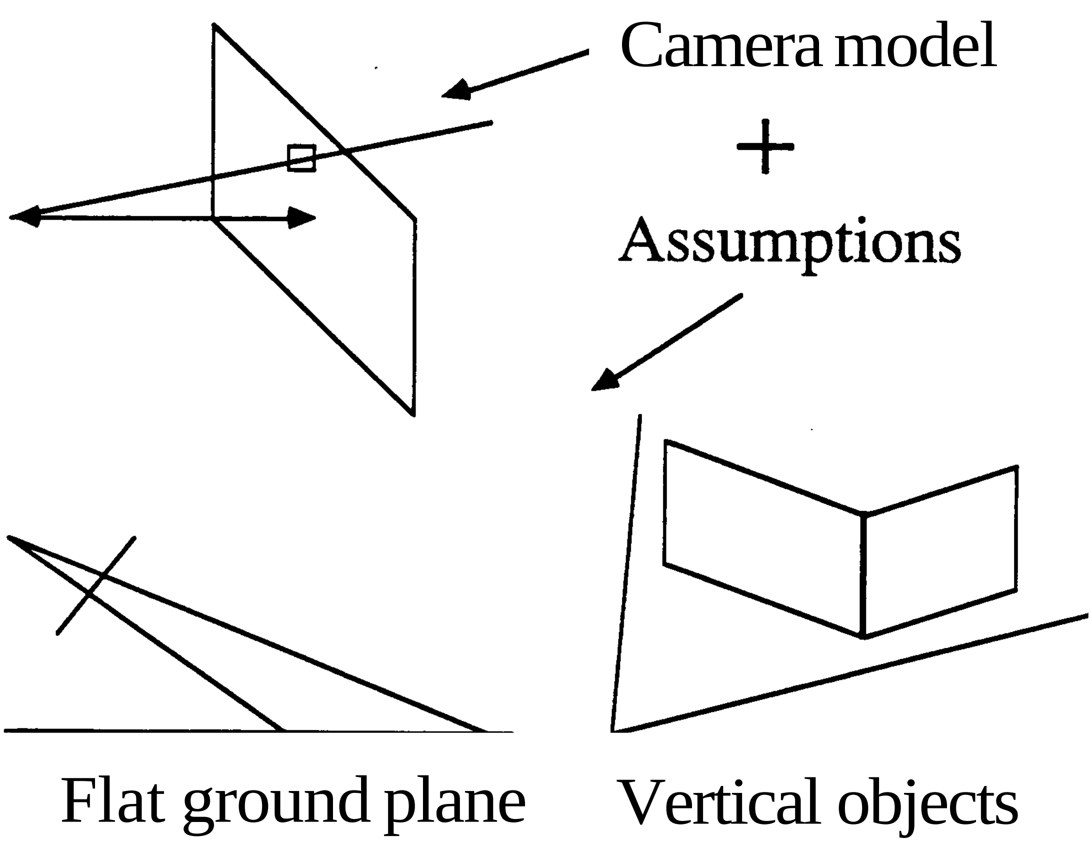

Example: Road following (U. Maryland)

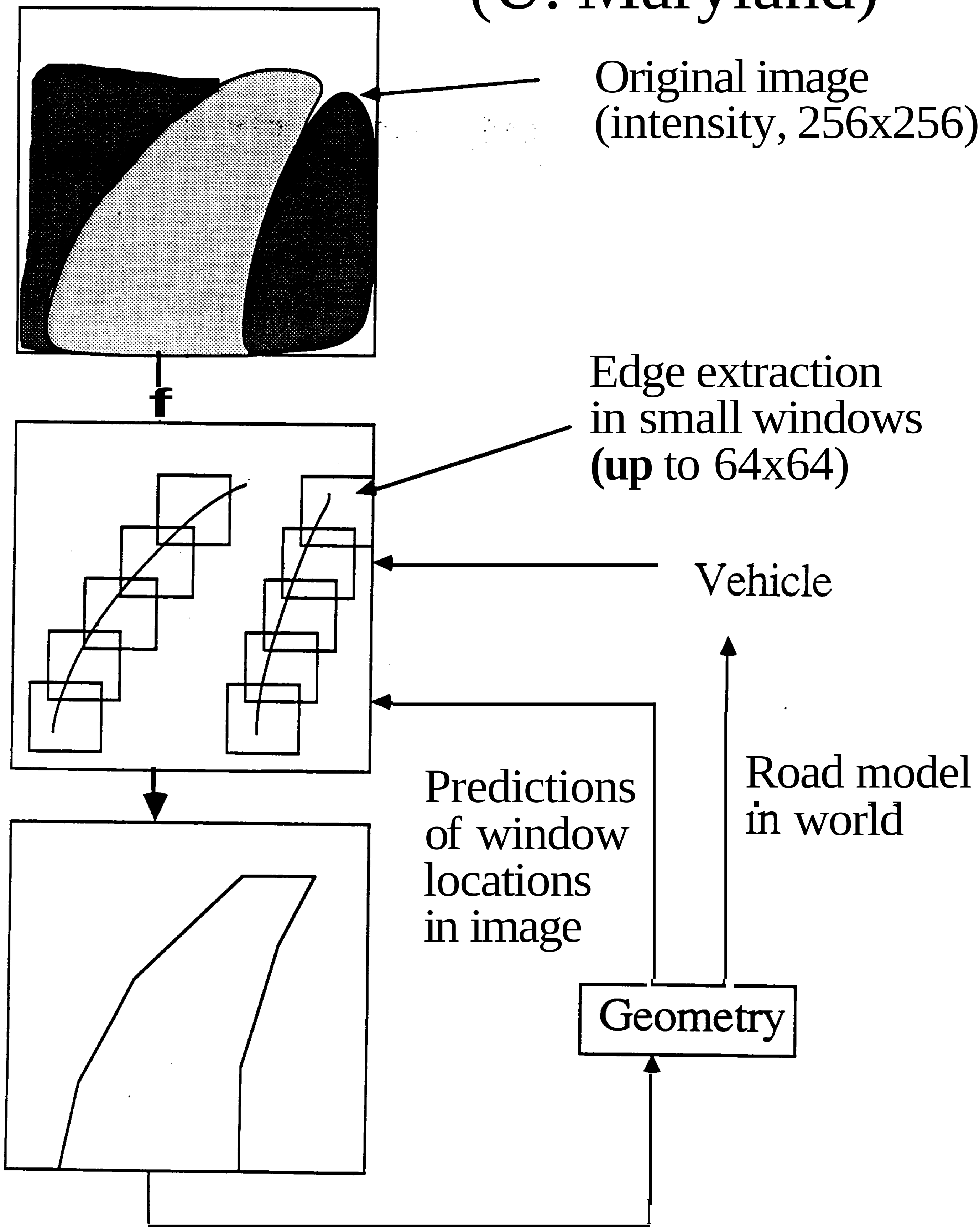

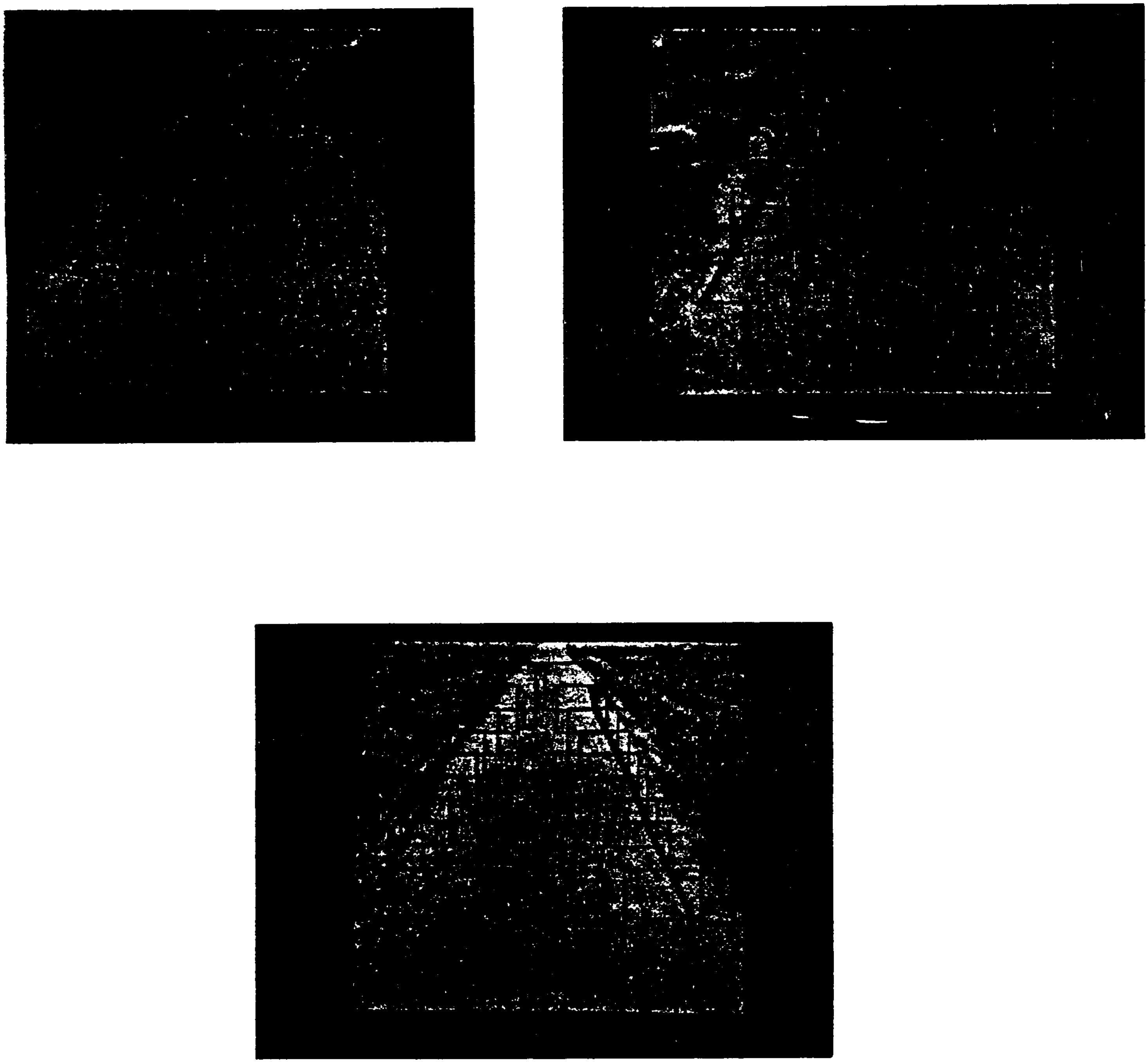

Figure 2c. The original image, along with the windows and located road boundaries

Passive depth estimation

The location of a point can be computed from its projections from differents viewpoints. From different cameras (stereo), or from different positions (e.g. motion).

- How to find good matches between images ?
- What to match ? (features vs. pixels)
- Binocular vs. trinocular ?
- How to use the vehicle's motion ?

PASSIVE STEREO

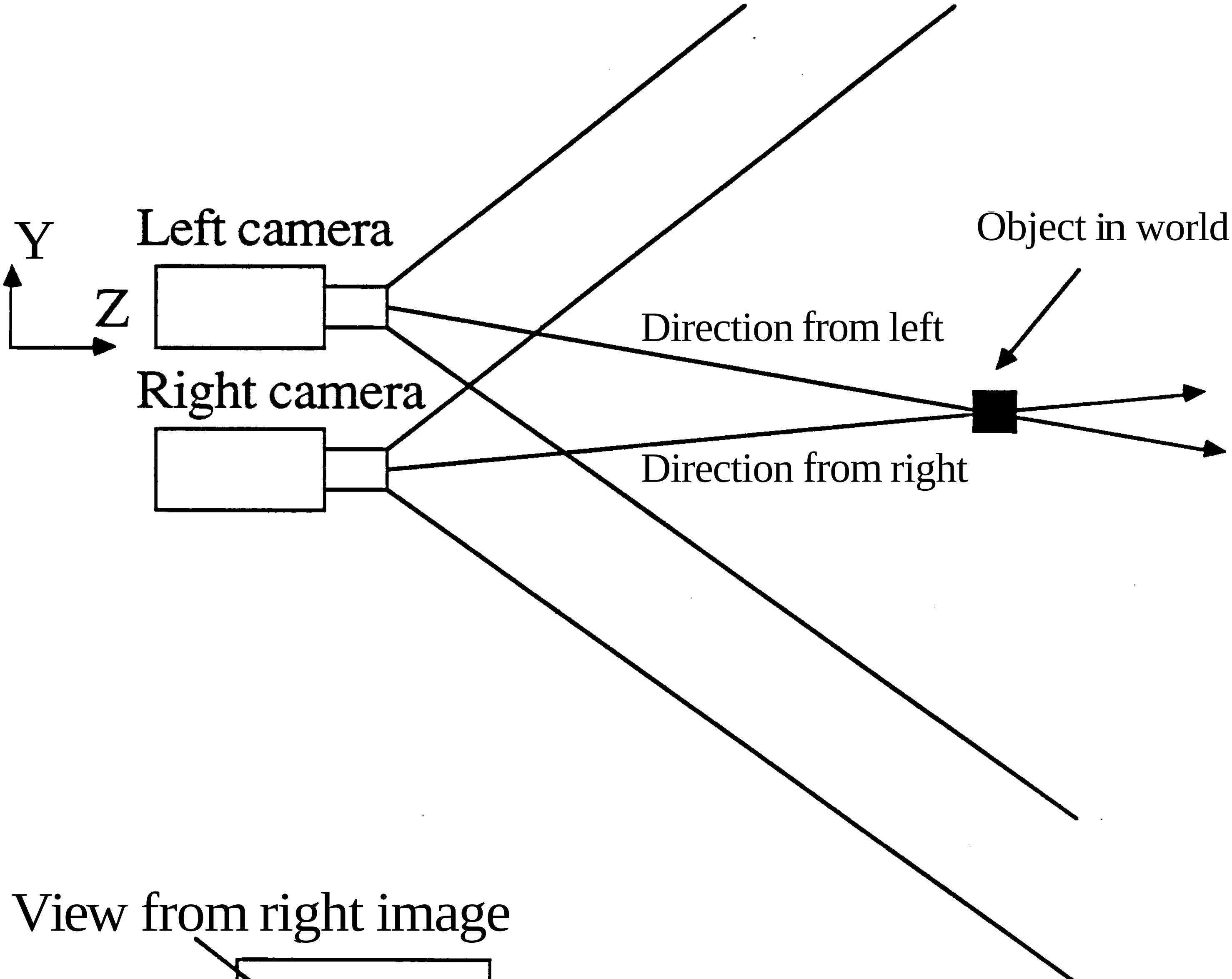

View from right image

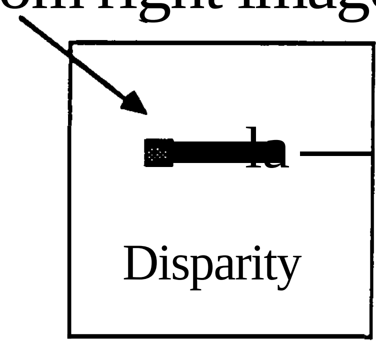

View from left image

$$\begin{cases} \mathbf{x} = f.X/(f - Z) \\ y = f.Y/(f - Z) \end{cases}$$

Finding good matches

- Similarity measures
- Epipolar constraints
- Ordering constraints
- Coarse-to-fine
- Small range of disparity values
- Overdetermination: trinocular techniques

Example: Mobi (Stanford)

- Goal: Navigation in hallways
- Two-cameras stereo
- Features: vertical edges
- Initial matches: similarity of grey level curves around edges
- Local consistency: similarity of grey level curves between edges
- Constraint propagation

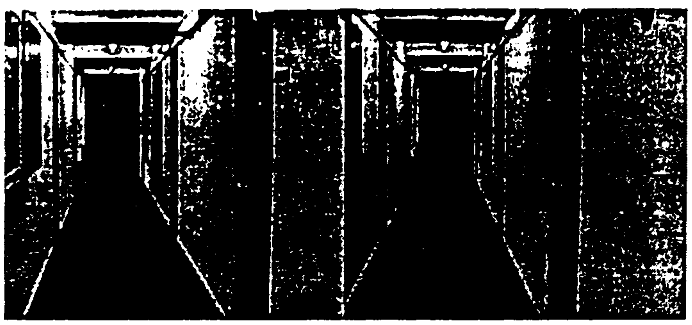

Figure 2. Stereo pair of images seen by Mobi while roaming through our lab

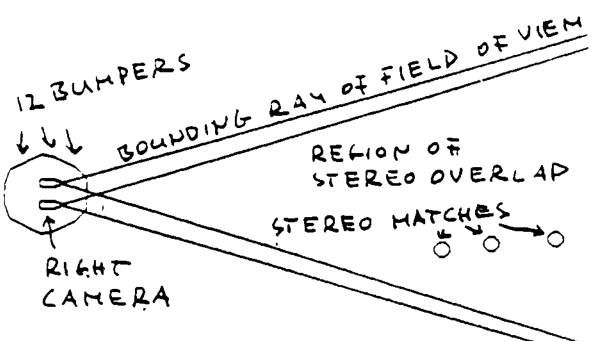

Figure 3. Model of Mobi with cameras and field of view. The stereo matches are from the image figure 2.

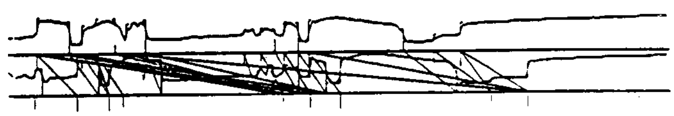

Figure 4. **Stereo match proposals and grey level curves**

Trinocular stereo

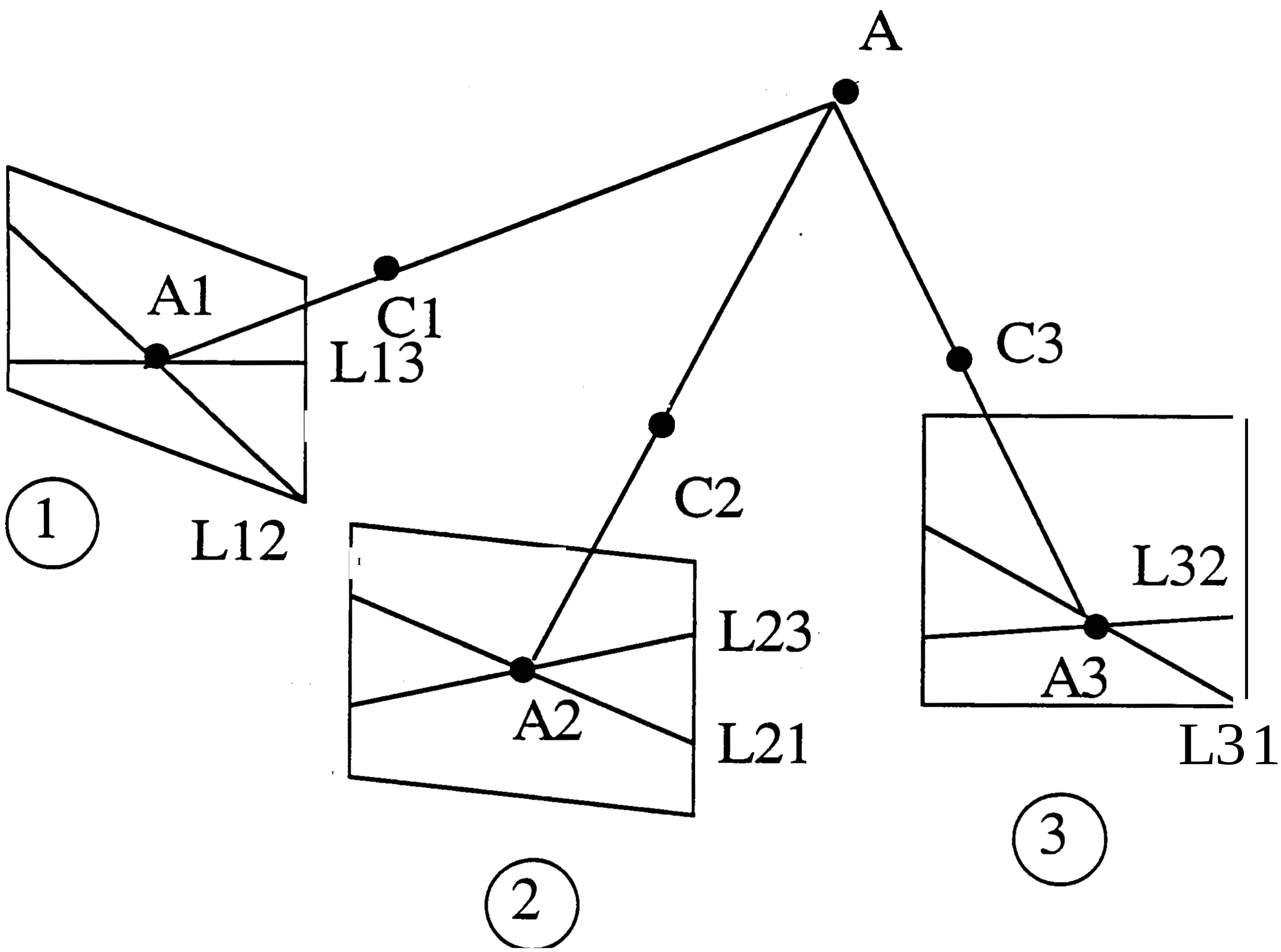

A1 and **A2** are images of the same point only
if there is an A3 at the intersection of L31 and L32.

→ No search.

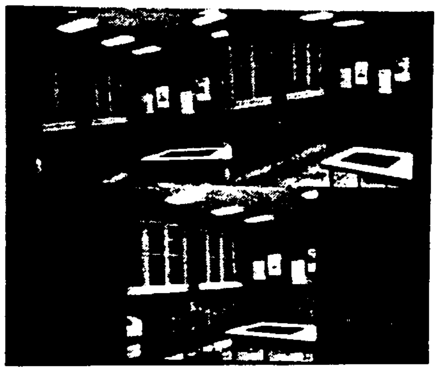

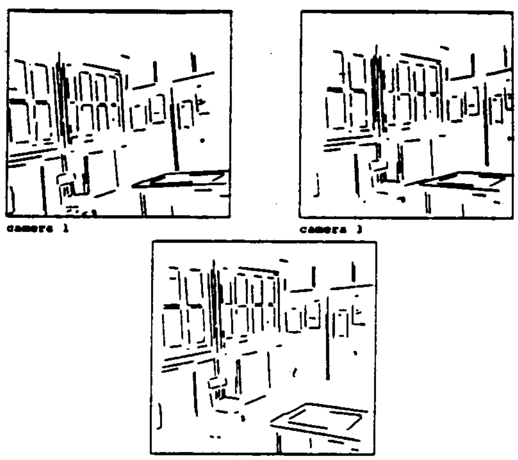
camera 1
camera 3
camera 2
na/15.12/pl.75.6dl

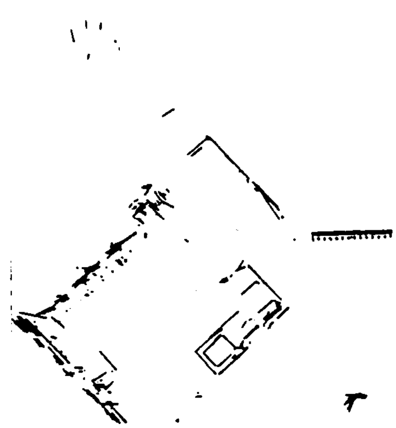

Using vehicle motion

Use depth estimates from previous positions to:

- Predict matches and reduce the search
- Improve (reduce uncertainty) of current depth estimates

FIDO (CMU)

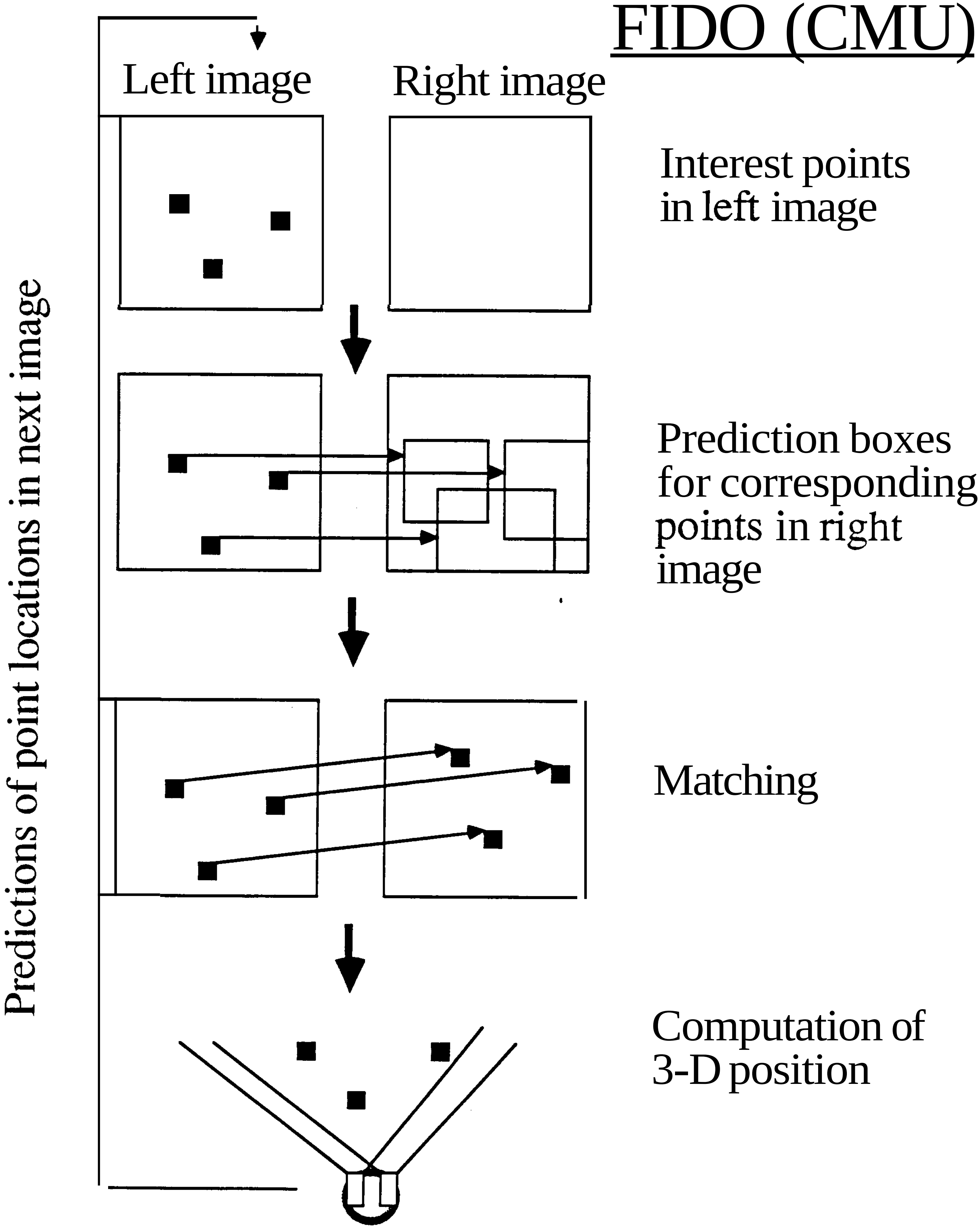
Left image
Right image
Interest points in left image
Prediction boxes for corresponding points in right image
Matching
Computation of 3-D position
Predictions of point locations in next image

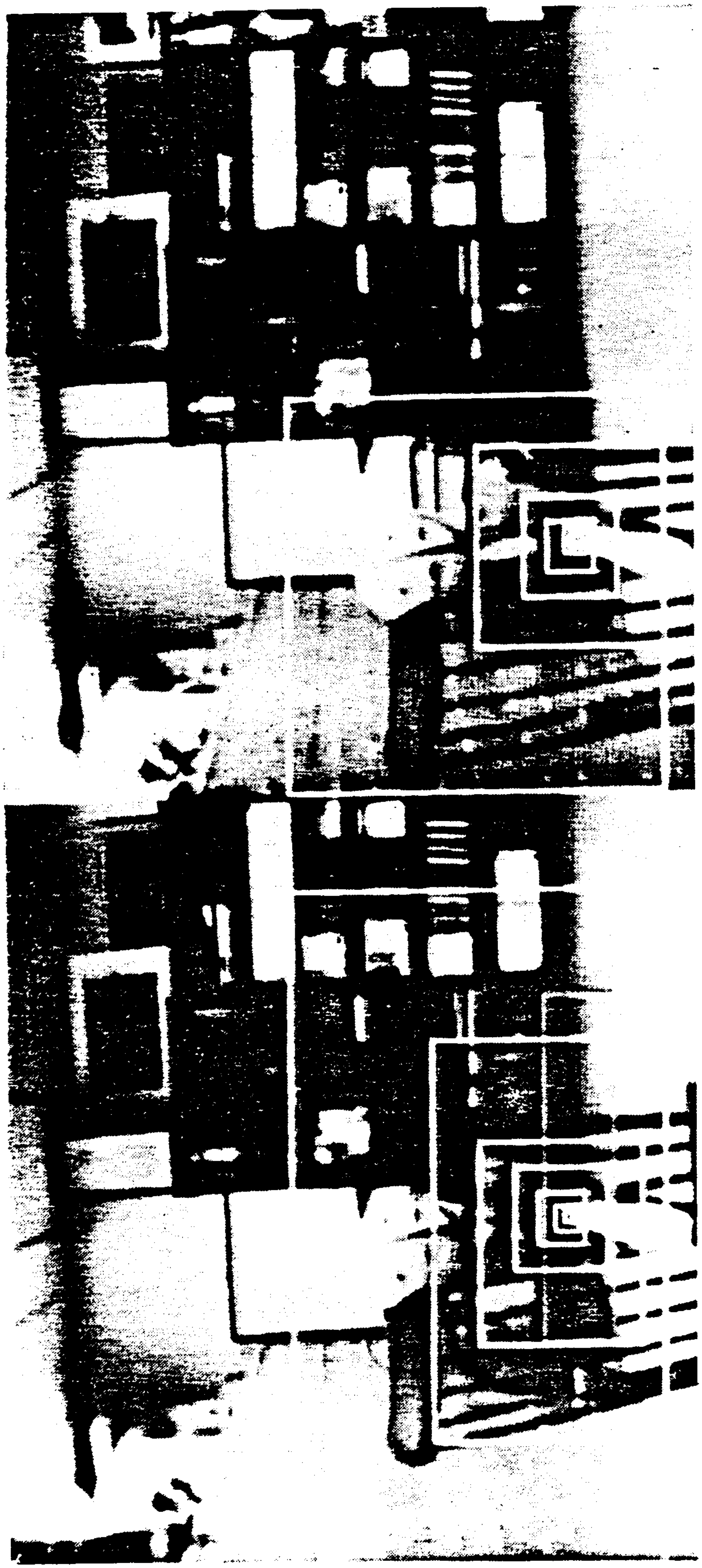

Pixel-based (or iconic) techniques (Example: Matthies' depth from motion)

- Do not match features
- Correlate images directly
- f_t and f_{t-1}: intensity image
- d: disparity at pixel (x, y)

$$e(d, x, y) =$$

$$\int\int w(\lambda,\eta)[f_t(x-d+\lambda, y+\eta)-f_{t-1}(x+\lambda, y+\eta)]^2 d\lambda d\eta$$

Minimum gives best d and uncertainty $Var(d)$. Depth map is updated over time:

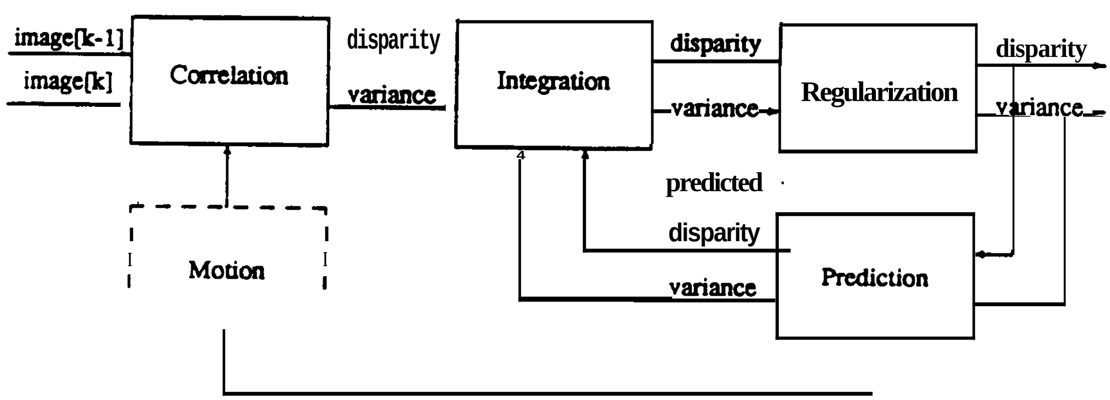

Figure 2: Iconic depth estimation block diagram

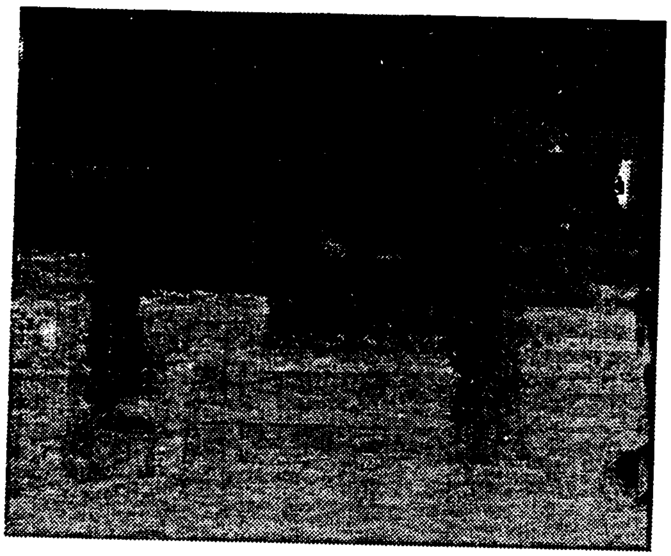

(a)

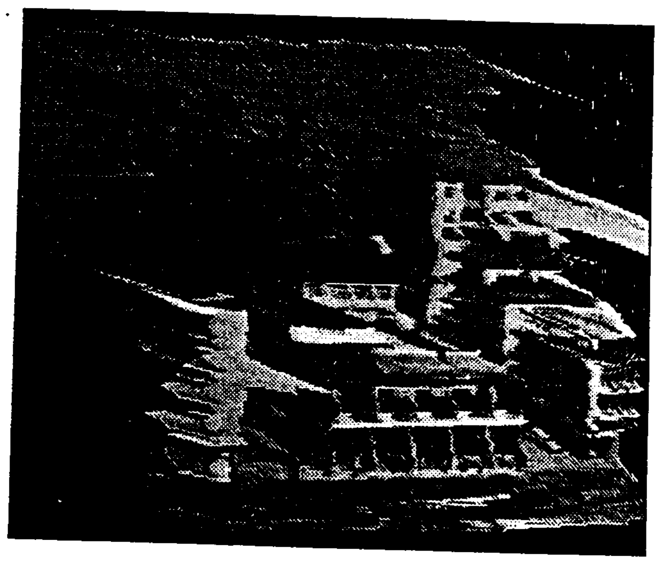

(b)

Uncertainty from passive depth estimation

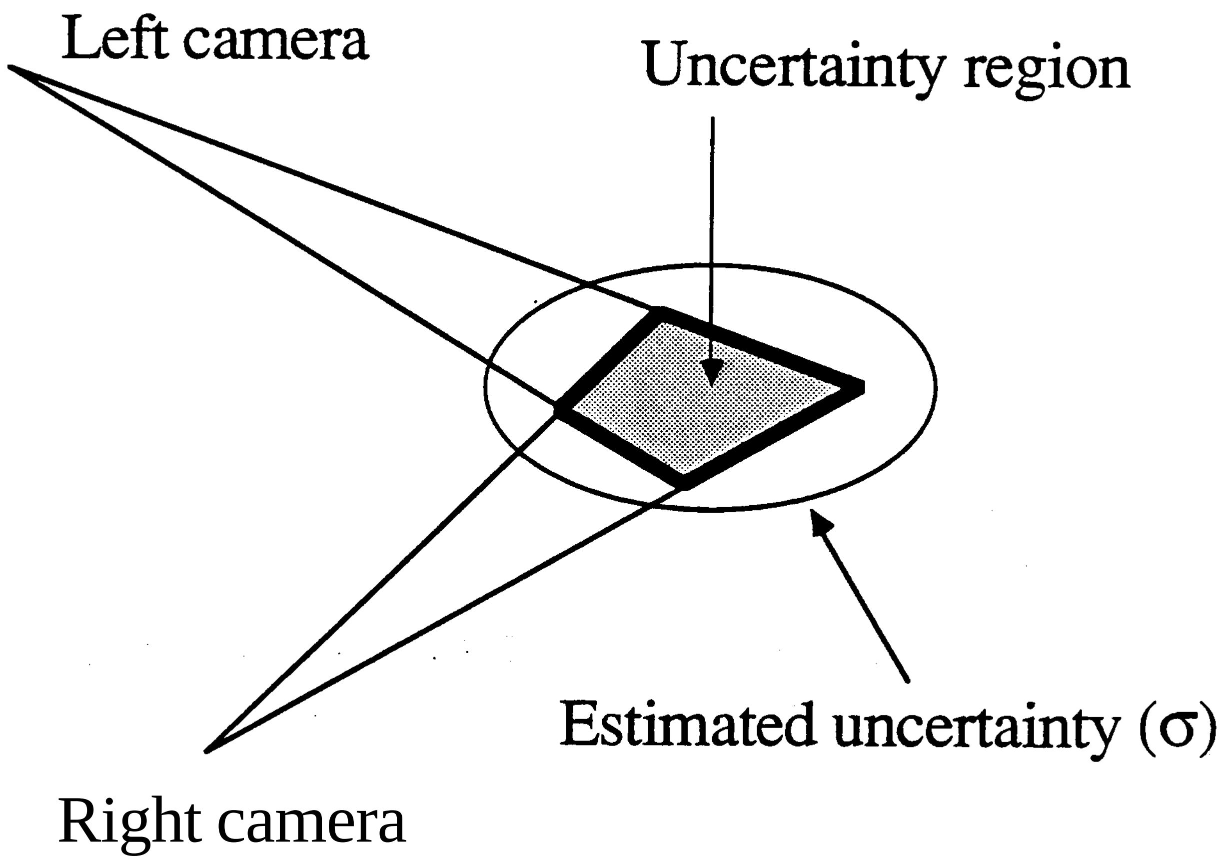

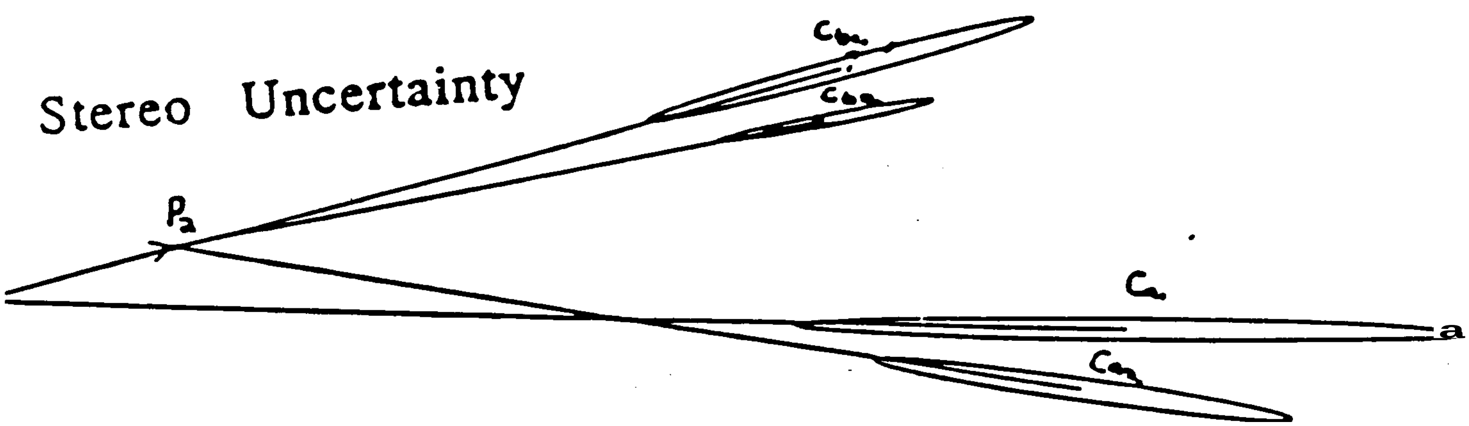

Sonar

Time-of-return of sound wave.
Typical characteristics:

- Single depth measurement
- Limited to 30 ft.
- 30° field of view (Polaroid)
- Low data rate
- Low cost

Applications:

- One unit:
  - Soft bumper
  - Surface (e.g. wall) tracking
- Sonar ring:
  - Obstacle avoidance
  - Map building (More later on that)

Sonar ring

(Typically 24 Polaroid units)

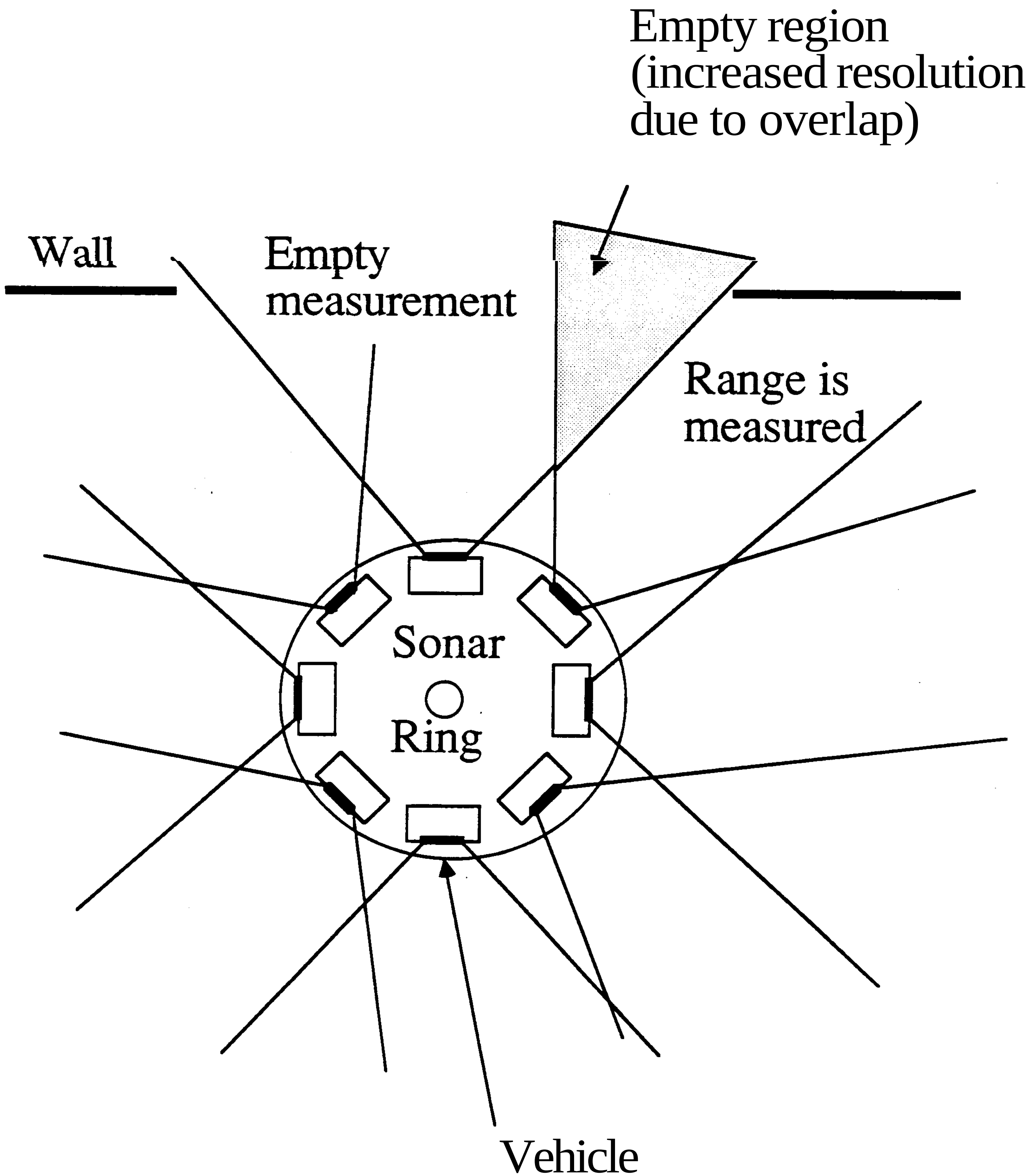

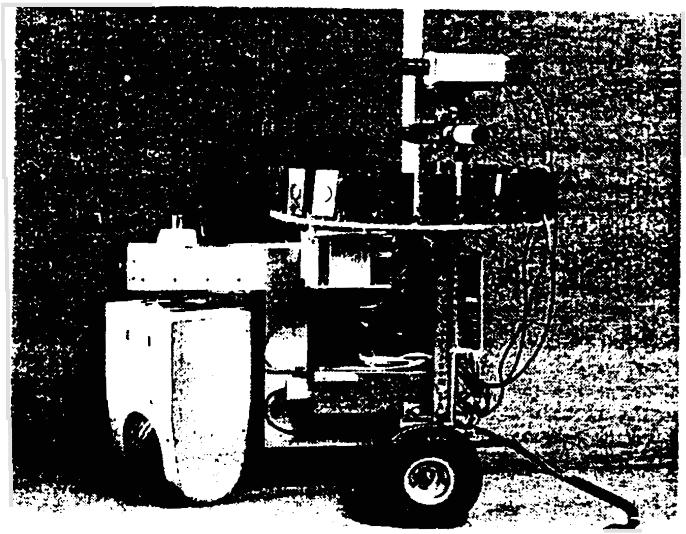

Figure 2: The *Neptune* mobile robot, with a pair of cameras and the sonar ring. For experiments in sensor integration, the cameras were mounted lower, so that their horizon line would be close to the cross-sectional view provided by the sonar ring.

Exceptions

FMC sonar for outdoor vehicle: 30KHz, 64 ft. range, 16 x 24 image

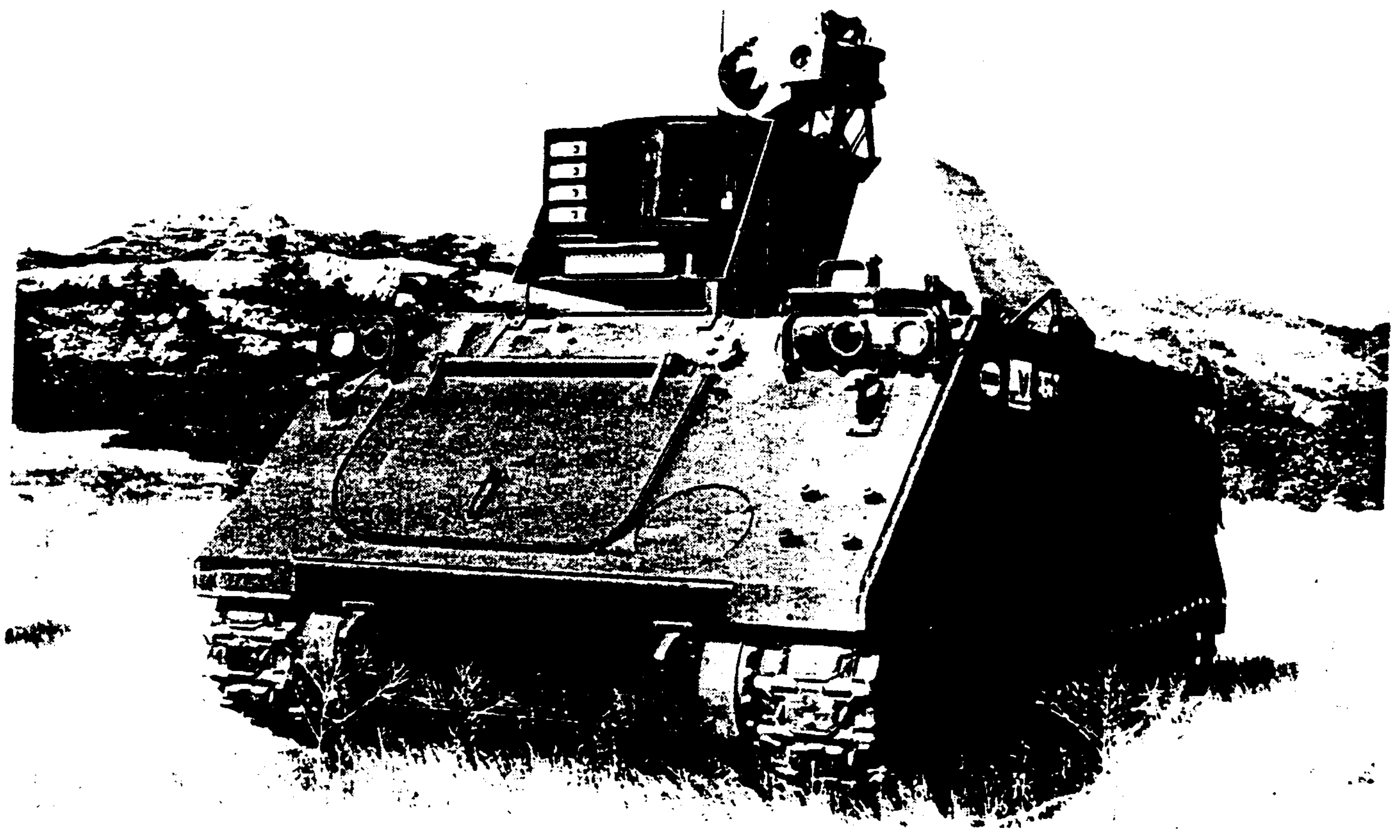

Exceptions

Underwater sonar imaging

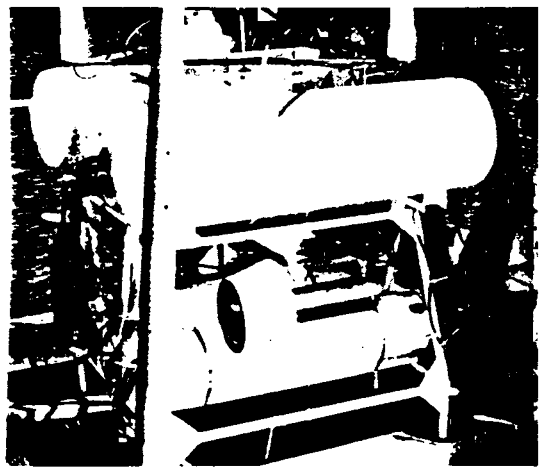

FIG. 1. Underwater robot EAVE-East (Experimental Autonomous Vehicle) in its launch cradle at the University of New Hampshire. The large white cylinders contain electronics: the smaller. lower white cylinders hold batteries: and the darker cylinders are thrusters.

Acoustic Scan

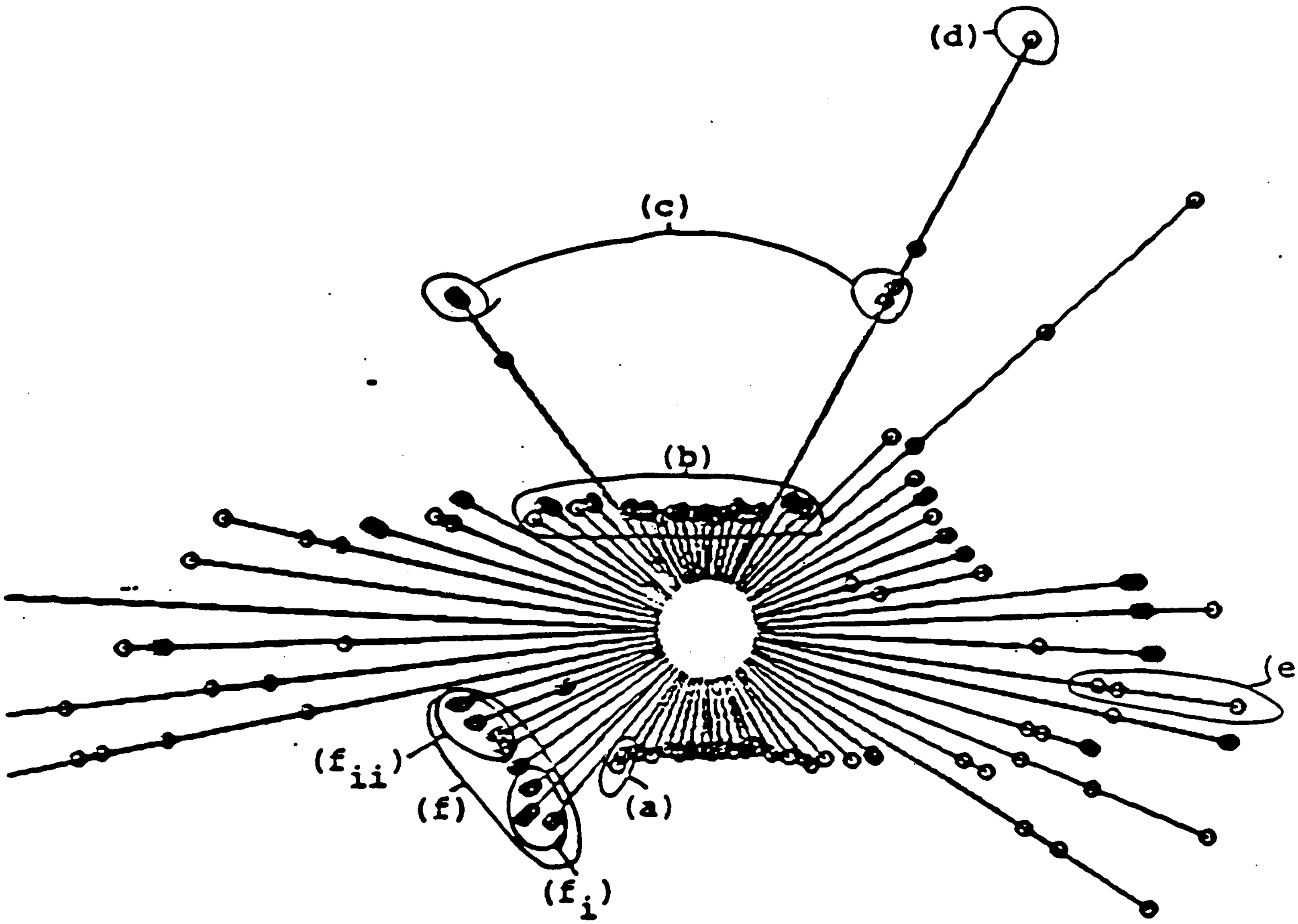

a) Random errors
b) LMS line fit
c) Specular reflections
d) Double reflections
e) Large angle of incedance
f) Reflections in a Dihedral

Laser range finders

Distance measurement by projection of a single laser beam. Two types

- Triangulation (Simple design but calibration problems on a mobile platform)
- Time-of-flight (Self-contained unit $\Rightarrow$ no calibration problems, better accuracy but state of the art technology)

Characteristics:

- Indoor or outdoor
- High resolution images (either 1-D or 2-D)
- Fast
- High resolution depth measurement
- High cost, fragile, power/resolution/speed tradeoff
- Sensitive to material properties (e.g. specular materials)

Laser range finders:

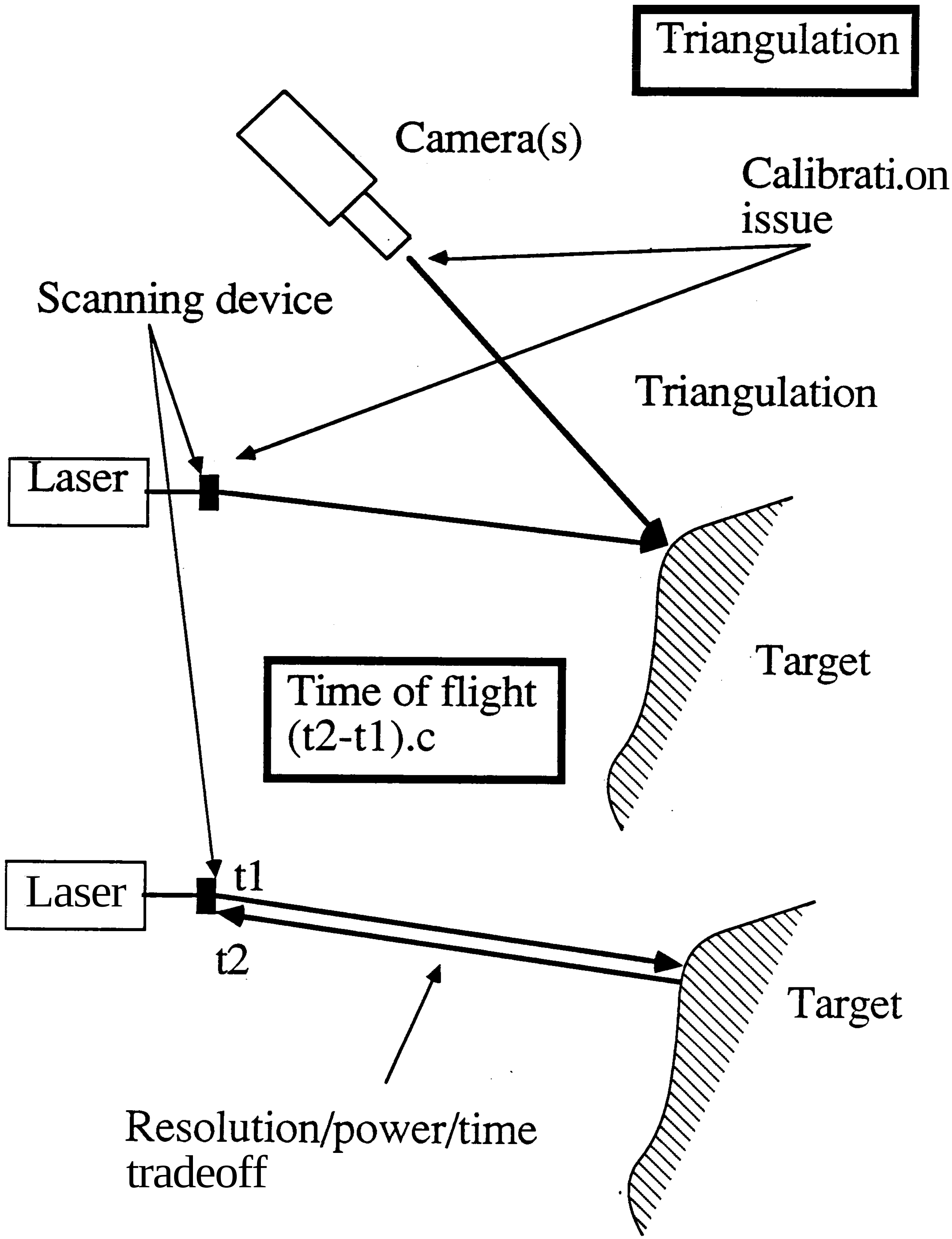

Example: HILARE (LAAS)

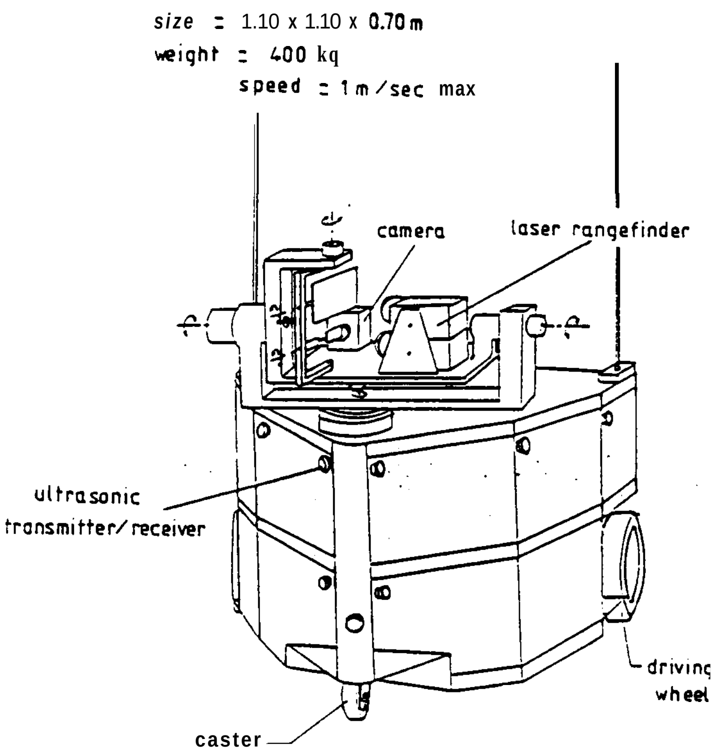

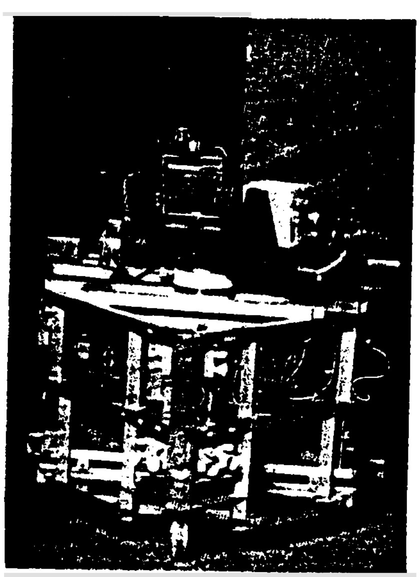

Figure 1

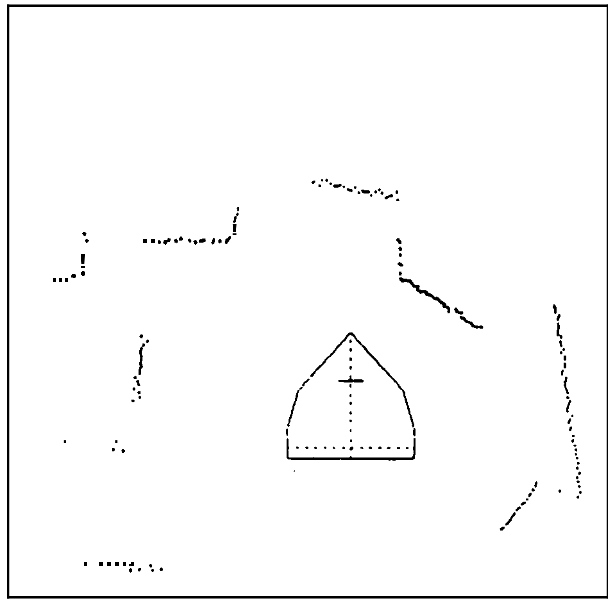

Figure 3 a : Actual data

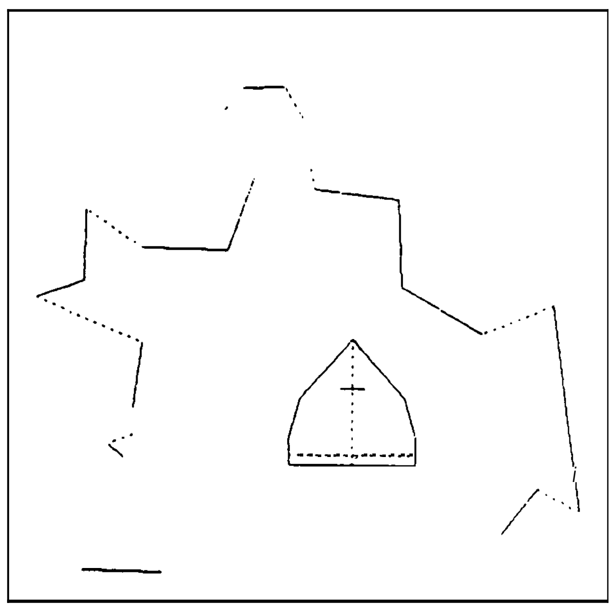

Figure 3 b : on-line polygonal representation

Figure 3 : Environment circular scanning
with the Laser range-finder

Example: Environmental Research Institute of Michigan (ERIM)

- Time-of-flight
- 64 x 256 range images, 30° x 80°
- Reflectance image
- 8-bit range from 0 to 64 feet (3 inches resolution)

Similar devices: Odetics, **ASV** sensor for Ohio State Univ. walking machine.

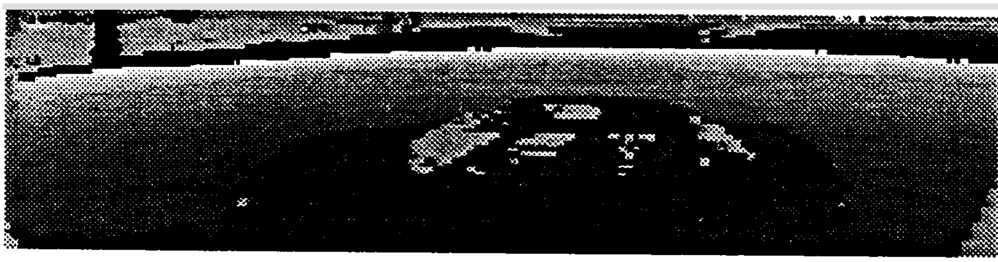

a image

Video image

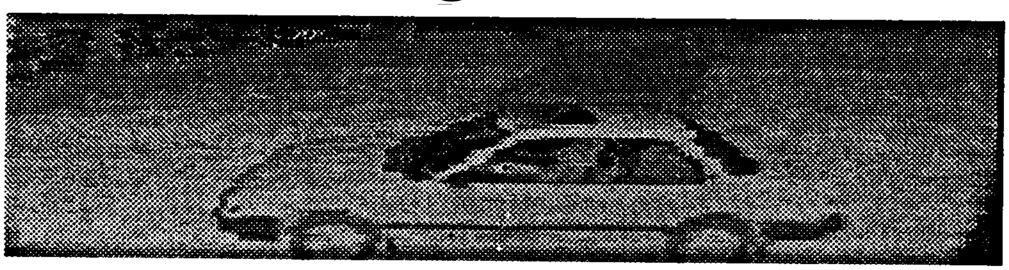

Reflectance **image**

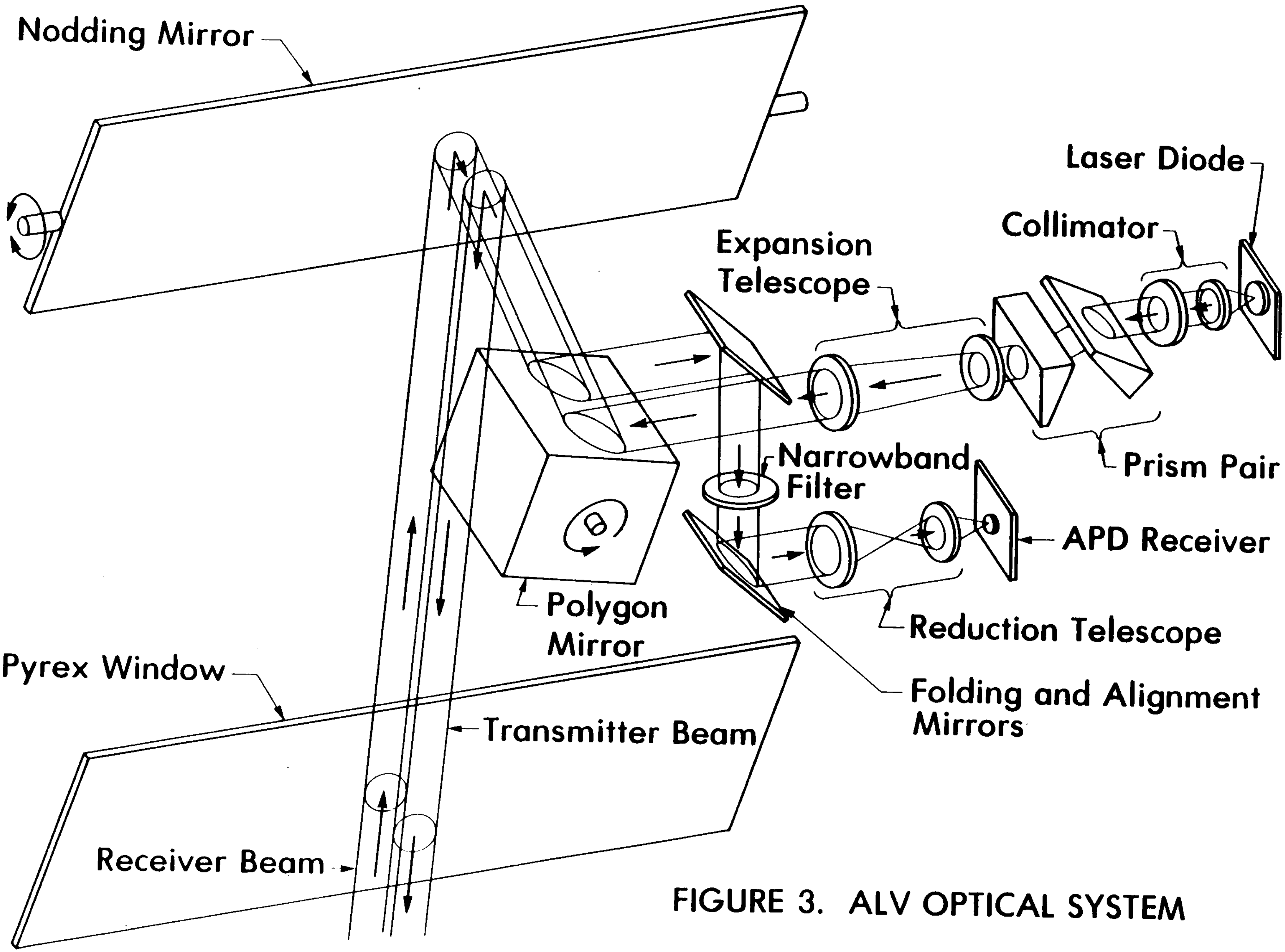

FIGURE 3. ALV OPTICAL SYSTEM

Representation of perceptual features for mobile robots

1. Representations of uncertainty and sensor fusion

   Special representations:

2. Terrain maps
3. probability maps

SENSOR FUSION:

How to combine observations from different sensors (e.g. passive stereo and active sonar)

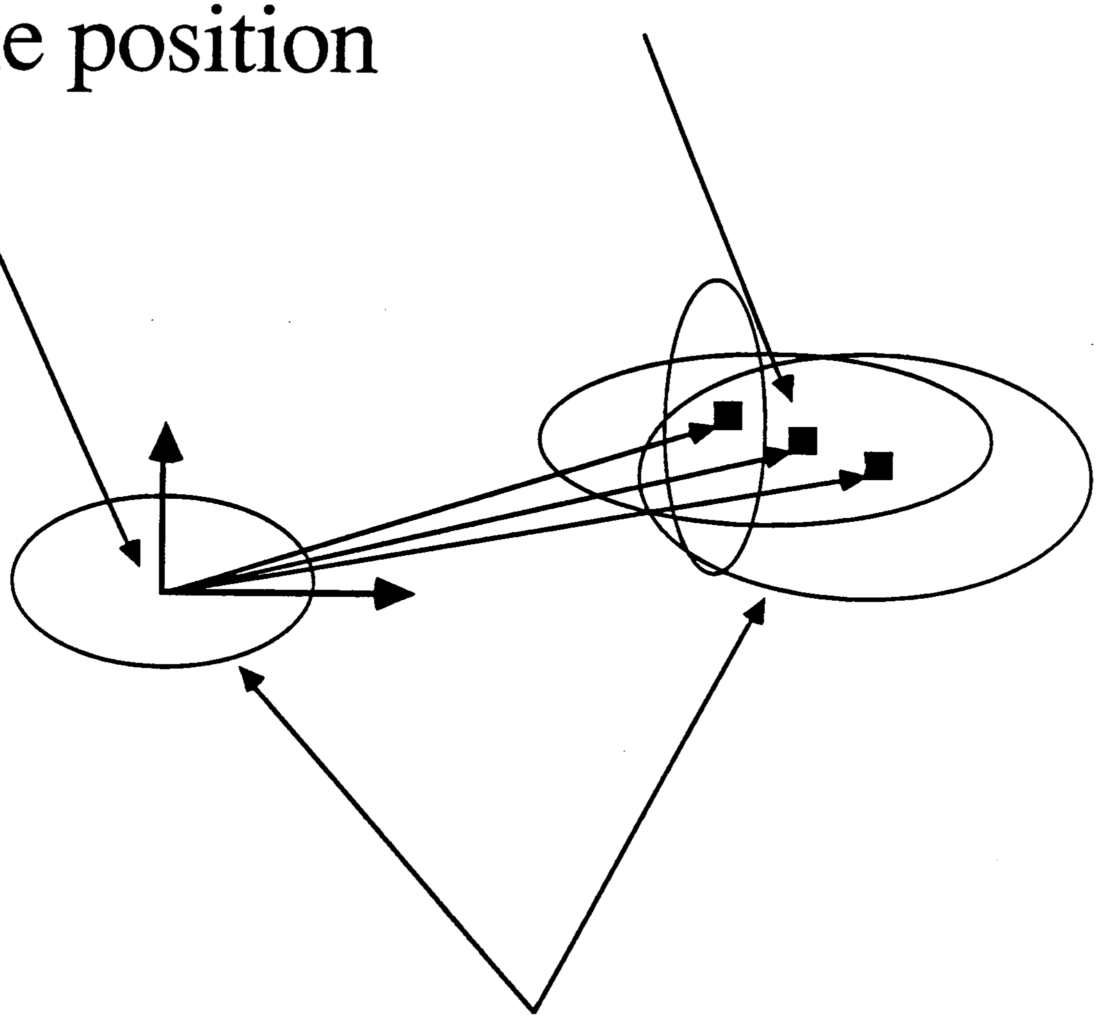

MOTION FUSION:
How to merge the two observations?

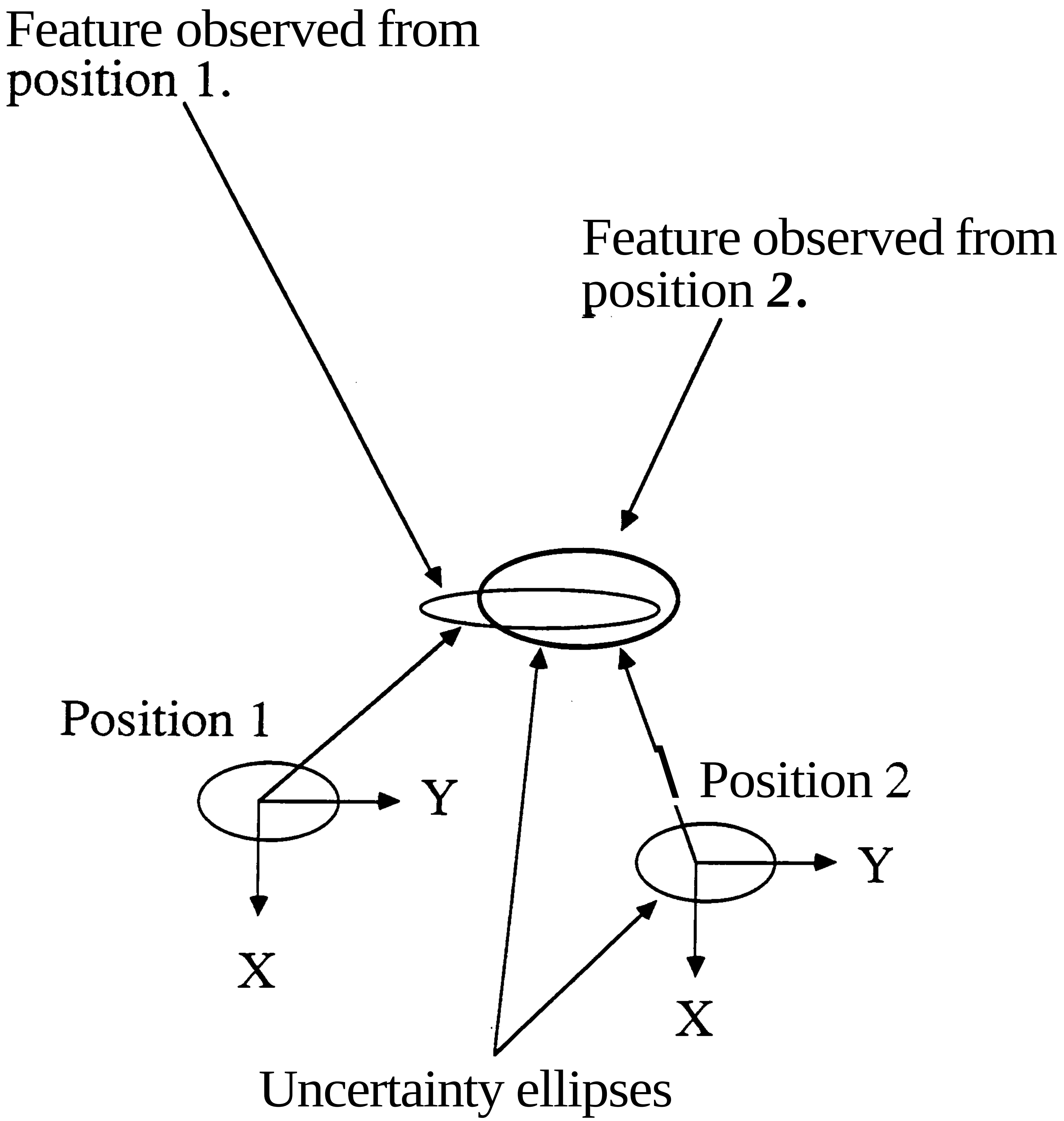

TRADITIONAL APPROACH

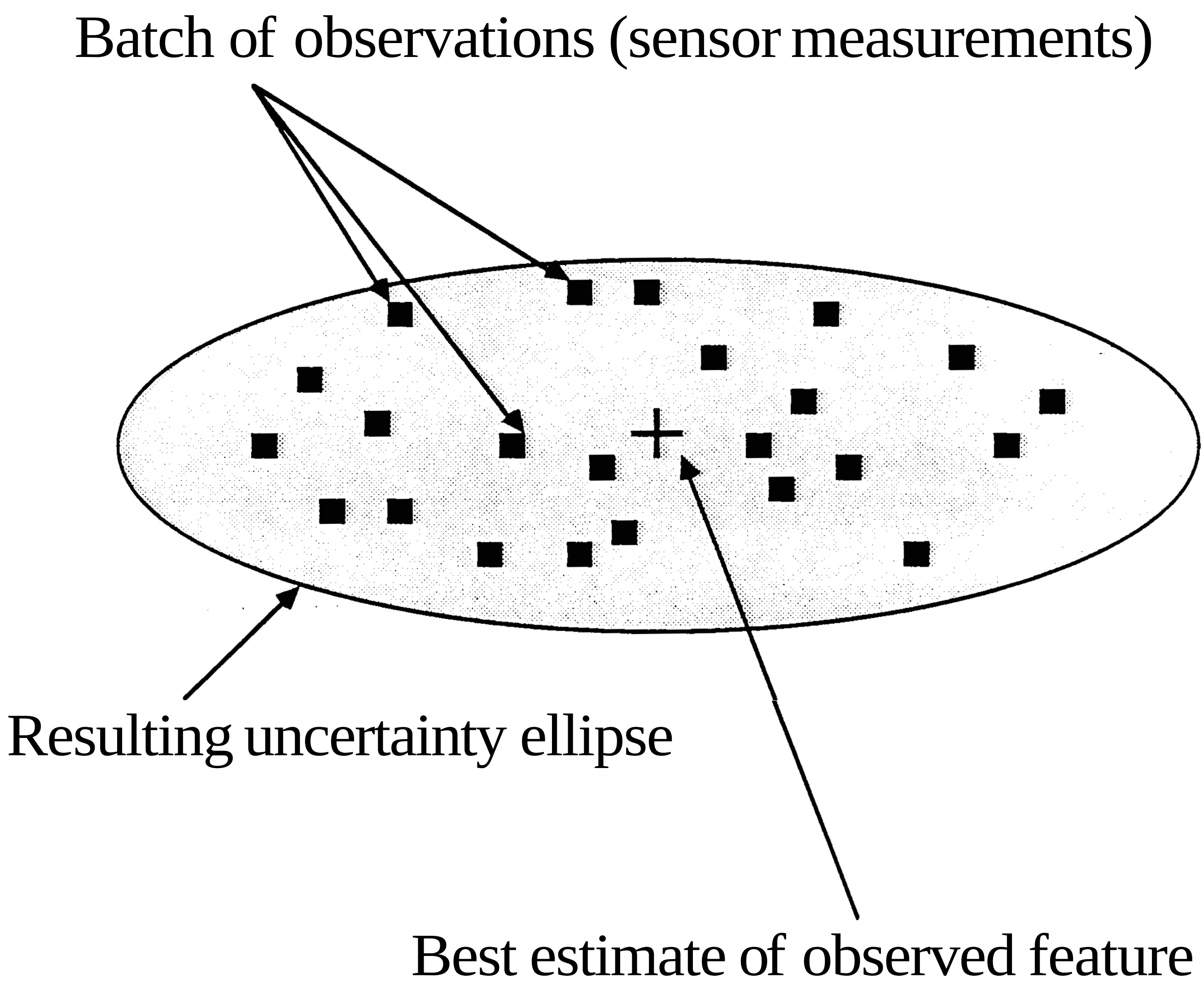

KALMAN FILTERING

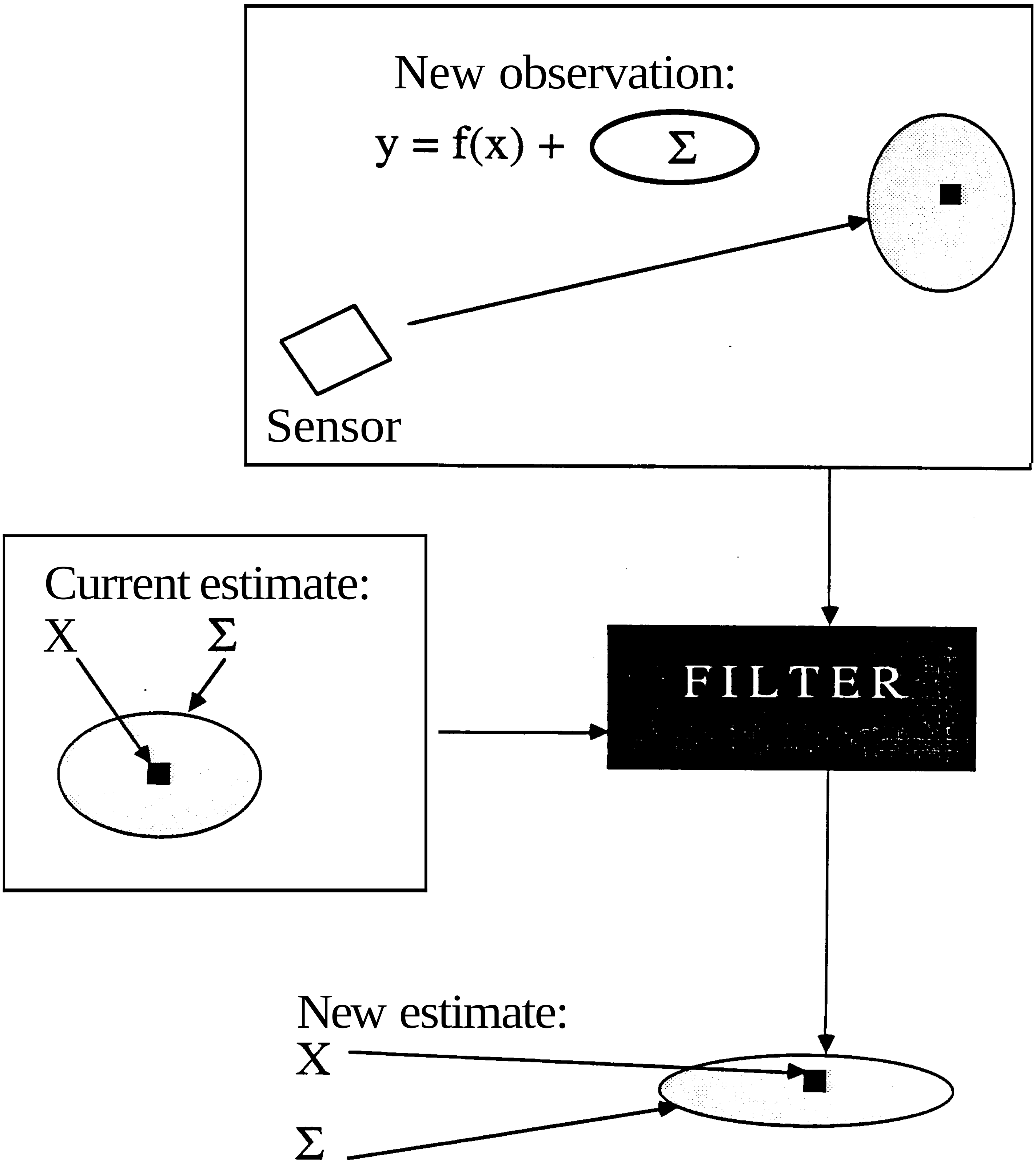

Linear Filtering

$$\underline{y} = H\underline{x} + \underline{v}$$

Where:

- $\underline{z}$ is a l x 1 measurement vector,
- $\underline{x}$ is the n x 1 vector to be estimated,
- H is an $l \times n$ matrix,
- and $\underline{v}$ is a random additive measurement error with l x l covariance matrix R.

The estimate of $\underline{x}$ is given by:

$$\min(\underline{y} - H\underline{x})^T R^{-1}(\underline{y} - H\underline{x})$$

The best estimate is:

$$\hat{\underline{x}} = (H^T R^{-1} H)^{-1} H^T R^{-1} \underline{y}$$

Justification: Maximum likelihood approach:

$$p(\underline{y}|\underline{x}) = \frac{1}{(2\pi)^{l/2}|R|^{1/2}} \exp[-\frac{1}{2}(\underline{y}-H\underline{x})^T R^{-1}(\underline{y}-H\underline{x})]$$

Bayesian approach

$$p(\underline{x}|\underline{y}) = \frac{p(\underline{y}|\underline{x})p(\underline{x})}{p(\underline{y})}$$

Best estimation according to minimum variance criterion:

$$\min \int (\hat{\underline{x}} - \underline{x})^T(\hat{\underline{x}} - \underline{x})p(\underline{x}|\underline{z})d\underline{x}$$

Solution is:

$$\hat{\underline{x}} = \int \underline{x}p(\underline{x}|\underline{y})d\underline{x} = E[\underline{x}|\underline{y}]$$

In case of a linear model, the best estimate is:

$$\hat{\underline{x}} = (P_0^{-1} + H^T R^{-1} H)^{-1} H^T R^{-1} \underline{y}$$

Where P_0 is the a priori covariance matrix of $\underline{x}$.

Recursive filtering

New problem:

$$\underline{z}_k = H_k \underline{x}_k + \underline{v}_k$$

We want to find the best estimate $\hat{\underline{x}}_{k+1}$ based on a new measurement $\underline{z}_k$ and the previous estimate $\hat{\underline{x}}_k$.

Recursive solution:

$$\hat{\underline{x}}_{k+1} = \hat{\underline{x}}_k + K_k[\underline{y}_{k+1} - H_{k+1}\hat{\underline{x}}_k]$$

Where $\boldsymbol{K_k}$ is a gain matrix given by:

$$K_k = P_k H_{k+1}^T (R_{k+1} + H_{k+1} P_k H_{k+1}^T)^{-1}$$

And the covariance matrix of $\hat{\underline{x}}_{k+1}$ is updated by:

$$P_{k+1} = (I - K_k H_{k+1}) P_k$$

Extended Kalman filter

New problem: we have an observation $\underline{z}$ that depends on the a parameter vector $\underline{a}$ by the relation:

$$\boldsymbol{f}(\underline{z}, \boldsymbol{a}) = 0$$

and $\underline{z} = \underline{z}\prime + \underline{\epsilon}$, where $\underline{\epsilon}$ is additive noise. Given an estimate $\underline{a}^*$ and a new measurement $\underline{z}$ what is the new estimate of $\underline{a}$?

Linearization of f

$$f(\underline{z}\prime, \underline{a}) \approx f(\underline{z}, \underline{a}^*) + \frac{\partial f}{\partial \underline{z}}(\underline{z}\prime - \underline{z}) + \frac{\partial f}{\partial \underline{a}}(\underline{a} - \underline{a}^*)$$

Linear measurement equation (as before):

$$\underline{y} = H\underline{a} + \underline{v}$$

where:

$$\underline{y} = -f(\underline{x}, \underline{a}^*) + \frac{\partial f}{\partial \underline{a}}\underline{a}^*$$

$$H = \frac{\partial f}{\partial \underline{a}}$$

and

$$\underline{v} = -\frac{df}{\partial \underline{x}}\epsilon$$

Building maps from matching line segments:
(Faugeras, Ayache, INRIA)

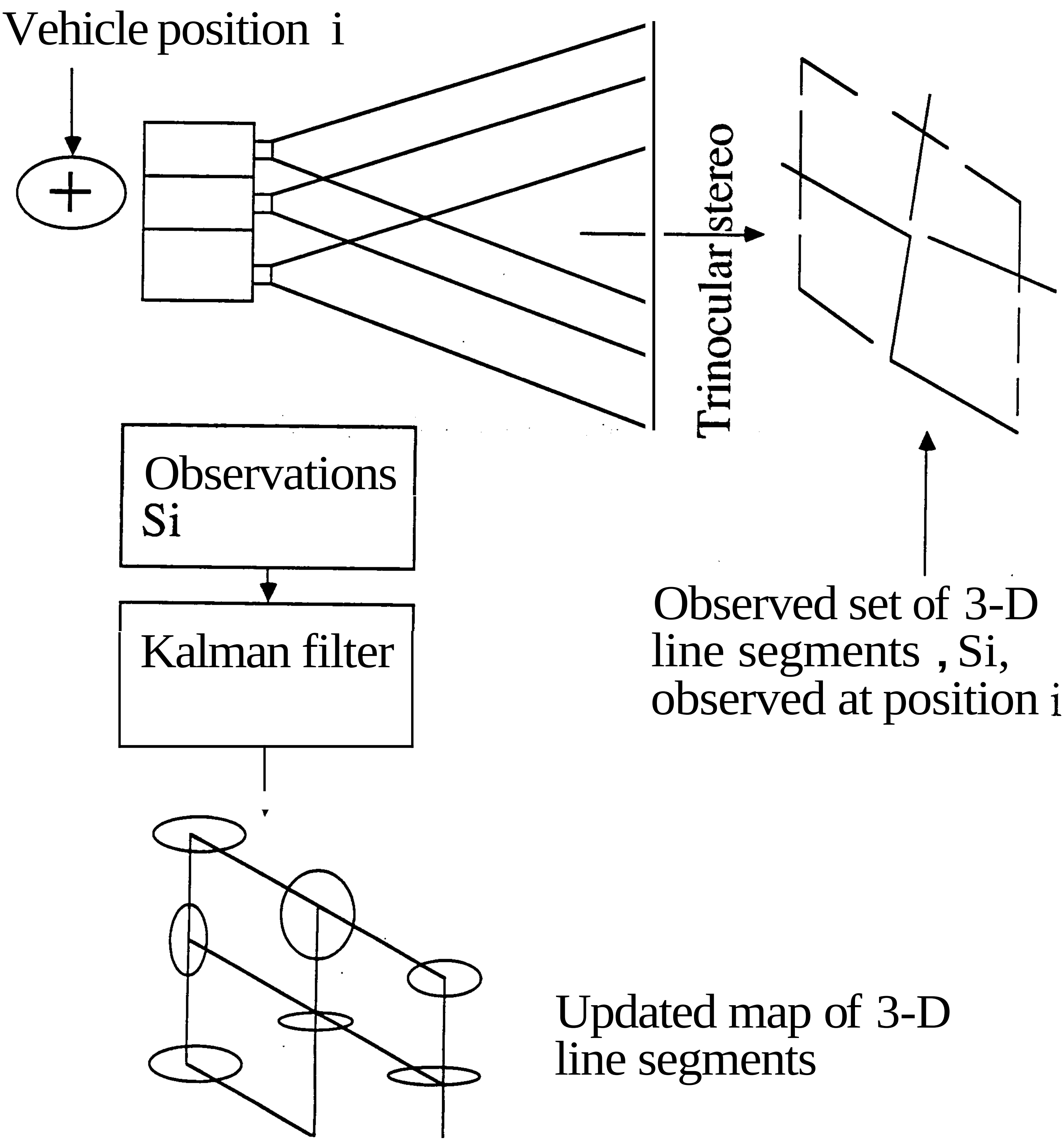

lication to line matching

esented by the intersection of

$$x = az + p$$

$$y = bz + q$$

o segments S_i $(i = 1, 2)$ supported
es L_i of parameters (a_i, b_i, p_i, q_i) with
matrix (from trinocular stereo) Λ_i
sformation T from frame 2 to frame
ariance matrix Λ, decide whether:

S_2 are two instances of the same segment, and

ompute the uncertainty (i.e. the co-
matrix) of the fused segment.

The EKF is used to compute:

1. The estimate of the transformed by T of S_2, $L'_2 = (a'_2, b'_2, p'_2, q'_2)$, and
2. The covariance matrix Λ'_2 computed from Λ_2 and Λ.

The two lines are matched if

$$d^2(L_1, L'_2) = (L_1 - L'_2)^T(\Lambda_1 + \Lambda'_2)^{-1}(L_1 - L'_2)$$

is greater than a threshold s corresponding to a probability of 95% (χ^2) distribution.

Figure 12:
Polygonal approximation of the edge points of a stereo pair of an office room observed in position 1

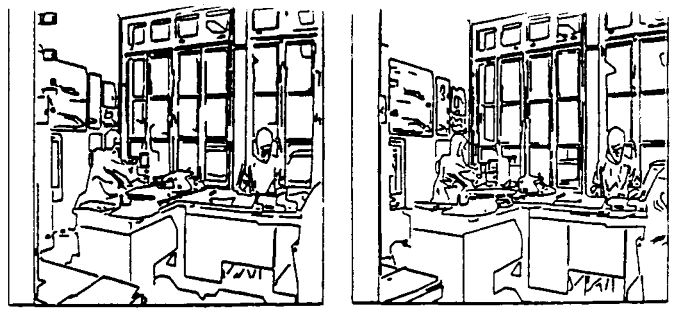

Figure 13: Polygonal approximation of the edge points of a stereo pair of the same office room observed in position 2

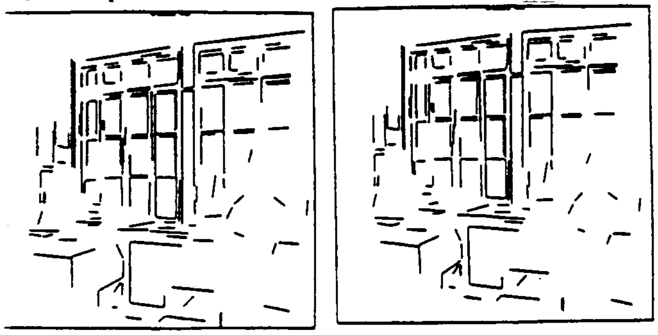

Figure 14: Edge segments matched in ~ P I pair of Figure 12

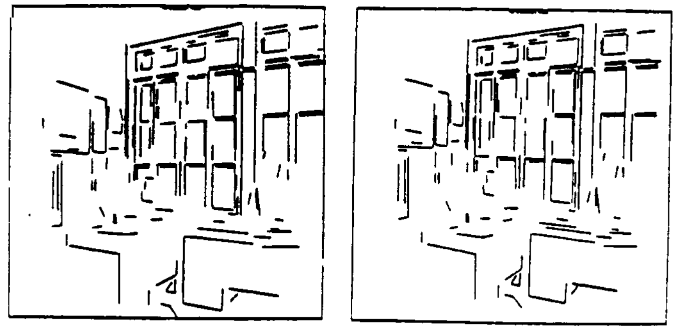

Figure 15: Edge segments matched in stereo pair of Figure 13

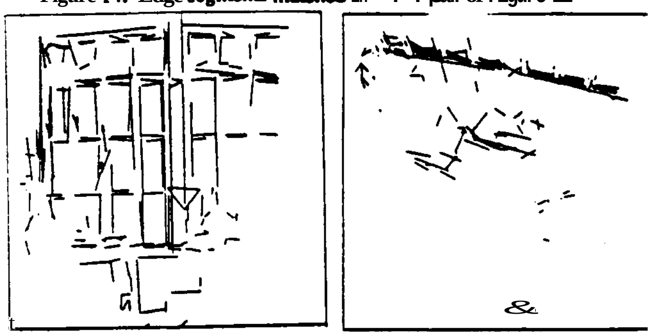

Figure 16: Horizontal and vertical projection of the reconstructed segments of the office room observed in position 1

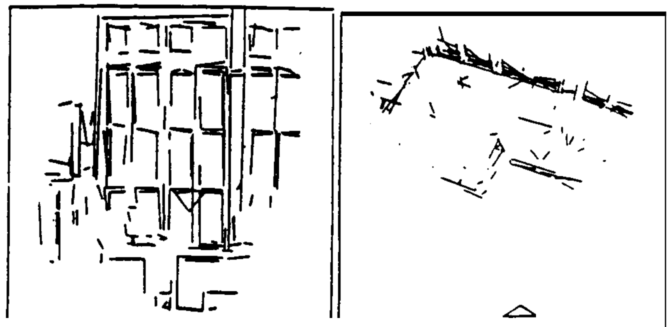

Figure 17: Horizontal and vertical projection of the reconstructed segments of the office room observed in position 2

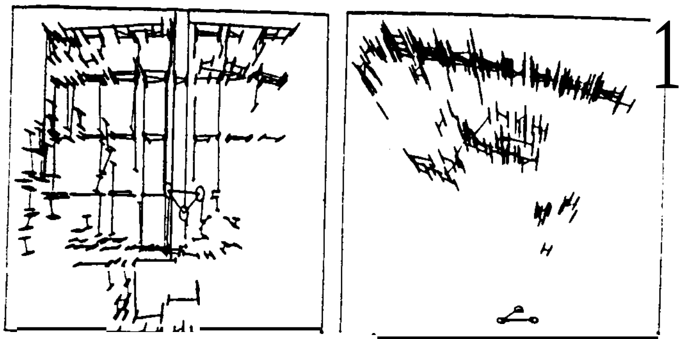

Figure 18: Covariance matrices attached to the endpoints of the reconstructed segments of the offiic room observed in position 1

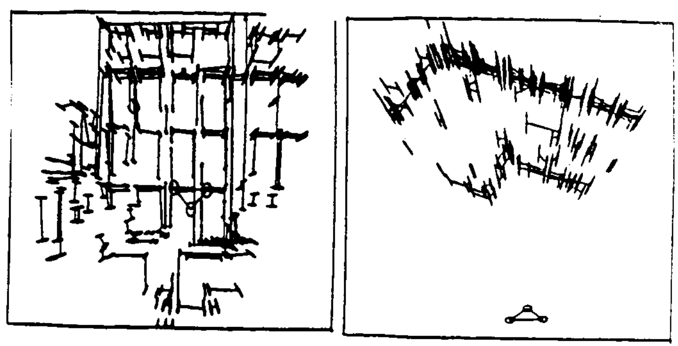

Figure 19: Covariance matrices attached to the endpoints of the reconstructed segments of the office room observed in position 2

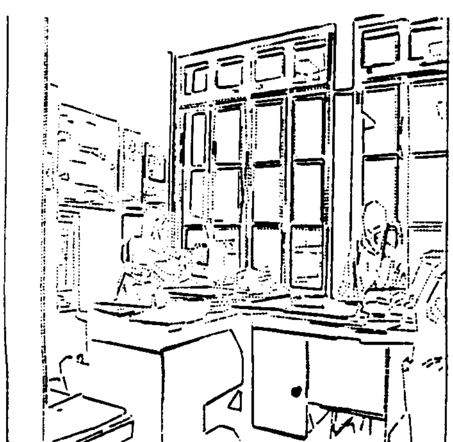

b)Application of the estimated motion to the segments of position 1 followed by a perspective projection (solid lines) on one of

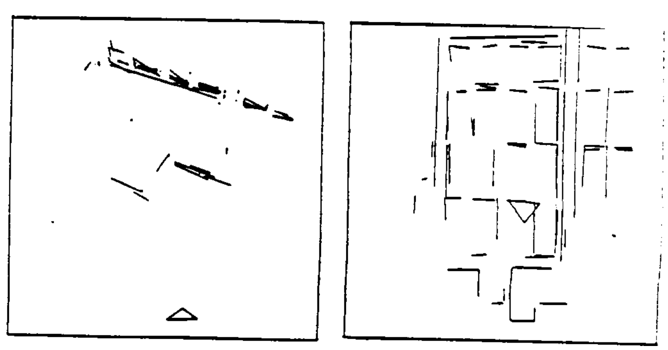

Figure 23: Fusion in position 2 of the segments reconstructed in positions 1 and 2

ELEVATION *MAPS*

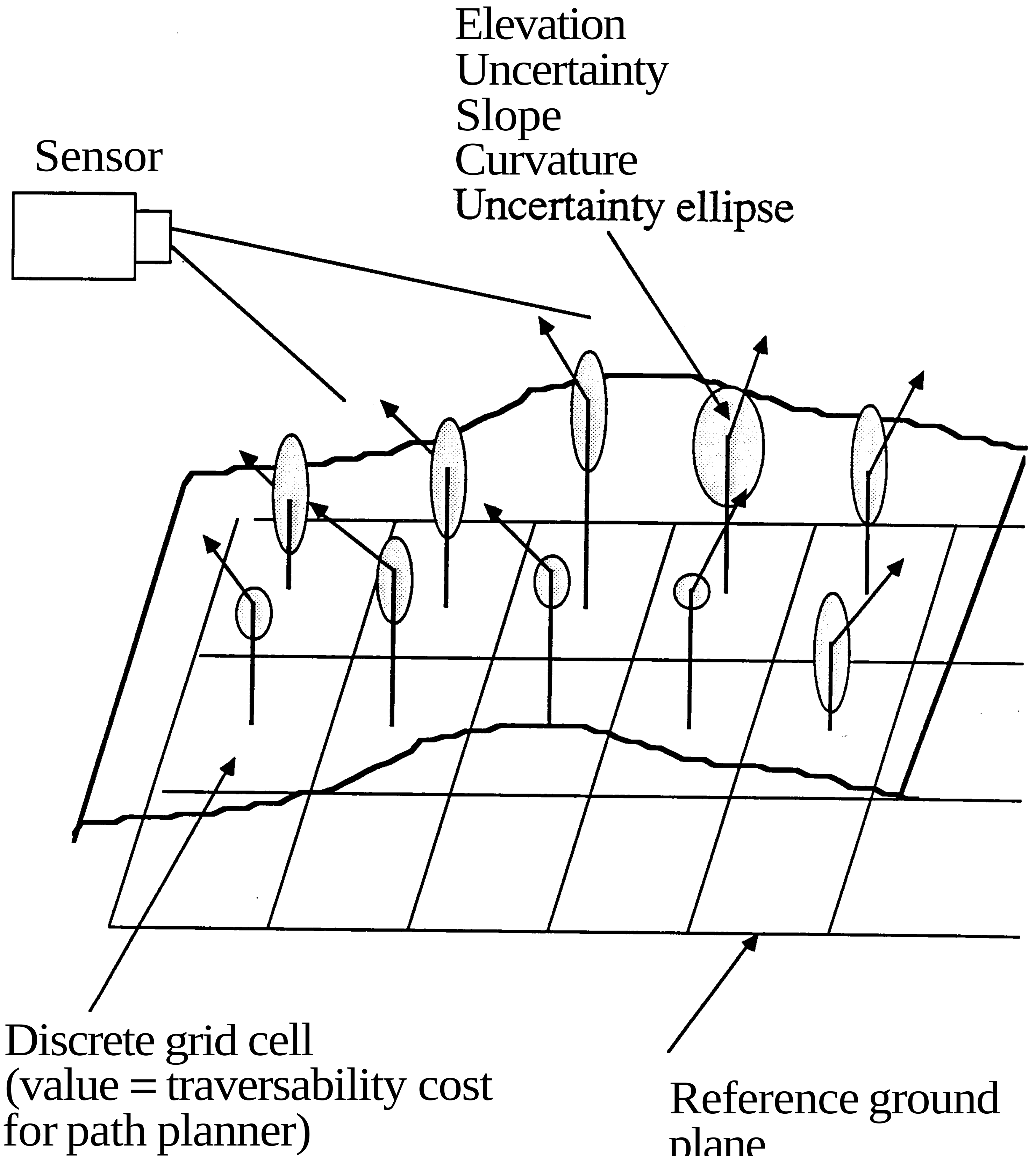

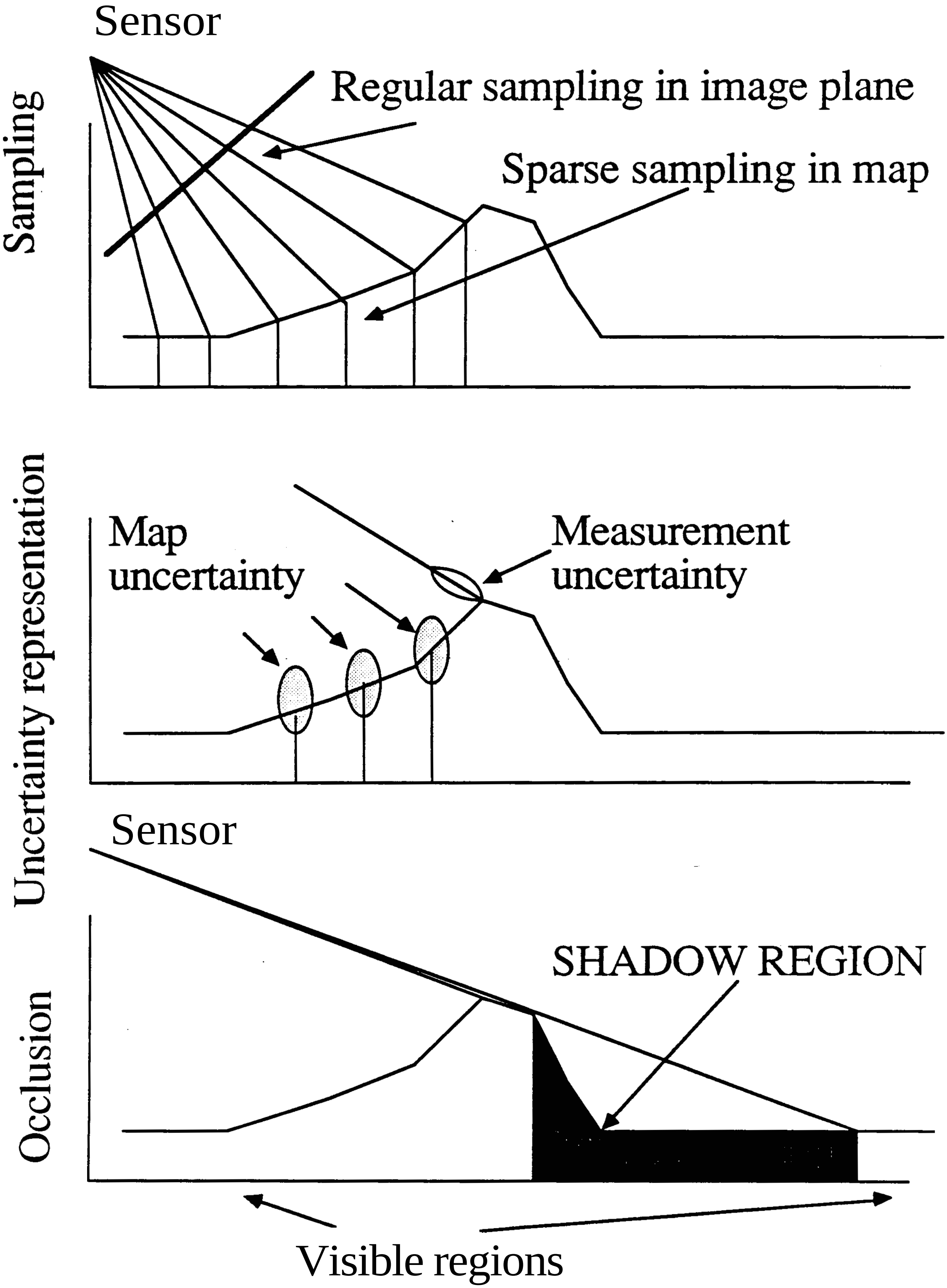
Sensor
Regular sampling in image plane
Sparse sampling in map
Sampling
Uncertainty representation
Map uncertainty
Measurement uncertainty
Sensor
SHADOW REGION
Occlusion
Visible regions

Application: cross-country navigation.

(K. Olin, D. Payton, Hughes AI Center)

Goal: Real-time perception for cross-country autonomous navigation. Local navigation uses an initial map-based plan.

Vehicle: Martin Marietta 8-wheels vehicle.

Sensor: ERIM laser range finder (delivers 64x256 range images, range is from 0 to 64 feet).

Environment: Outdoor rugged cross-country terrain, including bushes, gullies, rocks, and steep slopes.

Perception cycle for cross-country navigation

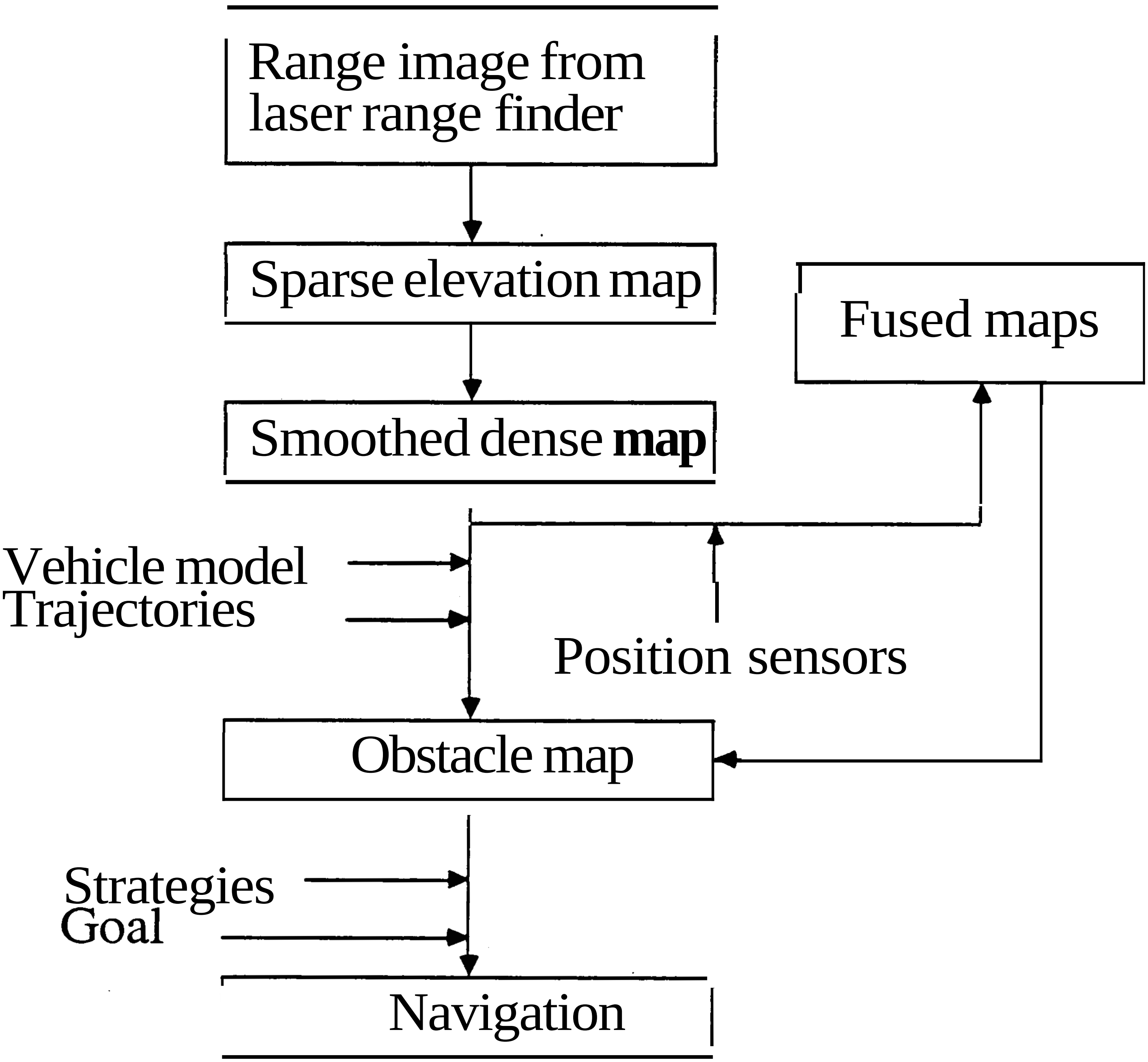

Vehicle model:

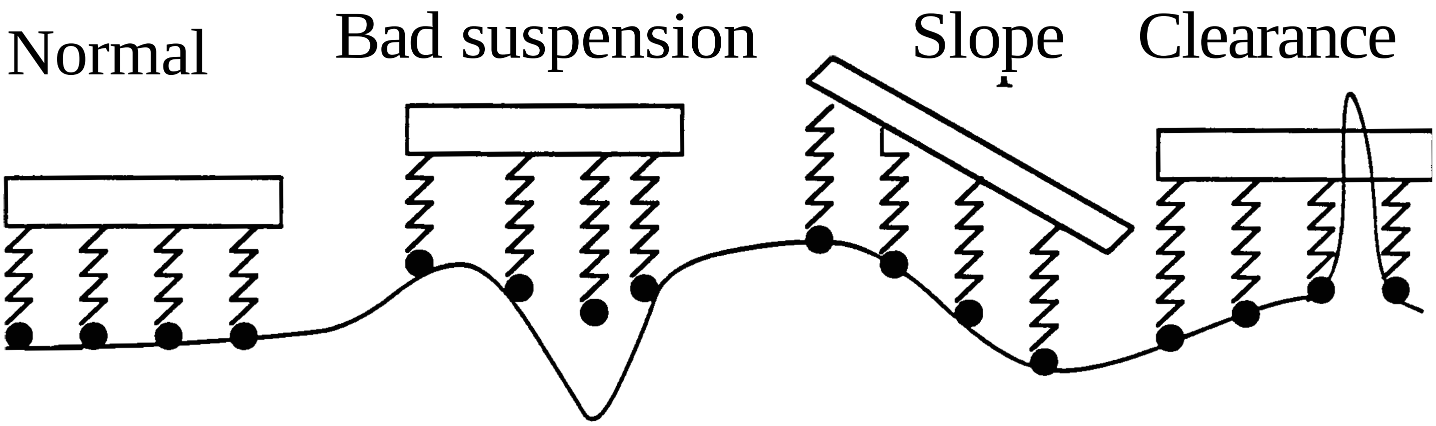

Navigation:

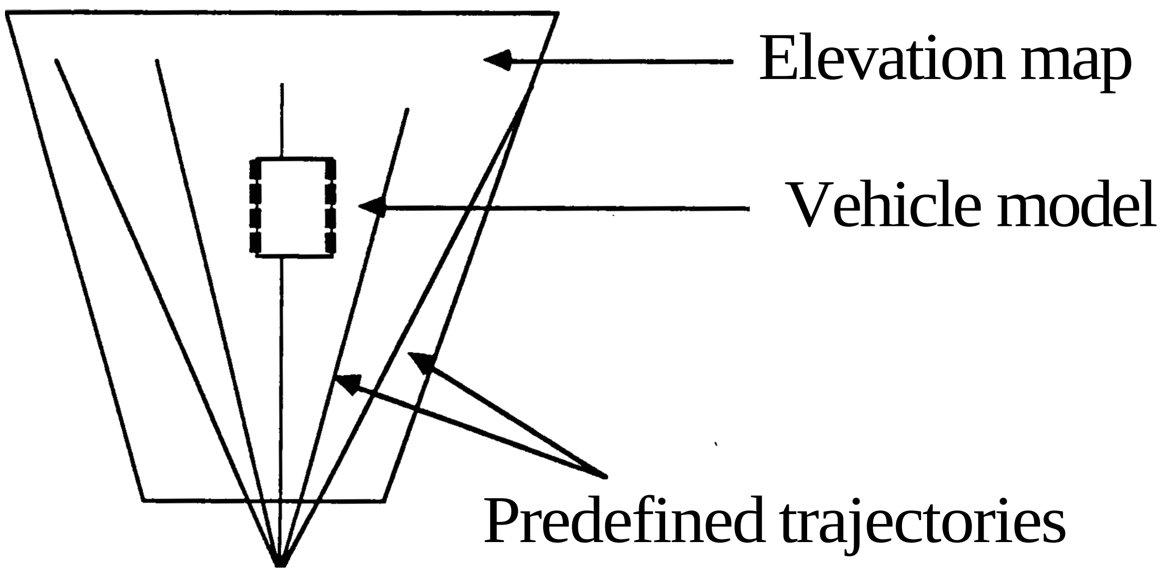

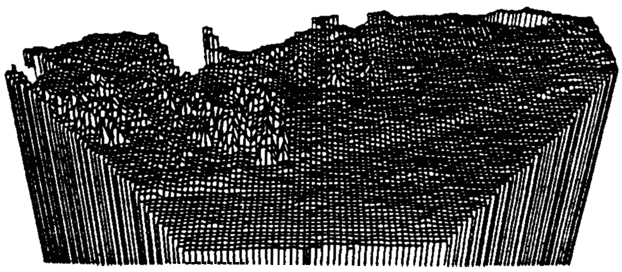

Figure 4. 3D view of CEM.

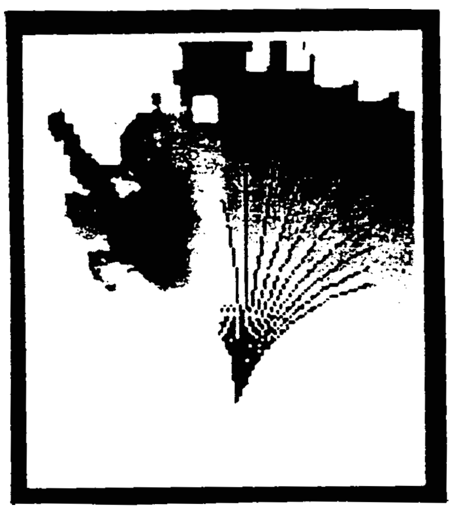

Figure 8. CEM from Figure 3 with curved trajectories.

Occupancy maps:

(Moravec, Elfes (CMU),
Stewart (M I / Woos Hole))

General description:

The world is represented by a set of regularily spaced cells (grid).

Each cell contains a probability P.

P is the probability that the cell is part of an object.

Each sensor rneaurernent is modelled as a distribution of probabilities over the grid.

The probability at a grid cell is computed by combining the contributions from many sensor measurements.

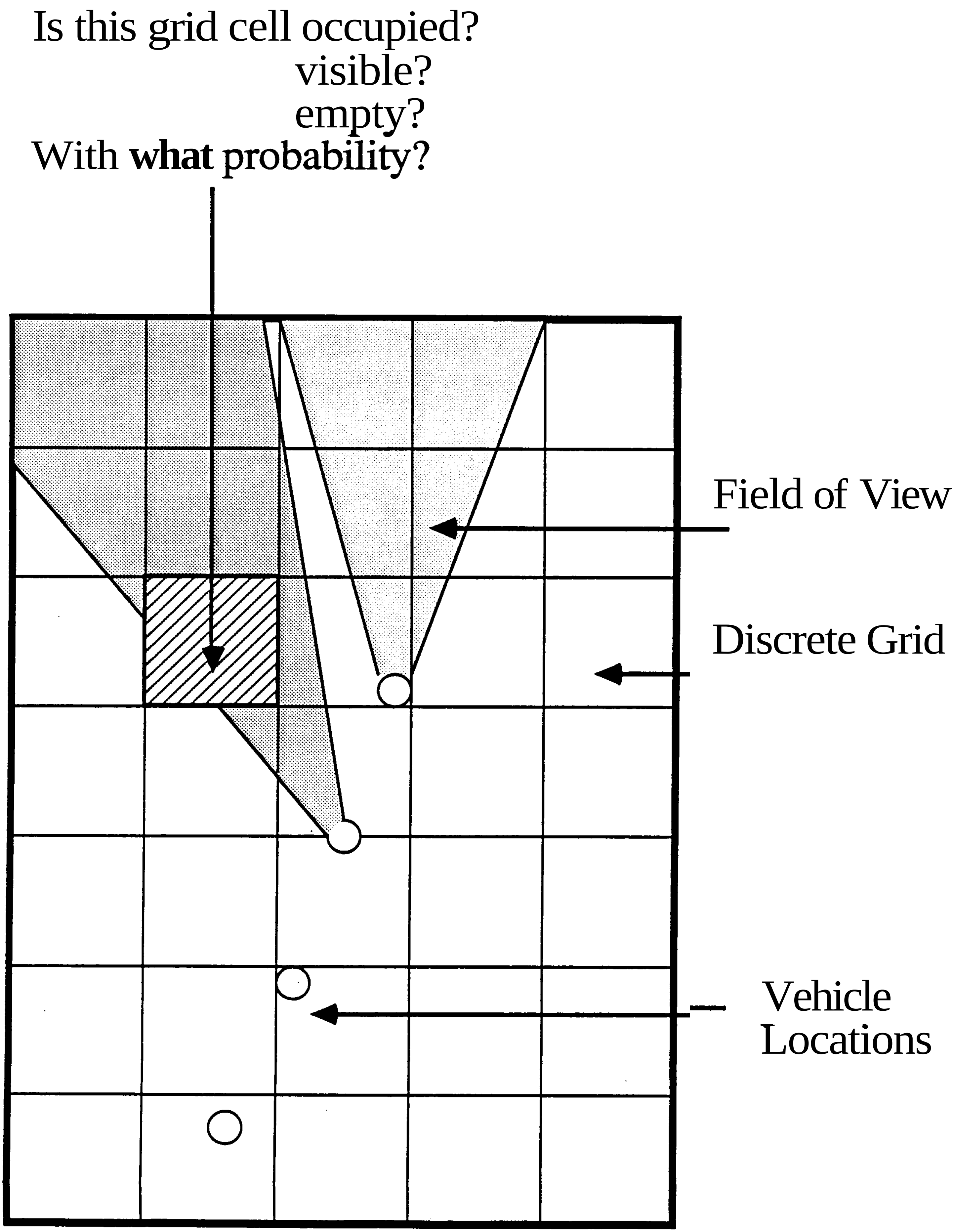
Is this grid cell occupied?
visible?
empty?
With **what** probability?
Field of View
Discrete Grid
Vehicle
Locations

3-D OCCUPANCY GRIDS

6 degrees of freedom:
R, **Tx,** Ty, Tz

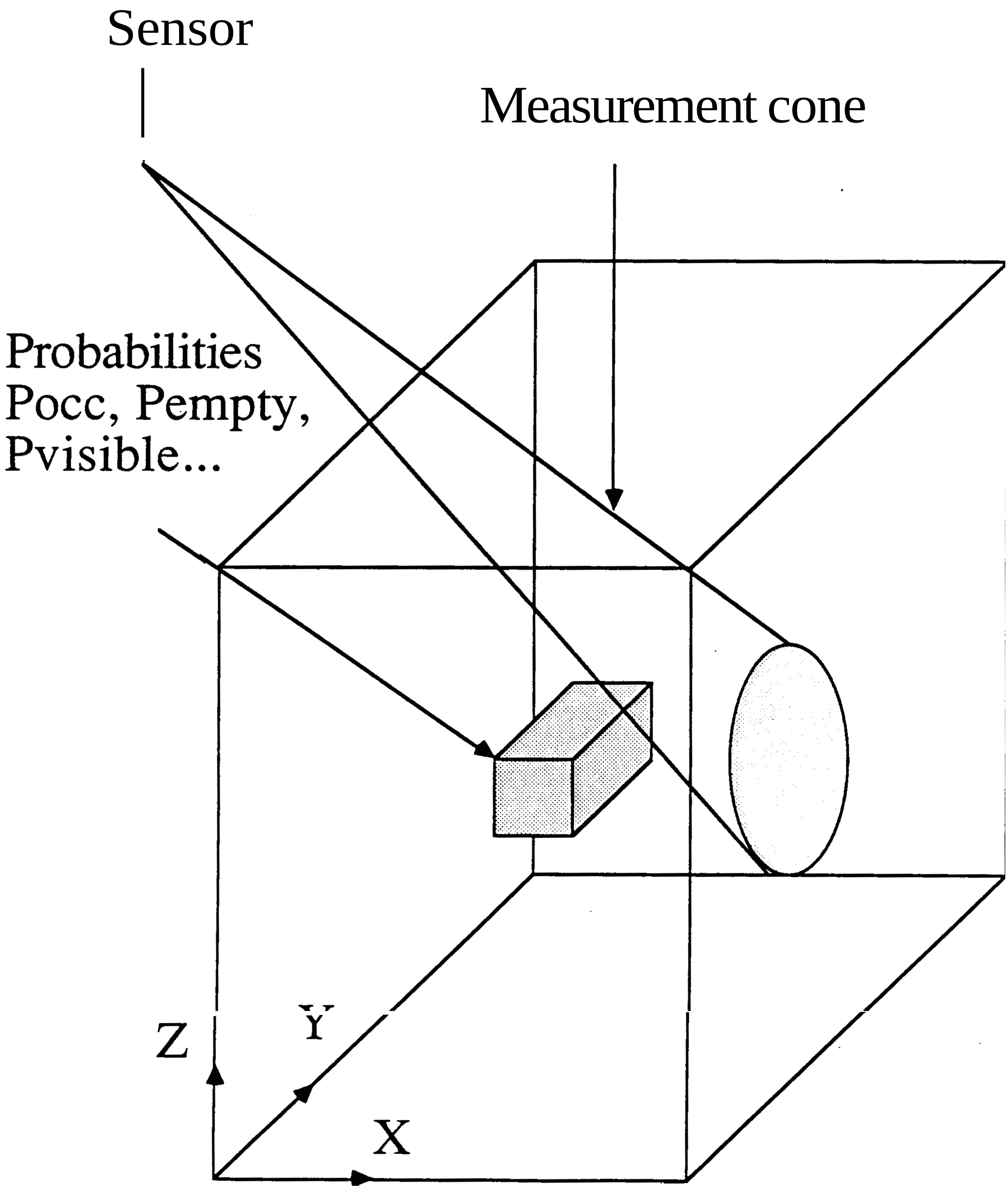

Applications:

Moravec/Elfes/Matthies:

Indoor robot with sonar and stereo cameras.
Occupancy map building from both sensors.
Used in navigation.

Stewart:

Underwater vehicle with sonar. Full 3-D occupancy map built from many images registered by using the vehicle's position sensors.
Extraction of surfaces from the 3-D grid.
Application: detailed bottom surface mapping.

Advantages:

Sensor model taken into account.

Feature extraction is not necessary.

Natural way of fusing multiple sensors.

Computing the probabilities

Problem: Define the probability that a given cell is in state s_i, given evidence (i.e. measurement) e. Bayesian model:

$$P(s_i|e) = \frac{P(e|s_i)P(s_i)}{\Sigma_j P(e|s_j)P(s_j)}$$

Simplest case: two states OCC and EMP, evidence e is a sensor range reading R.

$$P(OCC|R) = \frac{P(R|OCC)P(OCC)}{P(R|OCC)P(OCC) + P(R|EMP)P(EMP}$$

$P(R|OCC)$ and $P(R|EMP)$ are given by the sensor model, $P(OCC)$ and $P(EMP)$ are the current probability values in the map. Initially: $P(OCC) = P(EMP) = 0.5$ (no information).

Computing the probabilities

The simplifying assumption: $P(R|EMP) = 1 - P(R|OCC)$ provides intuitive properties:

$$P(OCC|R) = \frac{P(R|OCC)P(OCC)}{P(R|OCC)P(OCC) + (1 - P(R|OCC))(1 - P(OCC))}$$

- Updating independent of the ordering of measurements.
- $P(OCC) = 0.5$ (unknown) is **a** no-op.
- Conflicting measurements cancel.

Probabilistic sonar map (from Elfes && Matthies)

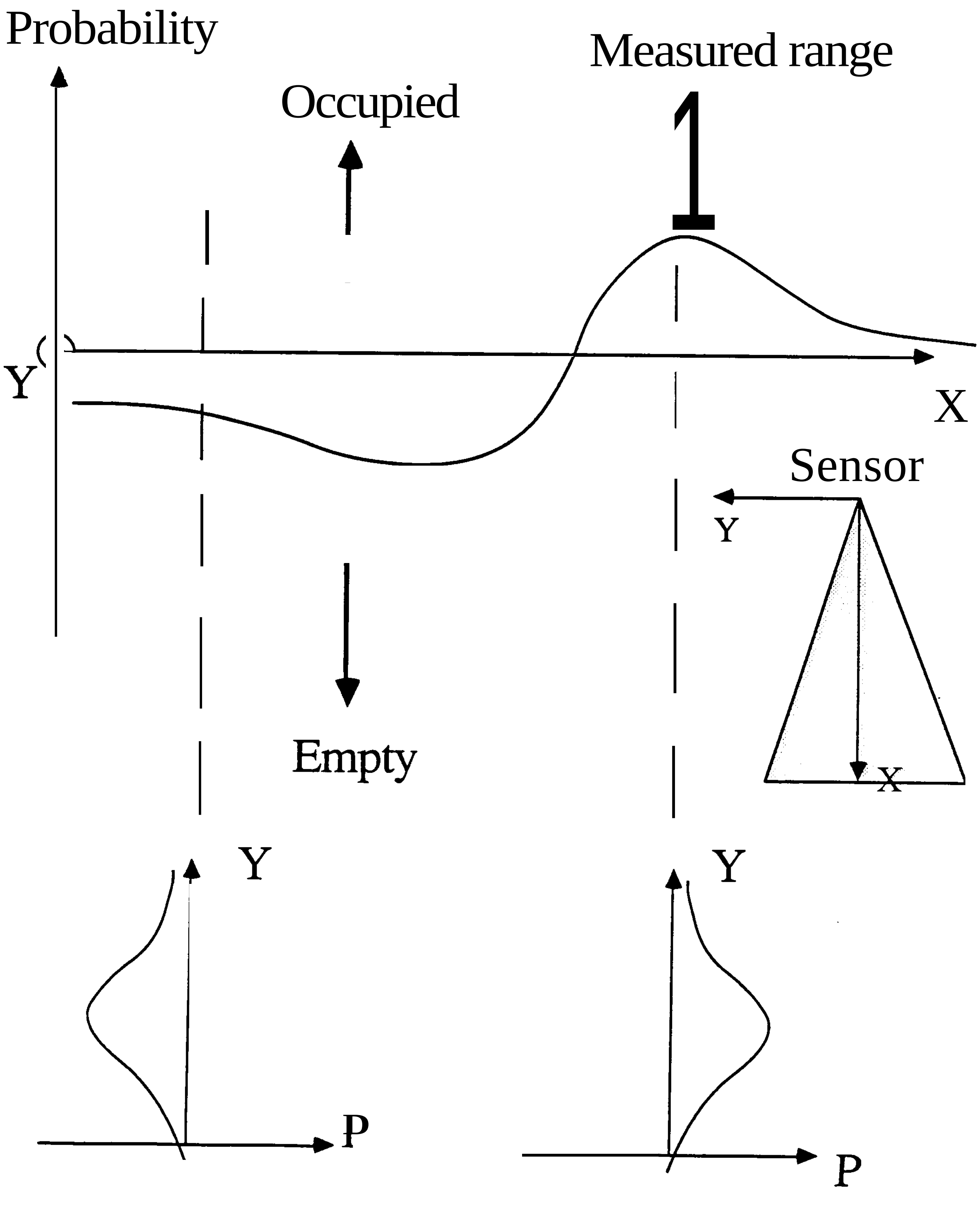

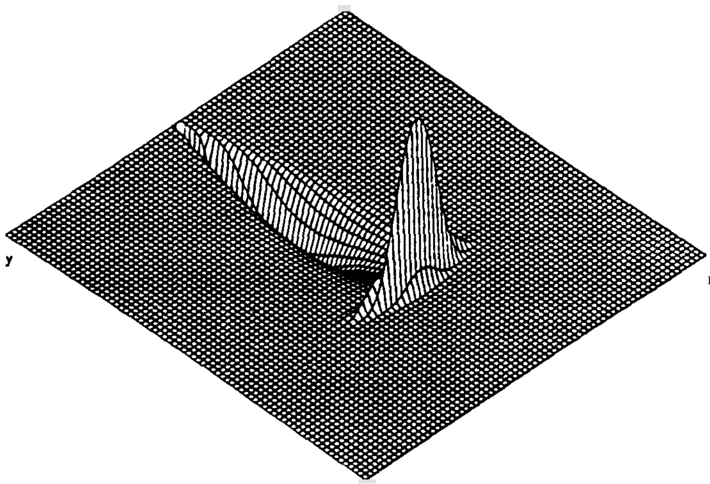

Figure 3: Probabilistic Sonar Sensor Interpretation Model. The probability profile shown corresponds to a reading taken by a sensor positioned at the upper left, pointing to the lower right. The plane shows the UNKNOWN level. Values above the plane represent OCCUPIED probabilities, and values below represent EMPTY probabilities.

Uncertainty from stereo

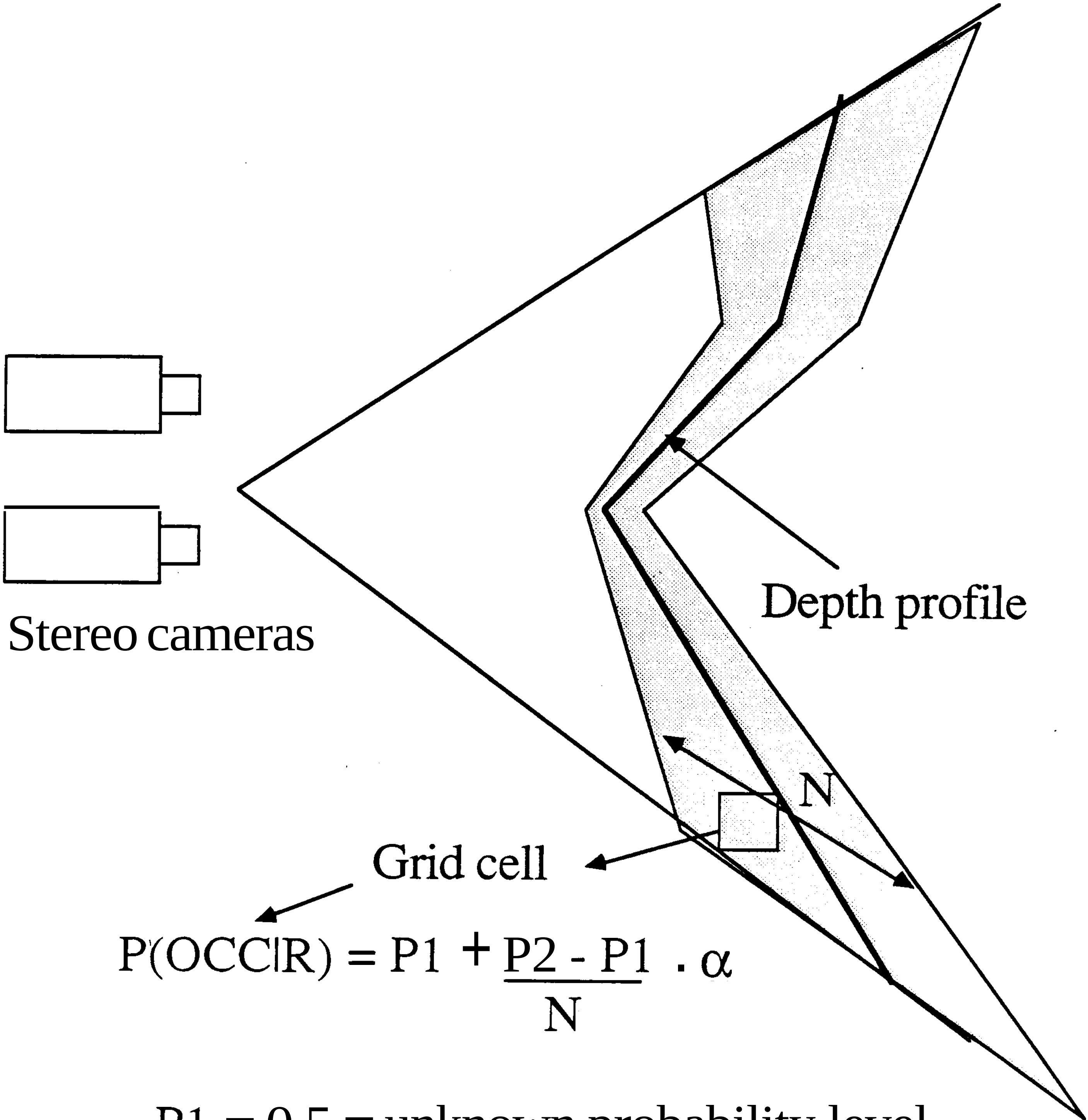

$$P(OCC|R) = P1 + \frac{P2 - P1}{N} \cdot \alpha$$

P1 = 0.5 = unknown probability level
P2 = maximum allowed P(OCC)
α = 1.0 at edge points, < 1.0 elsewhere

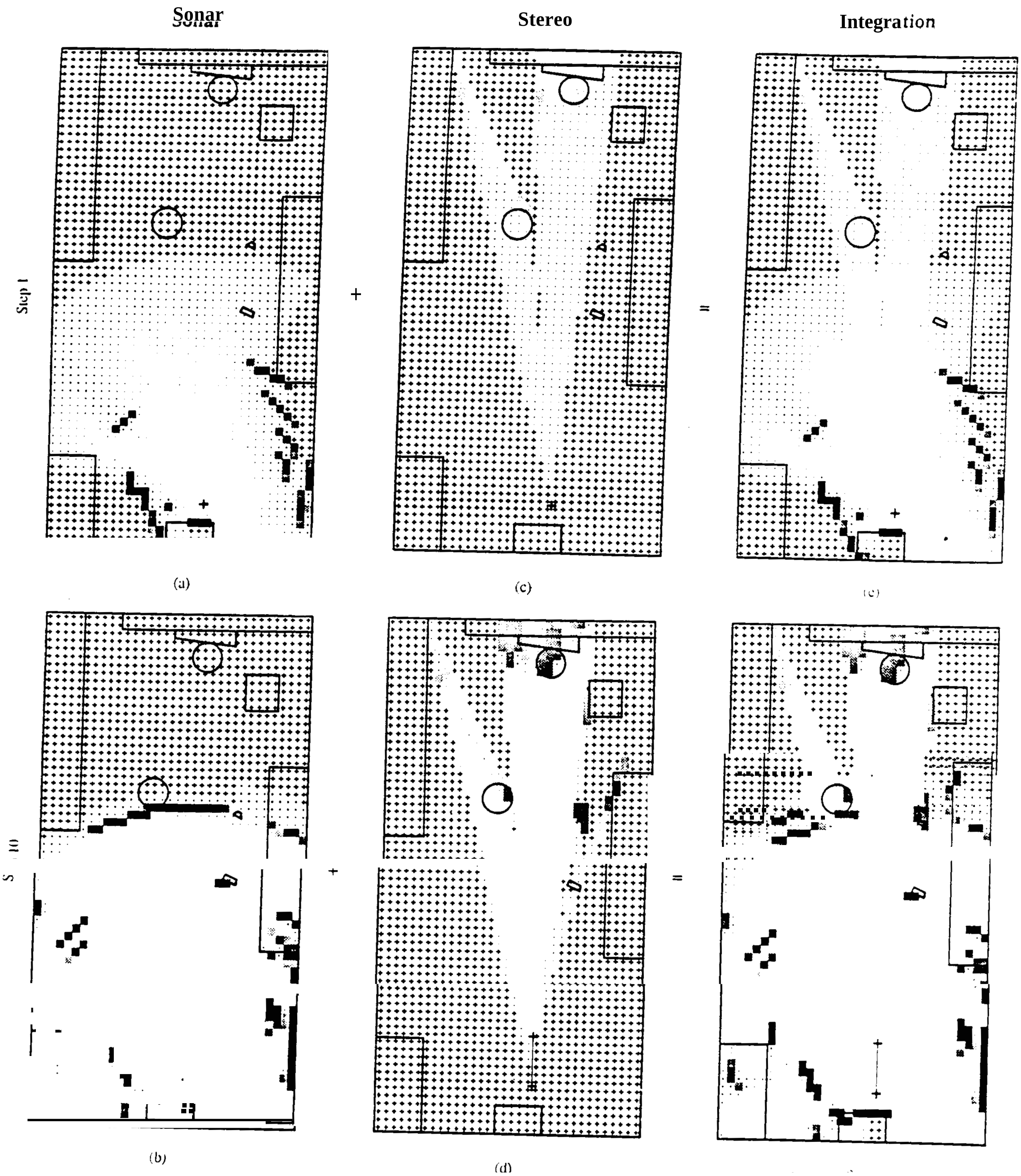

Figure 6: Occupancy Maps Generated by *Sonar*, Stereo and Sensor Integration. OCCUPIED regions are marked by shaded squares, EMPTY by dots fading to white space, and UNKNOWN by + signs.

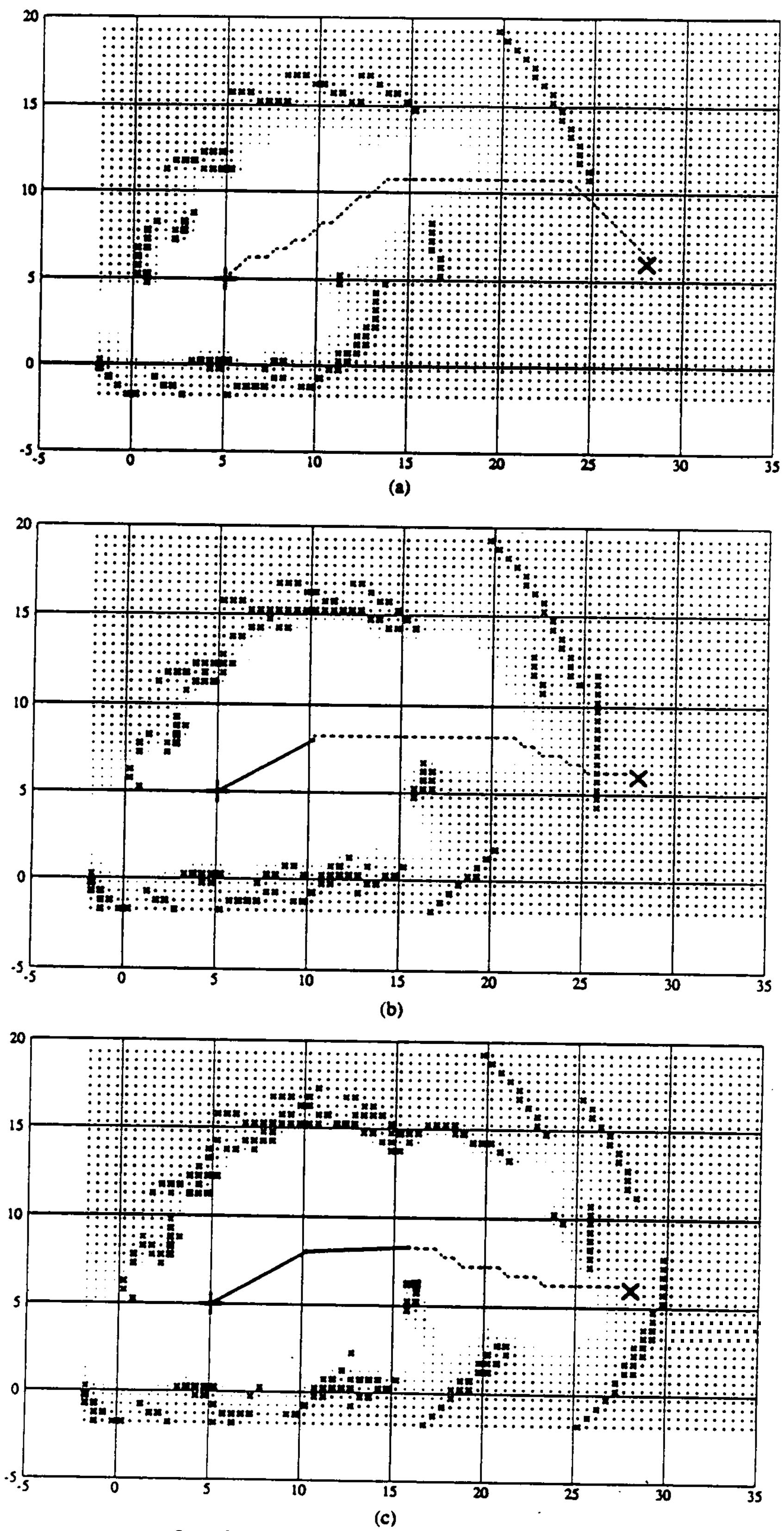

Fig. 13. Example run. This run was performed indoors, in Mobile Robot Lab. Distances are in ft. Grid size is 0.5 ft. Planned path is shown as dotted line. and route actually followed by robot as solid line segments. Starting point is solid + and goal, solid x .

Detailed description of an autonomous vehicle: the NAVLAB

Self-contained vehicle for:

- Road following with or without map.
- Object detection.
- Map building.

using:

- One color camera.
- One laser range finder.
- On-board computing (Suns).
- Controller.

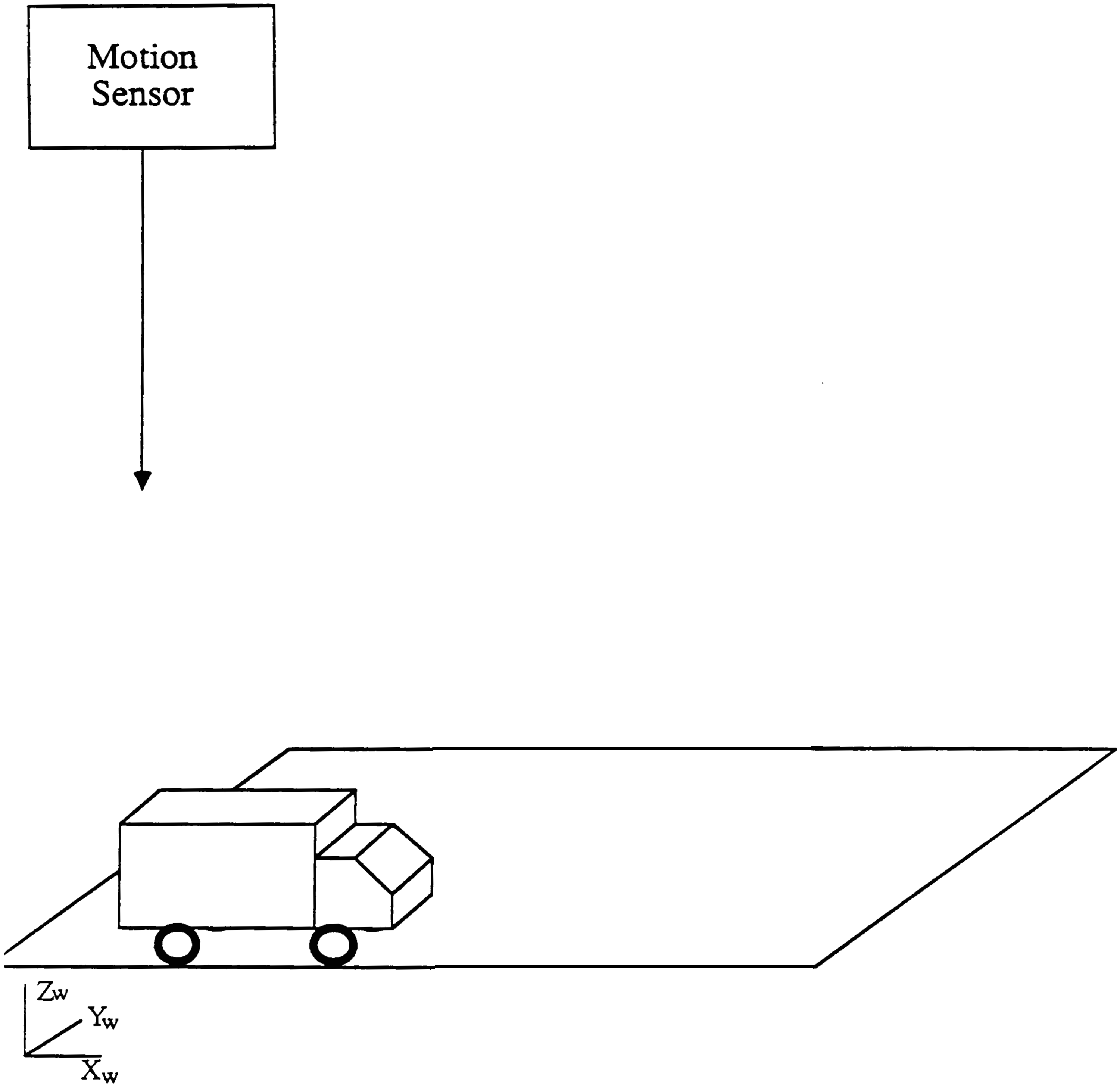
Motion Sensor
Zw
Yw
Xw

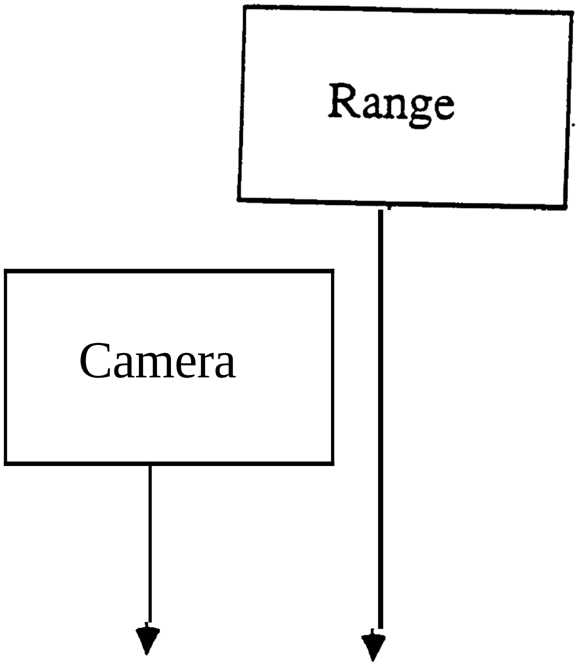
Range
Camera

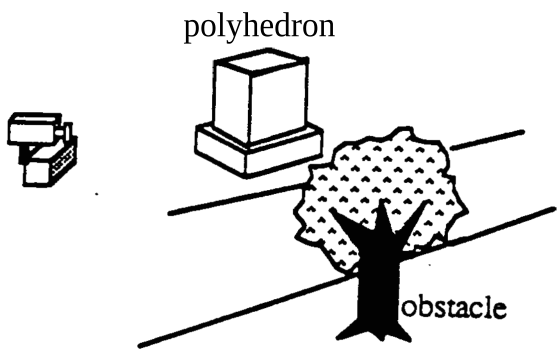
polyhedron
obstacle

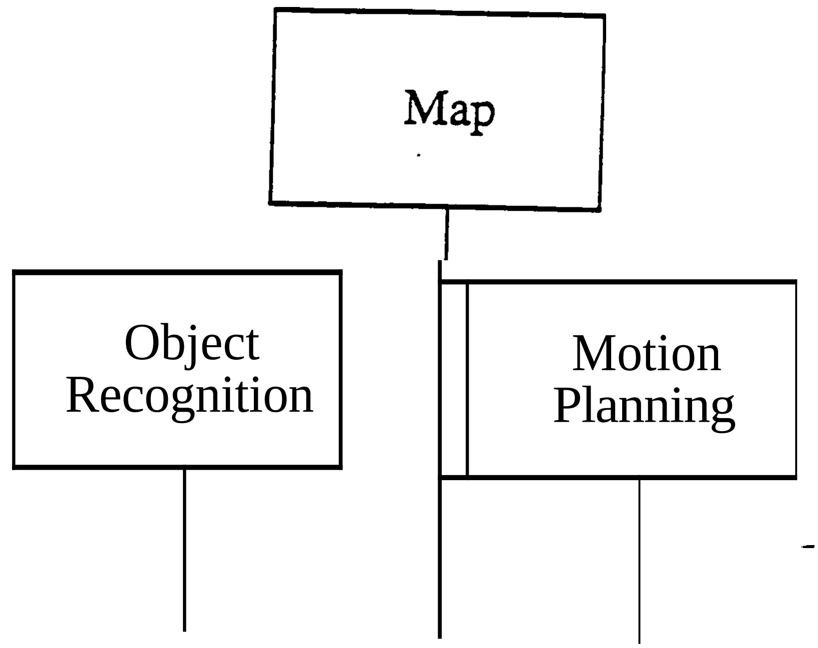
Map
Object Recognition
Motion Planning

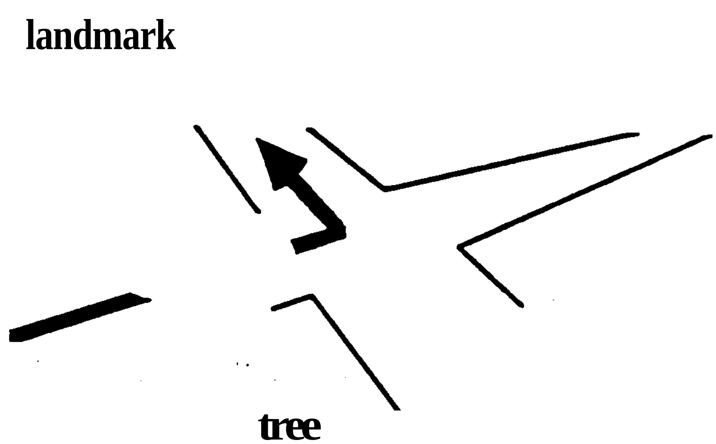
landmark
tree

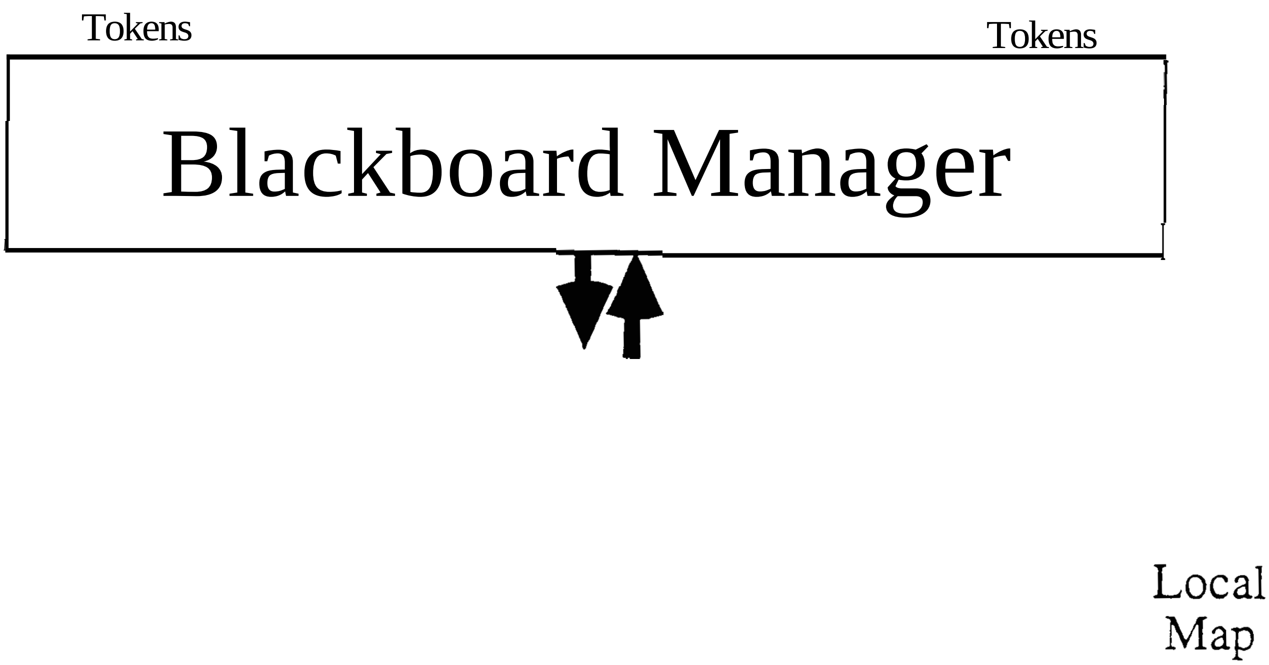

- Moving Coordinates
- Time
- Distributed Processing

Environment

- Paved curved roads.
- Non-uniform road appearance.
- Changing conditions (illumination, weather…etc).
- Discrete obstacles.
- Strong shadows from obstacles.

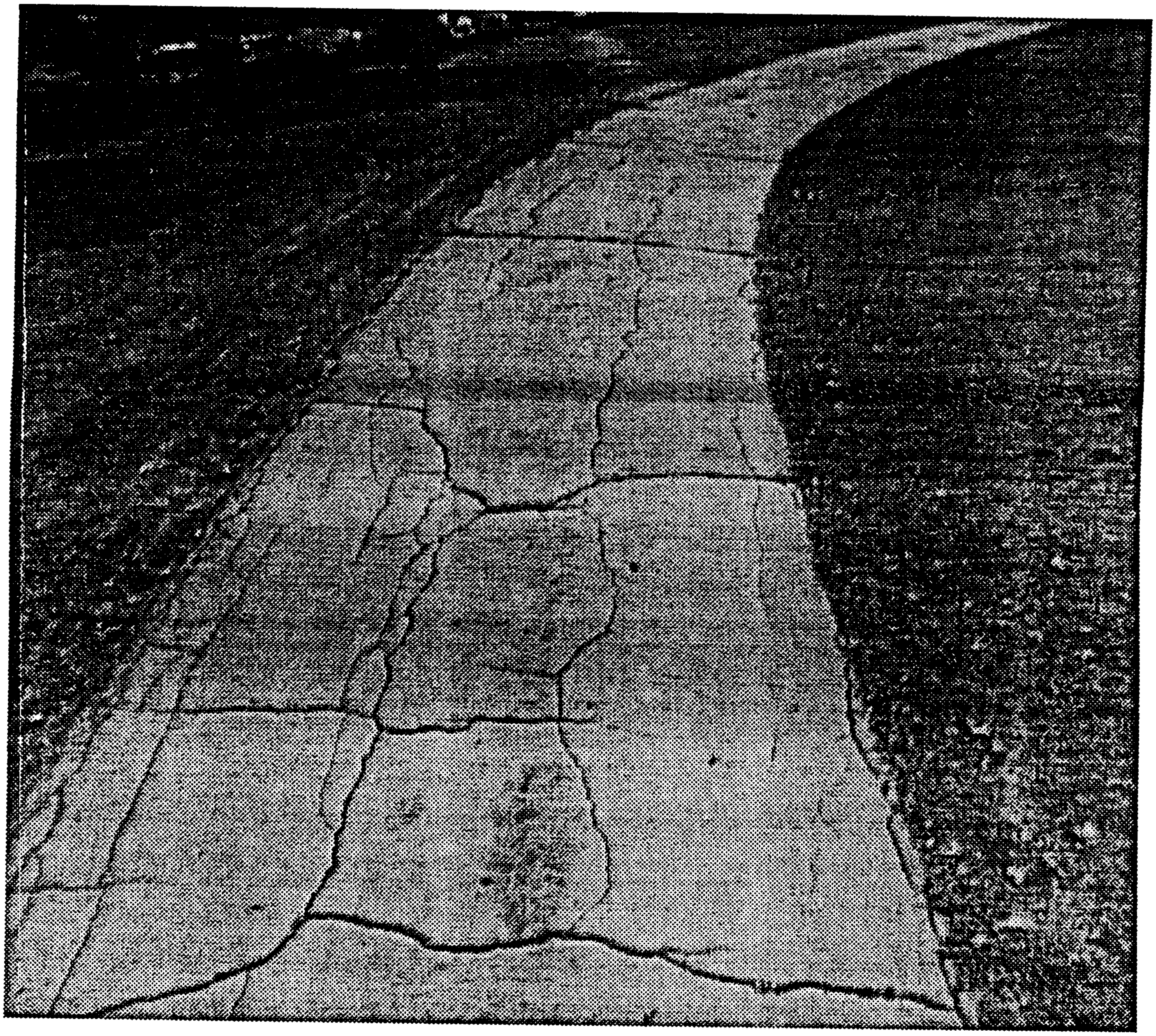

Components of the road following algorithm

- Color classification: The color of the road is significantly different than the background.
- Texture computation: The sides of the road are usually more textured.
- Road location in image: The geometry of the road must be determined.
- Calibration: The road detected in image space must be converted to the vehicle's co-ordinate system in order to steer the vehicle.

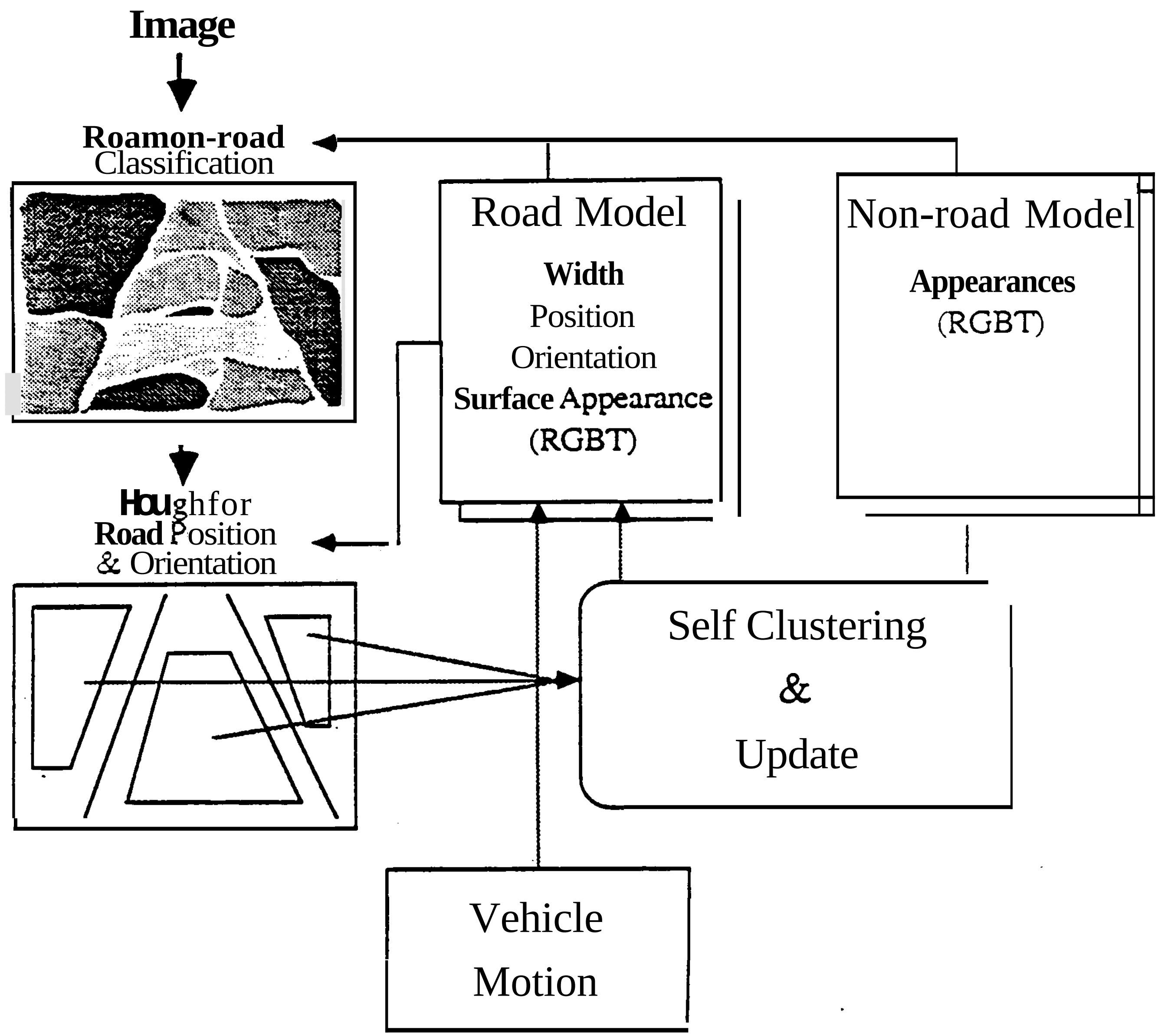
Image
Roamon-road
Classification
Road Model
Width
Position
Orientation
Surface Appearance
(RGBT)
Non-road Model
Appearances
(RGBT)
Houghfor
Road Position
& Orientation
Self Clustering
&
Update
Vehicle
Motion

Color classification

The color is divided into n classes. Each pixel is classified into one of the classes using the distance:

$$(X - m_i)^t \Sigma_i^{-1} (X - m_i)$$

Where:

- X is the (red,green,blue) vector at the current pixel.
- m_i is the mean (red,green,blue) value of class i
- Σ_i is the covariance matrix of class i

The set of classes is divided into road classes and non-road classes.

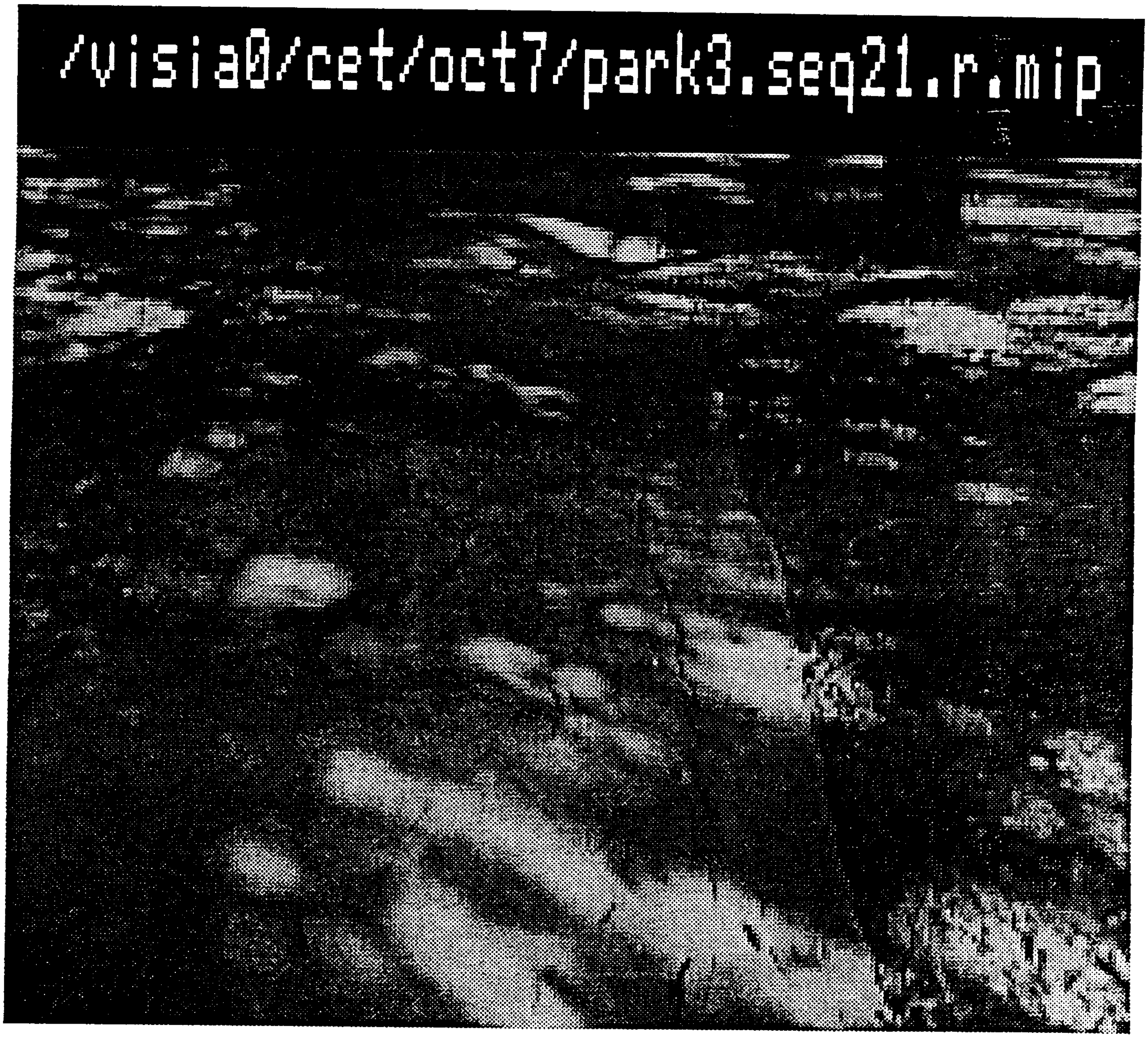
/visia0/cet/oct7/park3.seq21.r.mip

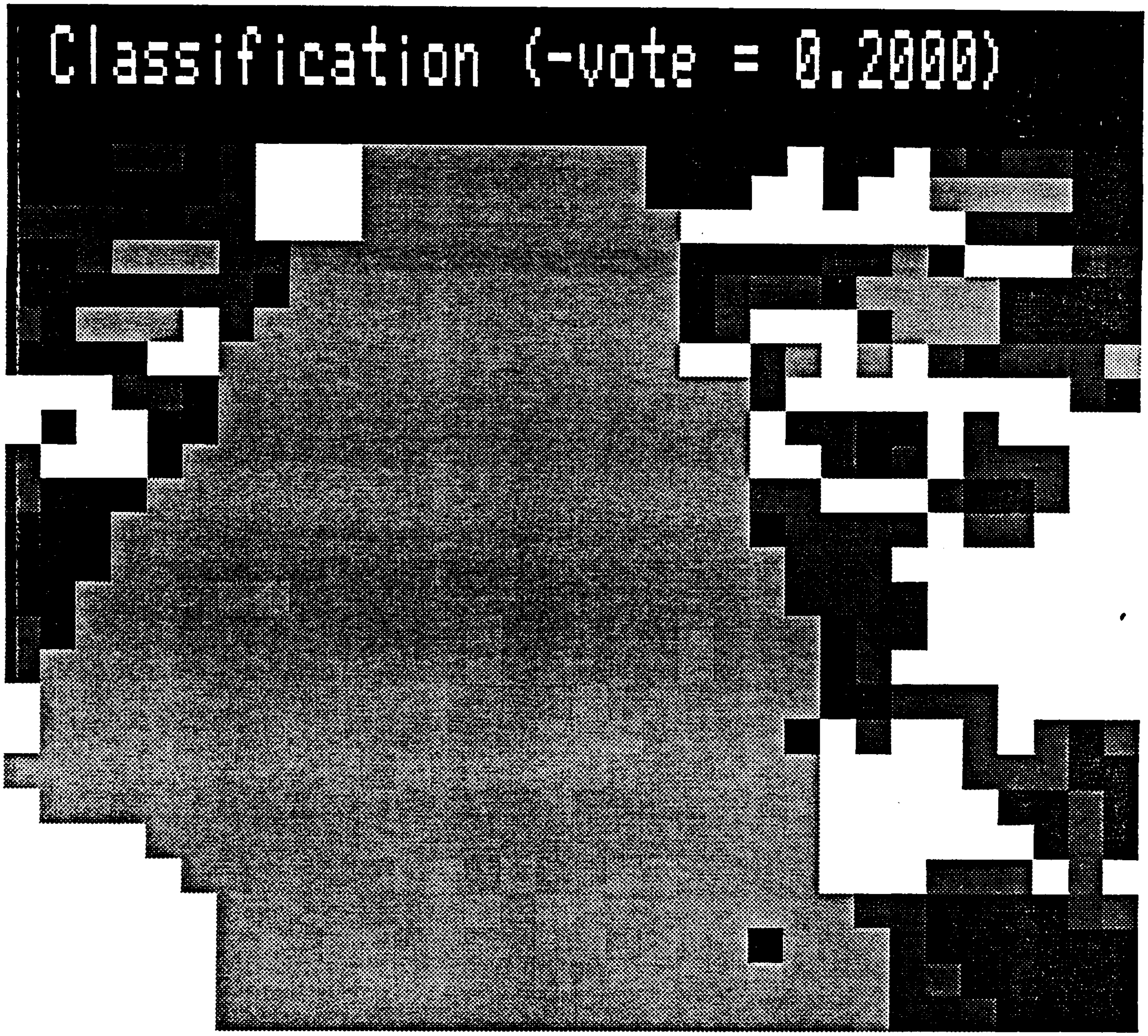
Classification (-vote = 0.2000)

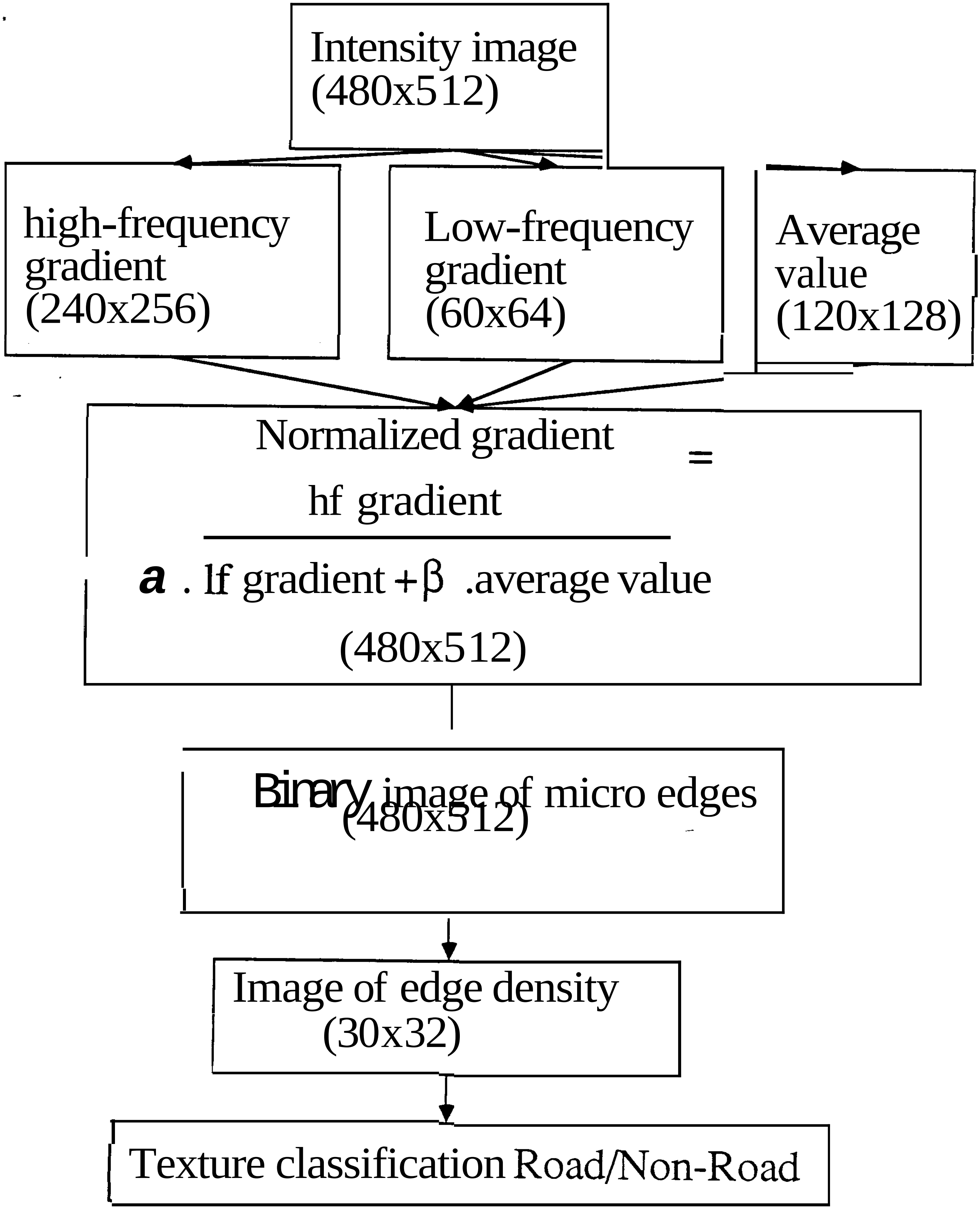
Intensity image (480x512)
high-frequency gradient (240x256)
Low-frequency gradient (60x64)
Average value (120x128)
Normalized gradient =
hf gradient
a . lf gradient + β .average value
(480x512)
Binary image of micro edges (480x512)
Image of edge density (30x32)
Texture classification Road/Non-Road

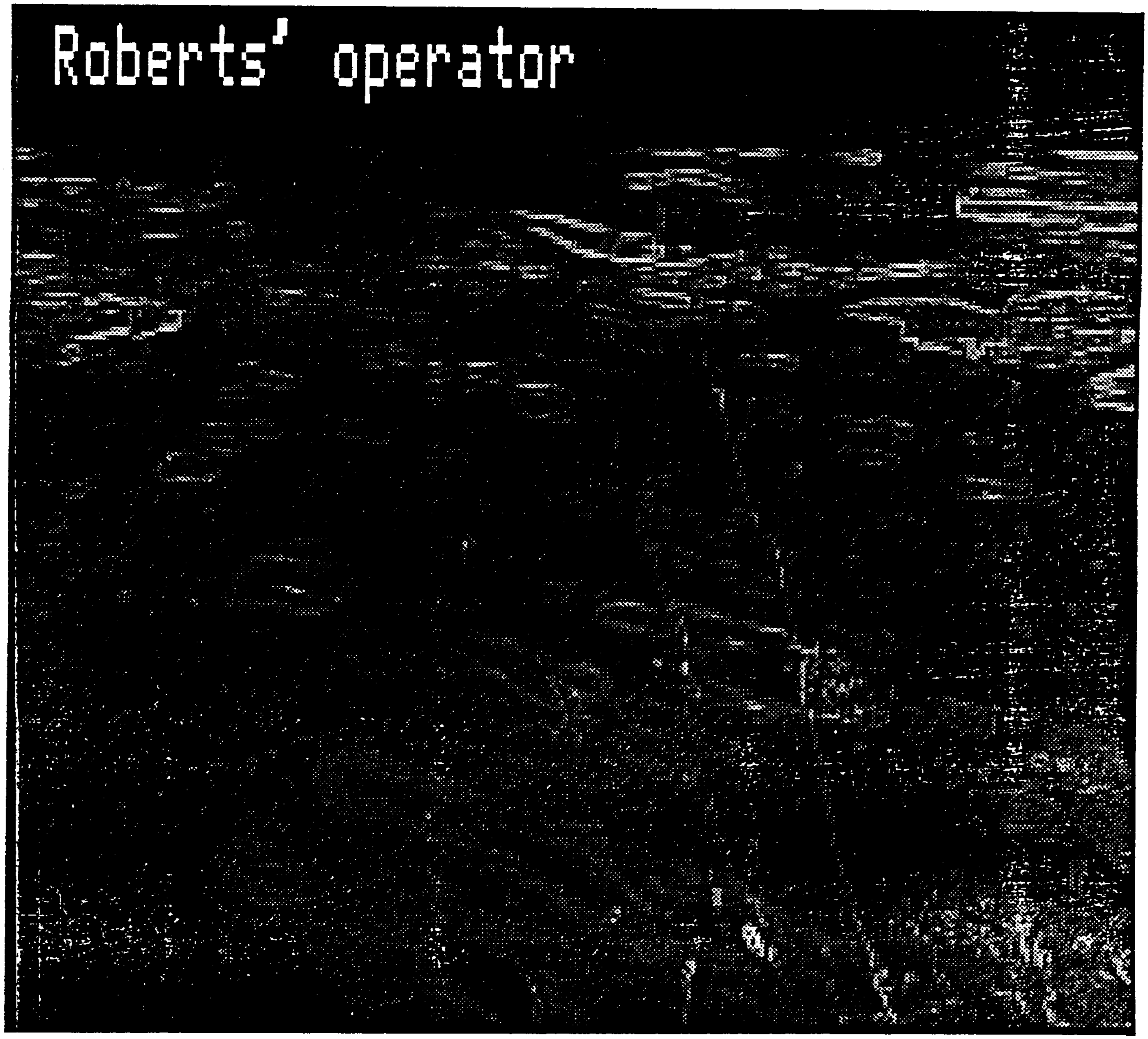
Roberts' operator

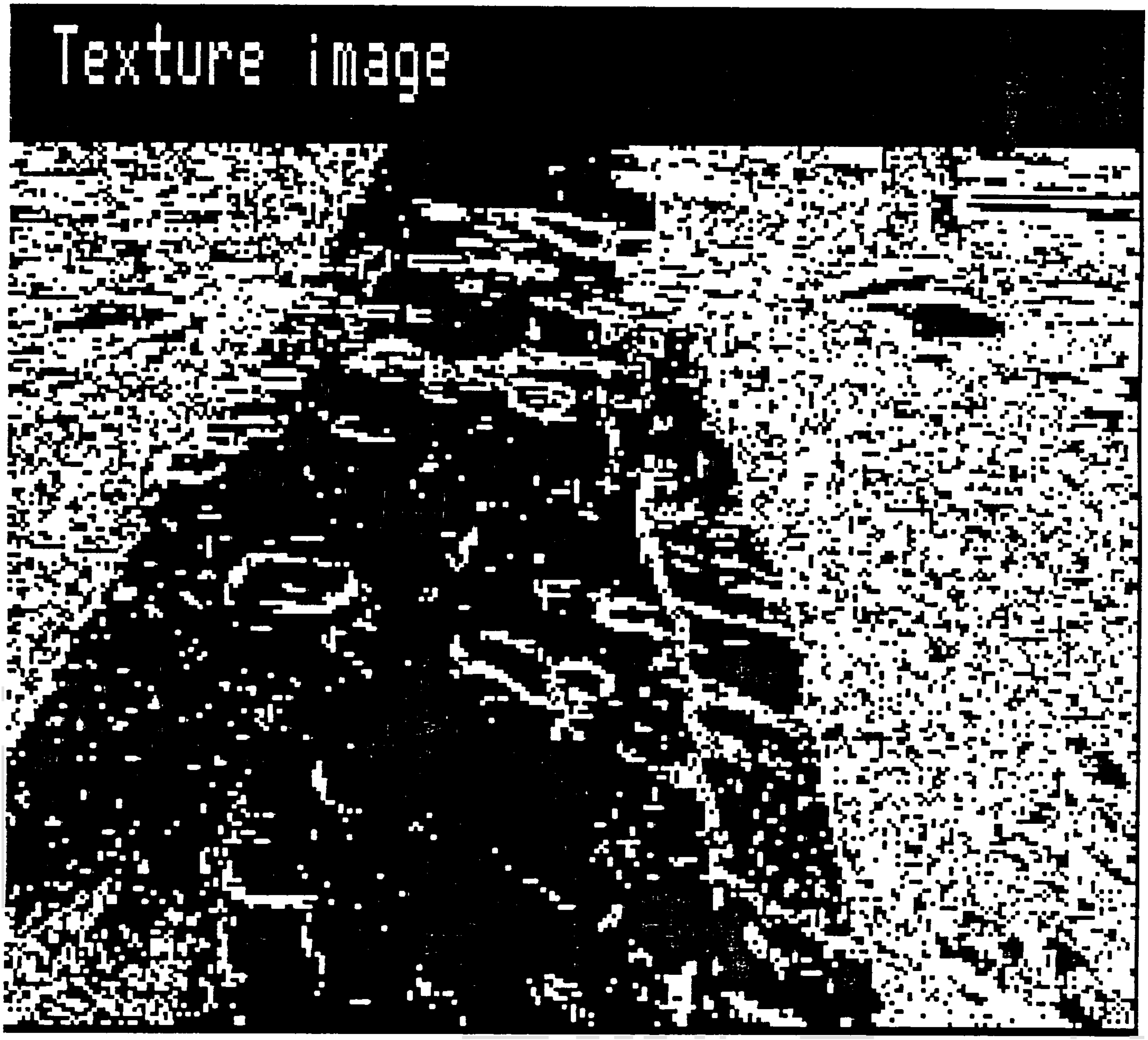
Texture image

Combining texture and color

For each class and each pixel:

$$P_i = (1-\alpha)P_i^T + \alpha P_i^C$$

Where

- P_i = confidence that the pixel belongs to class i
- P_i^T = confidence that the pixel belongs to class i based on texture
- P_i^C = confidence that the pixel belongs to class i based on color

Final confidence for each pixel:

$$C = \max(P_i, i \in Road) - \max(P_i, i \in NonRoad)$$

$C > 0 \iff$ the pixel is classified as road.

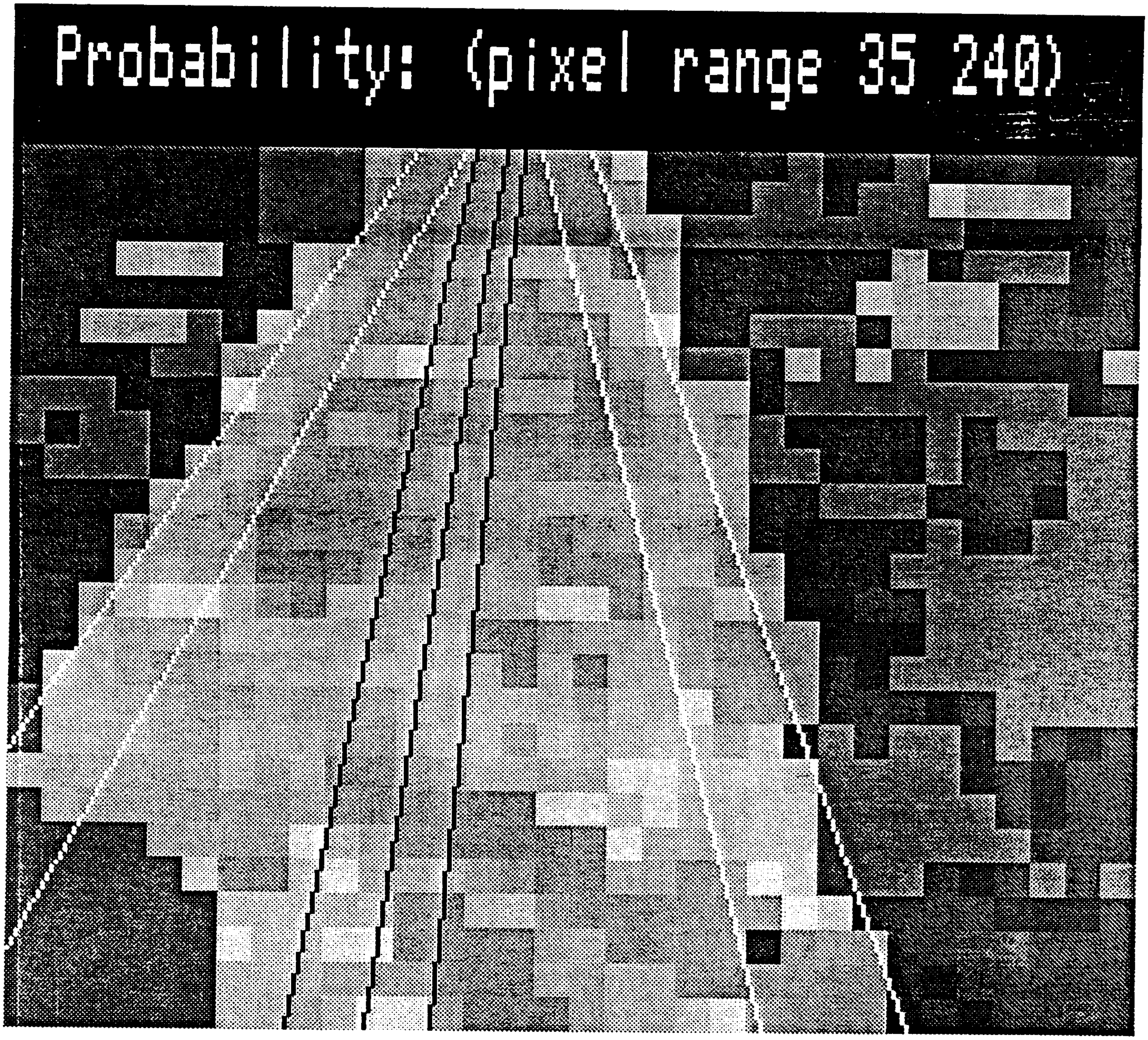
Probability: (pixel range 35 240)

Road representation

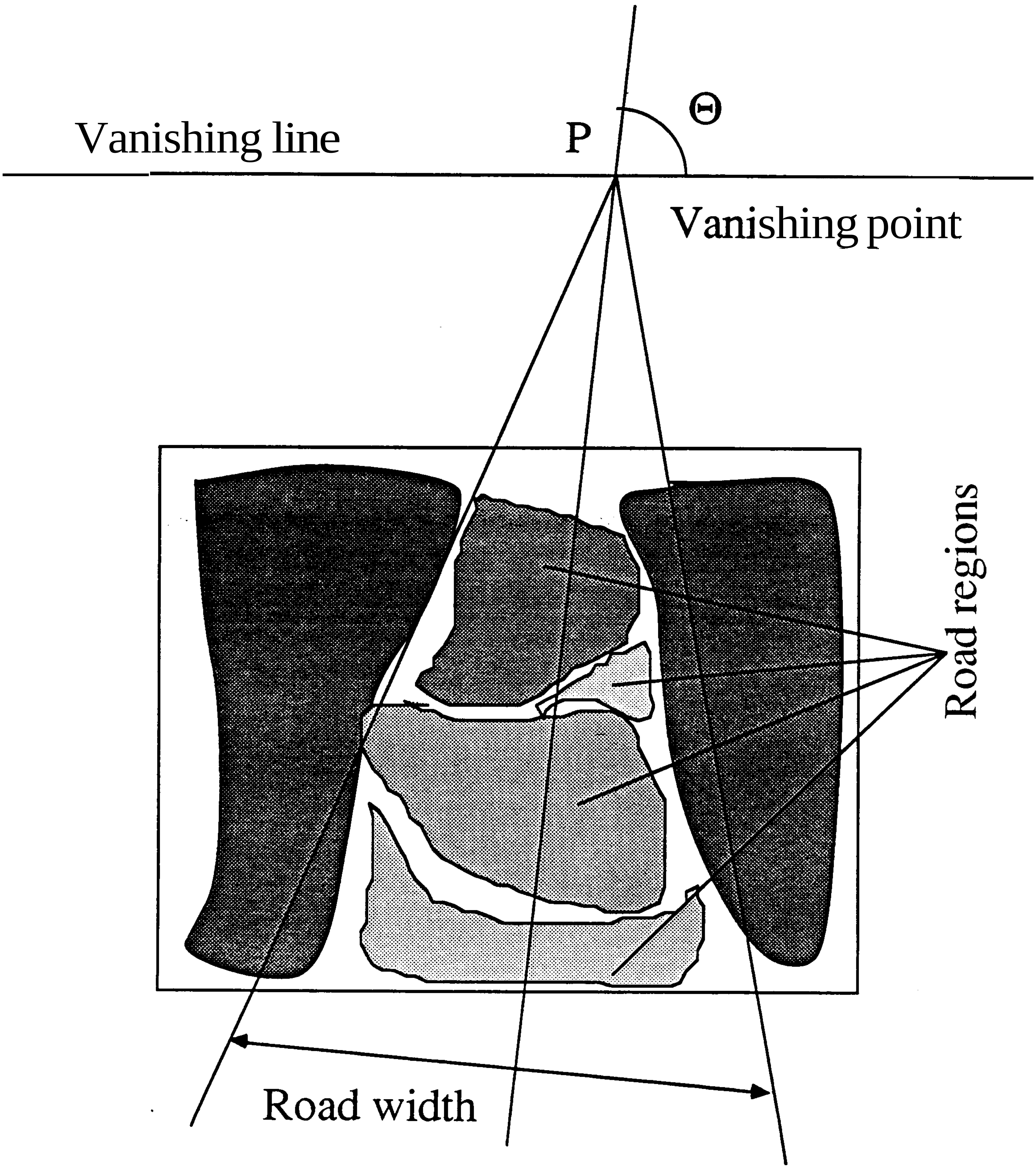

Hough transform

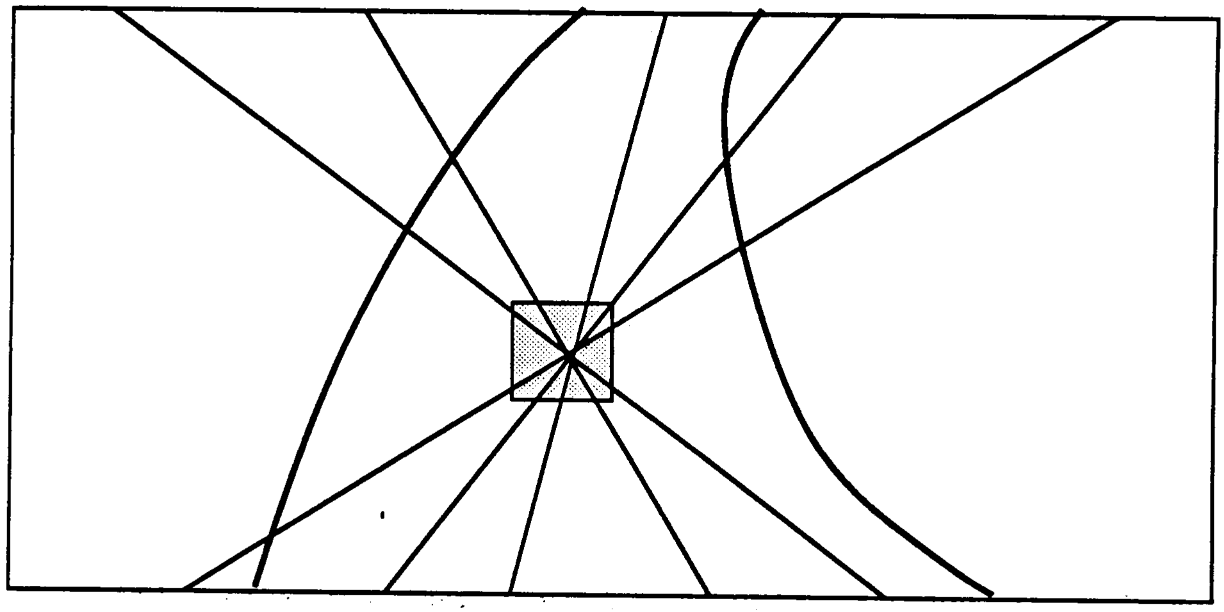

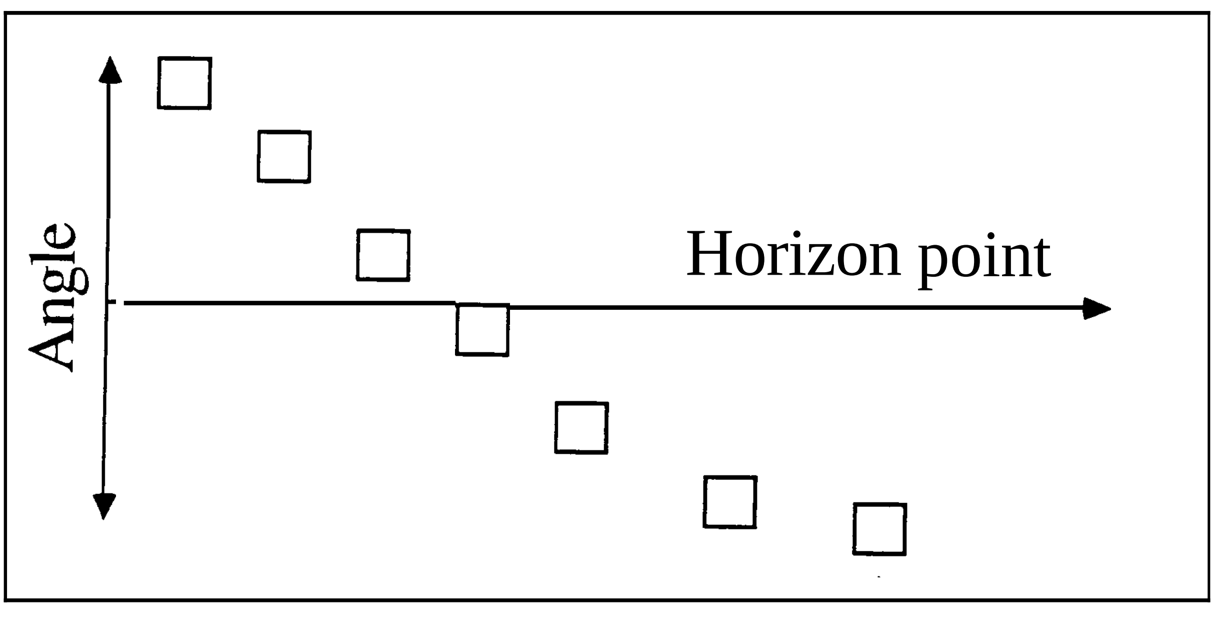

Voting algorithm

Quantized 2-D parameter space (P, θ) (32 levels for P, 20 levels for Θ)

An image point *(row,col)* can be votes for the set of road location:

$$(P, \theta) = (col + (row - r_{horizon}) \times \tan\theta, \theta)$$

Each pixel casts votes proportional to the road/non-road classification confidence.

The maximum in (P, θ) space is the reported road location.

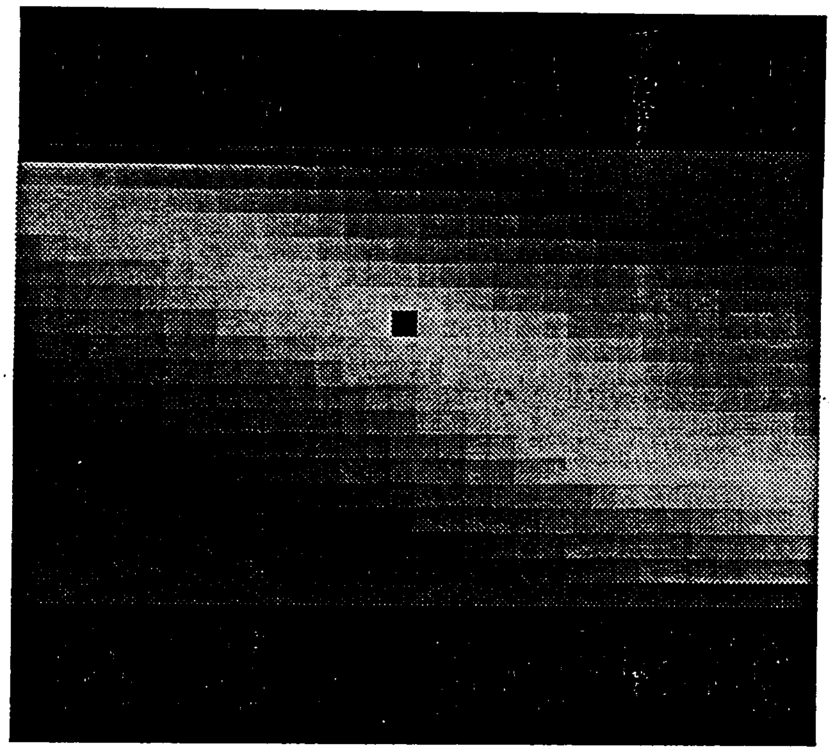

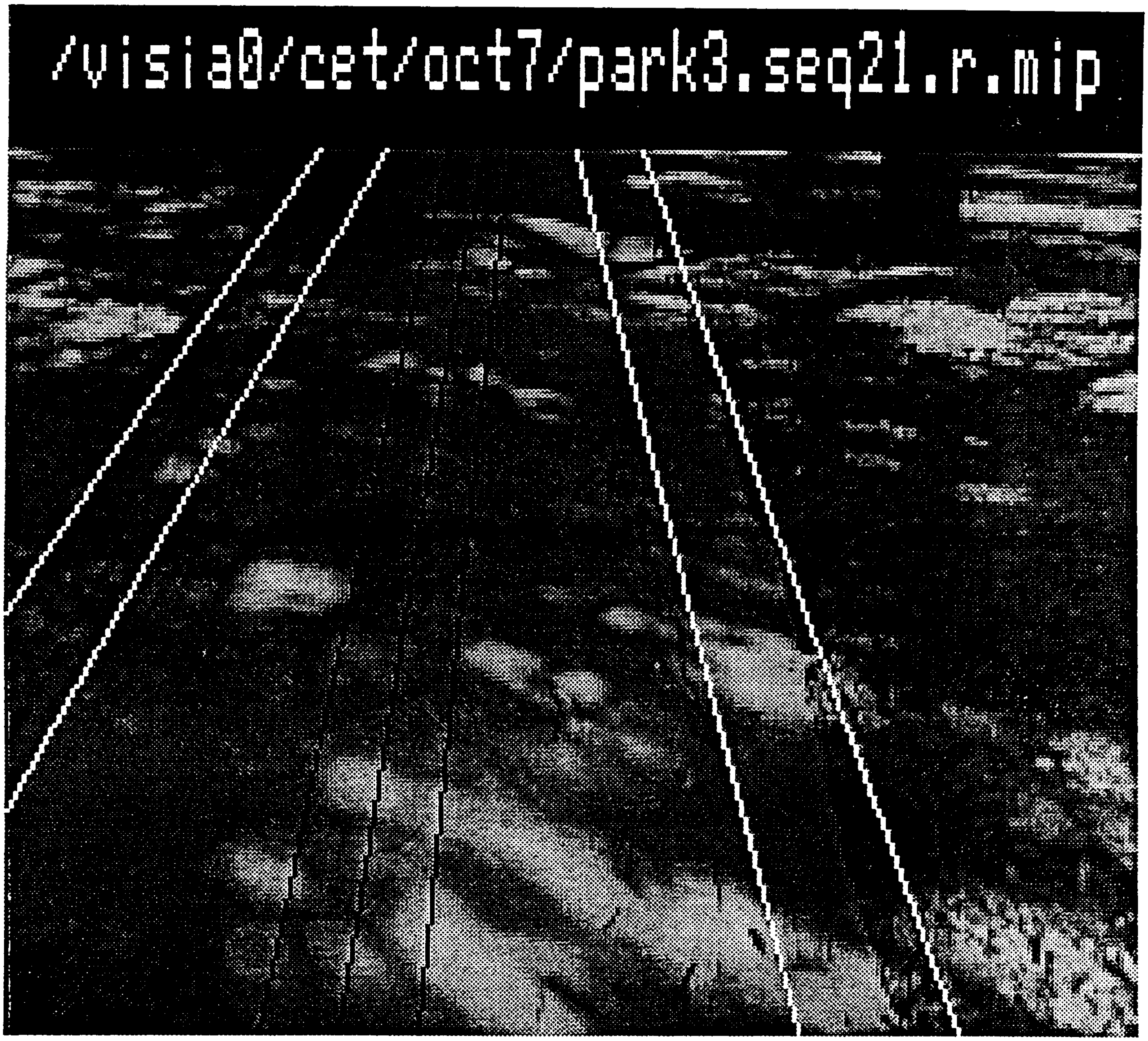
/visia0/cet/oct7/park3.seq21.r.mip

Processing cycle

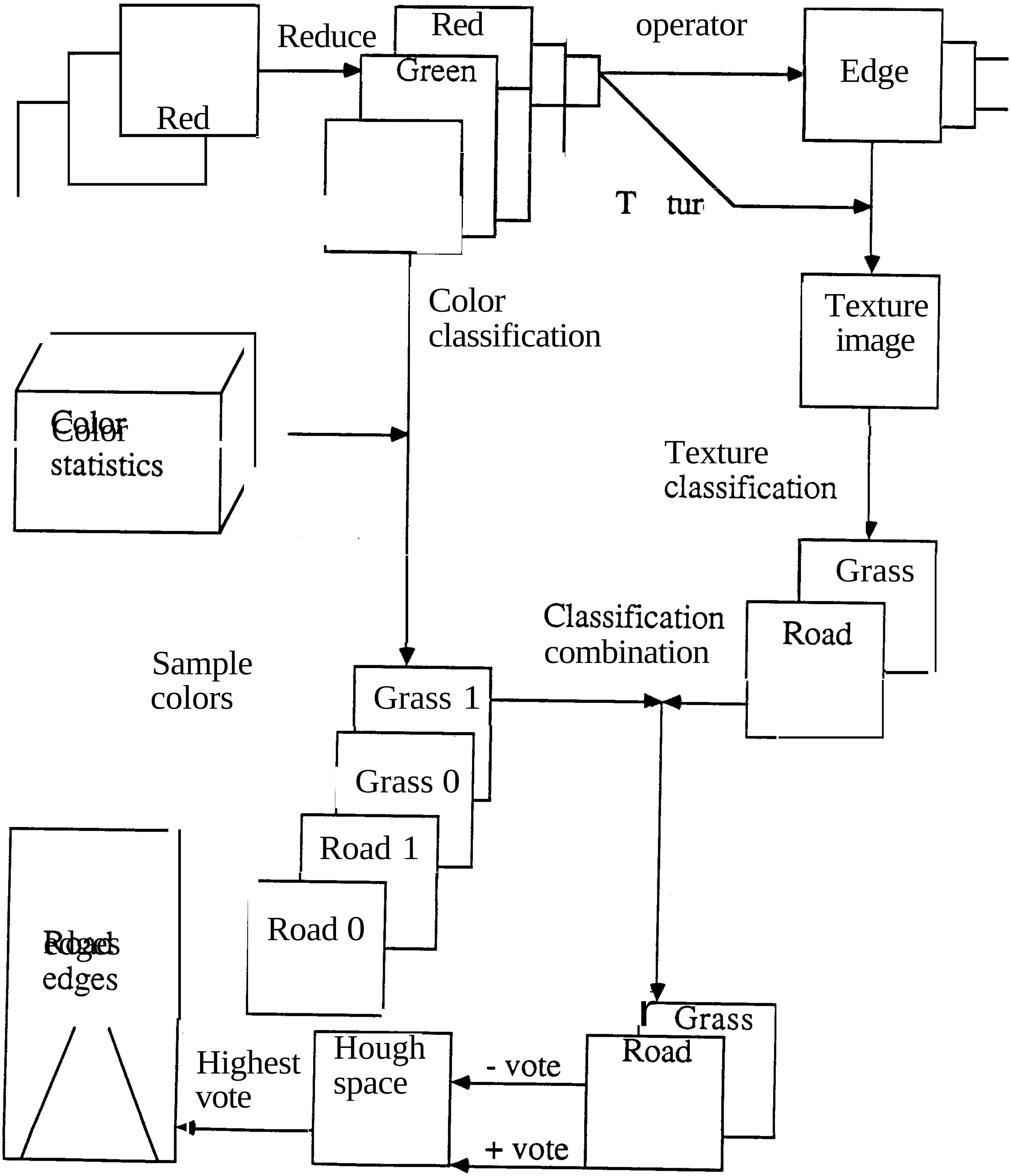

Simple calibration procedure

Measure the distance between rows ri and the vehicle.

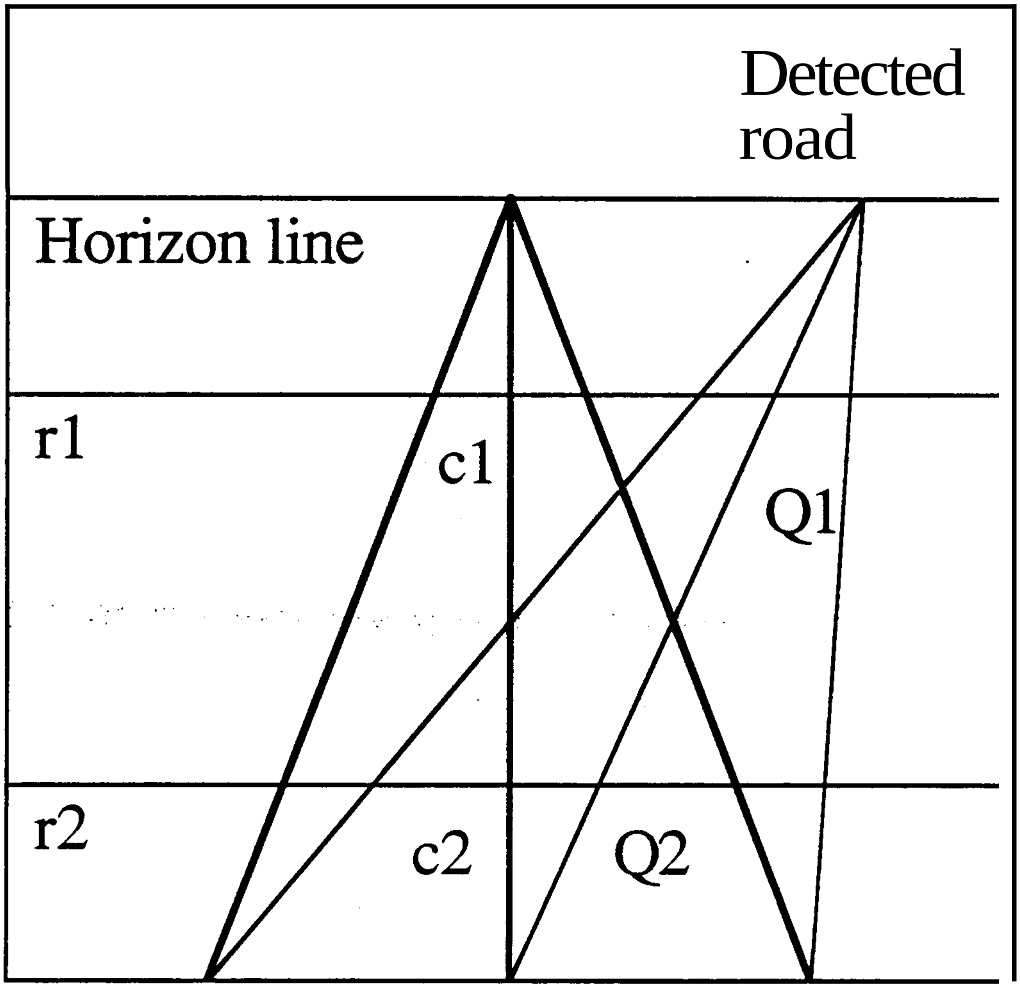

Distance between Qi and the center of the vehicle =

(Ci - ci)/ppmi

ppmi = pixels per meter at row ri.

Dynamic road following

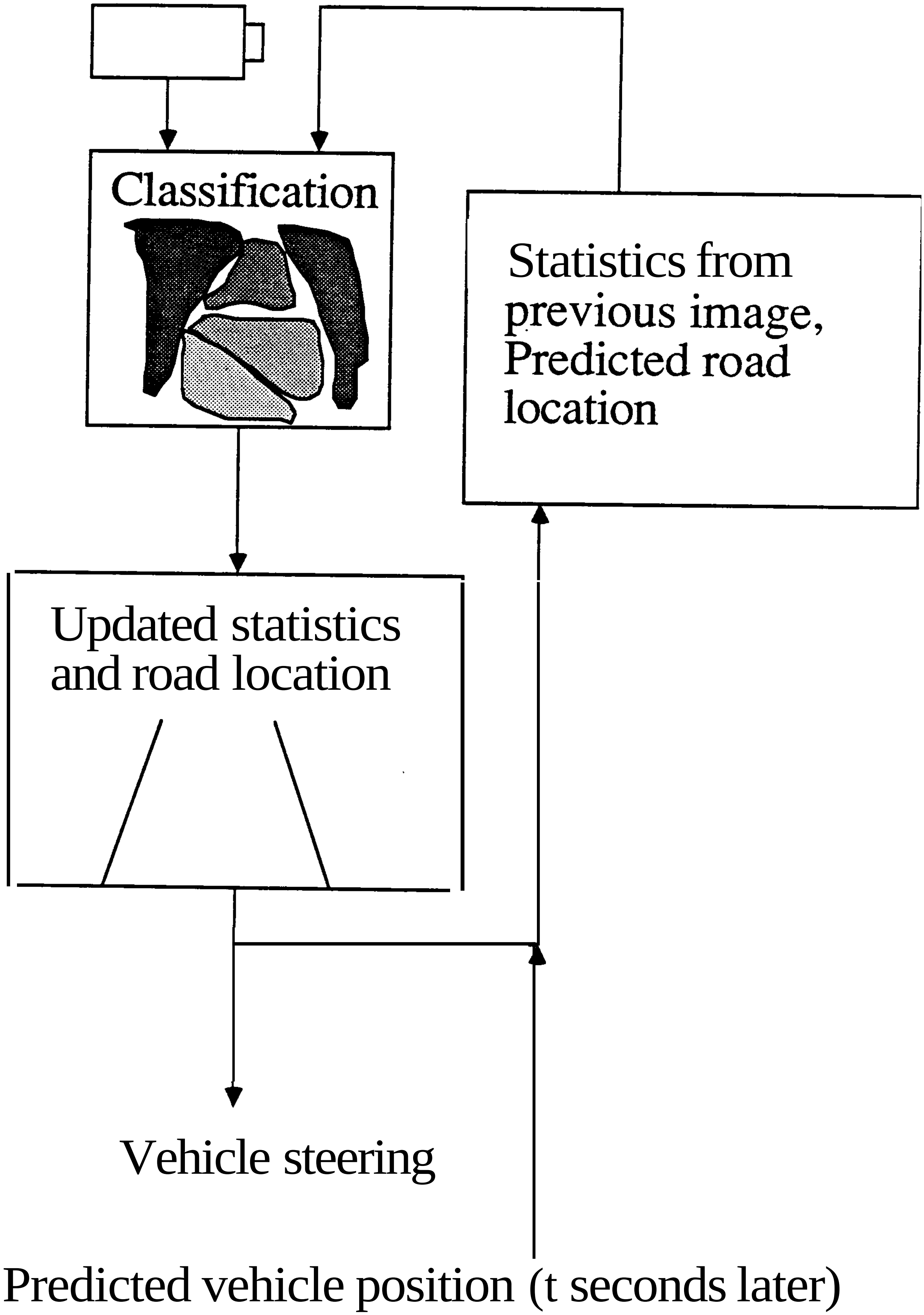

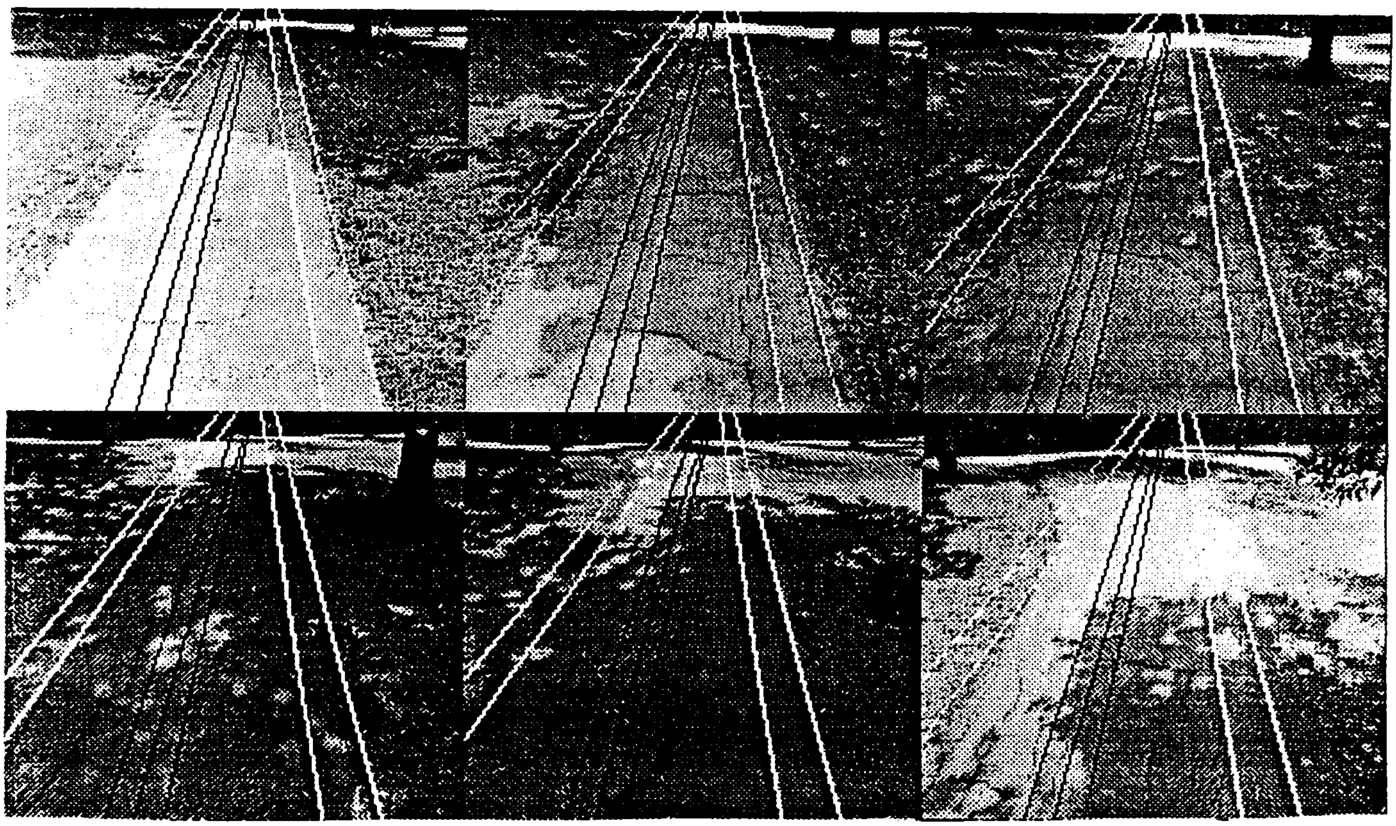

Some lessons from road following

- More accurate calibration is needed.
- More dynamic range in the color cameras is required to handled a wide range of conditions.
- More detailed road model (intersections, curved roads..).
- More flexible color classification.

Range data

Sensor:

- Time-of-flight laser range finder (ERIM)
- 64 x 256 range images, 30° x 80°
- Reflectance image
- 8-bit range from 0 to 64 feet (3 inches resolution)

Purpose:

- Obstacle detection ← path planning around discrete objects
- Terrain modeling ← path planning across open terrain
- 3-D map building ← exploration, incremental description improvement

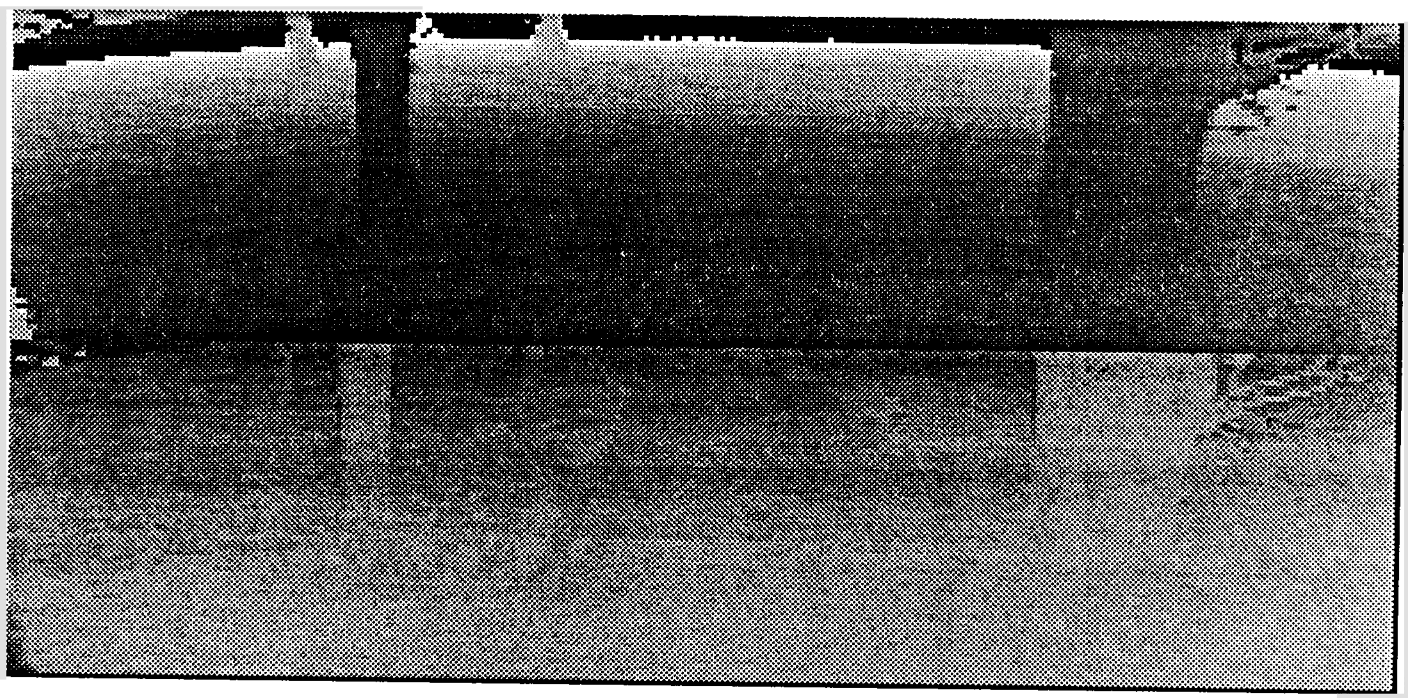

Obstacle detection

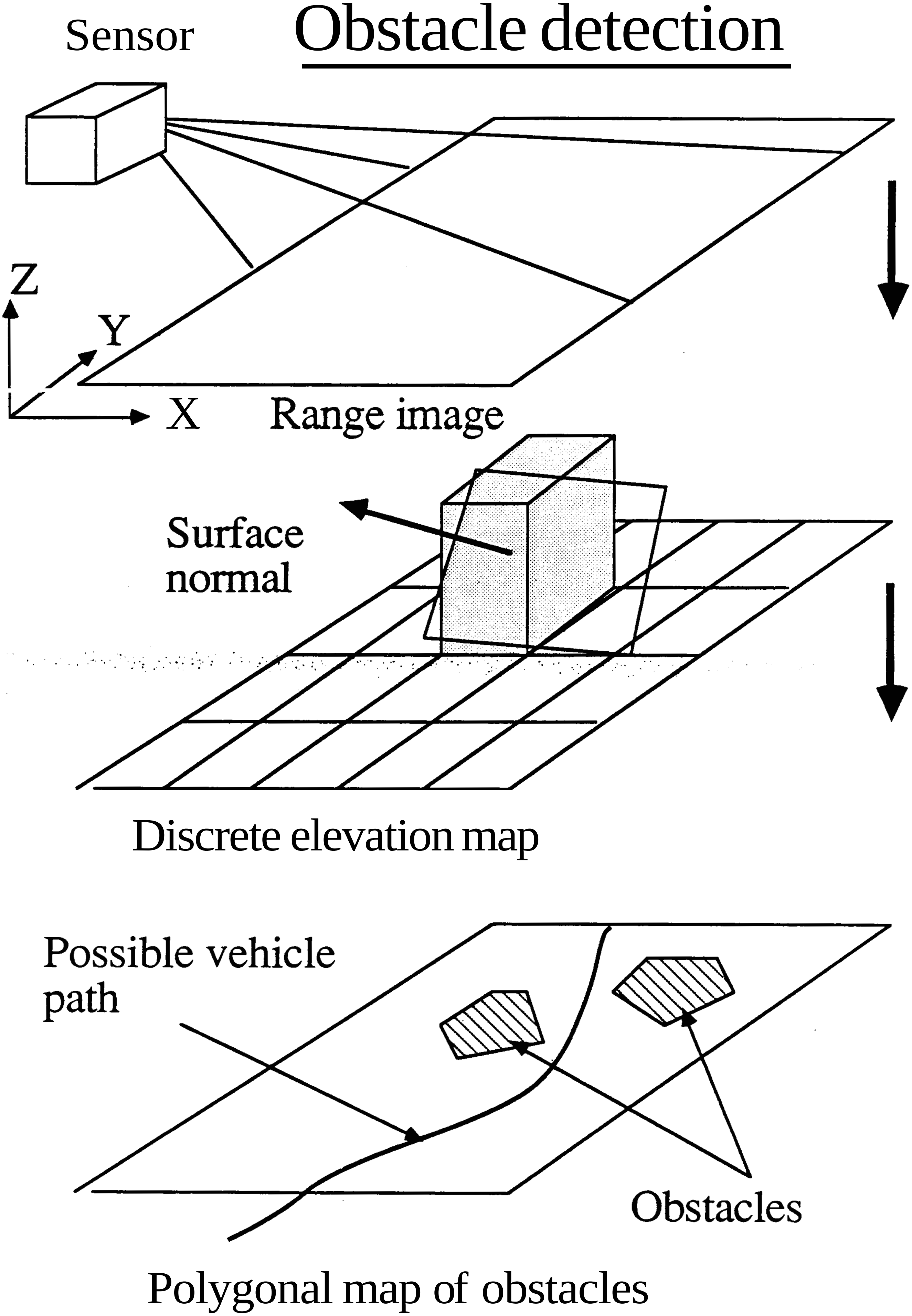

3-D map building

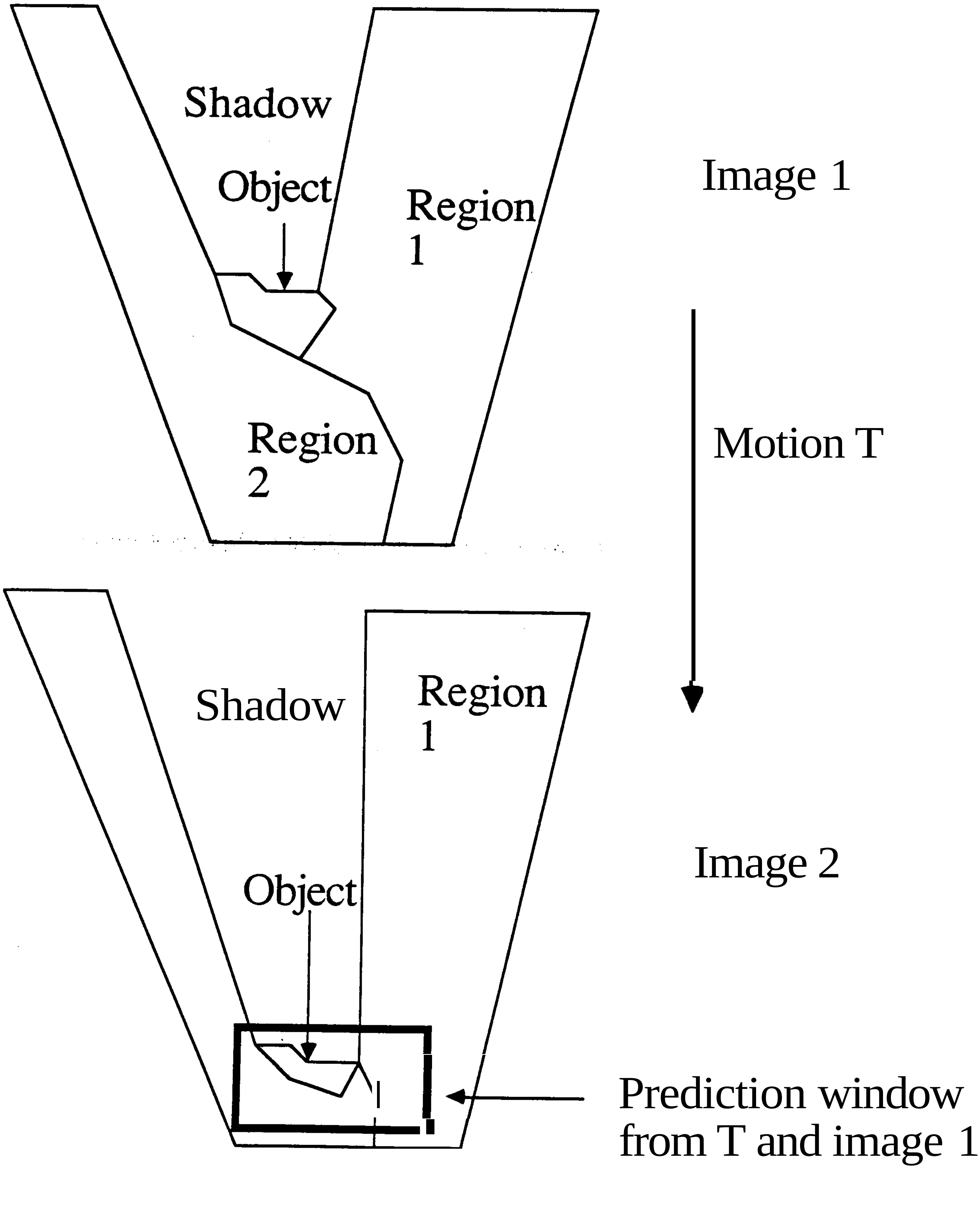

Range processing cycle

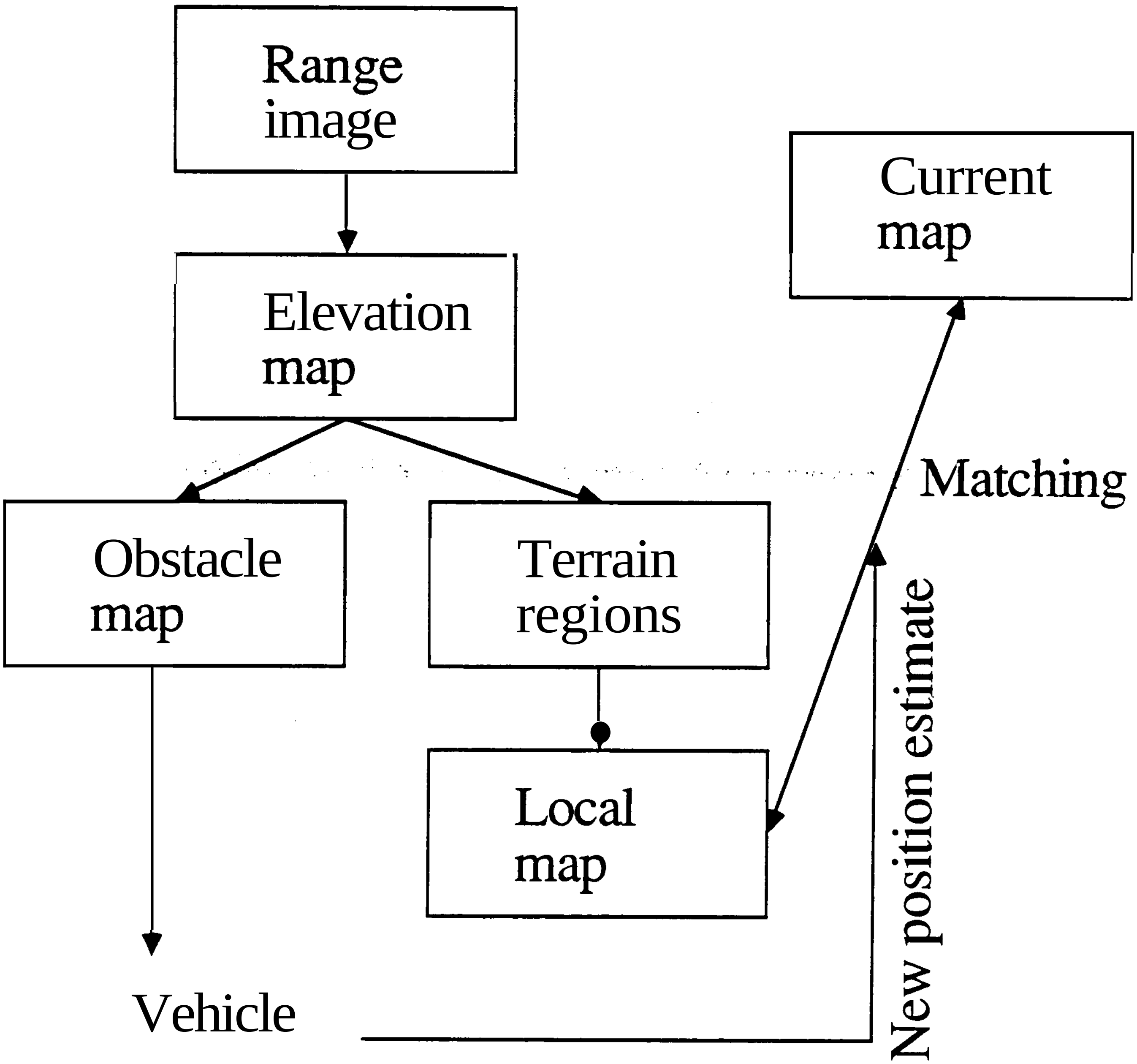

Terrain modeling

The part of the field of view that is not part of any object can be segmented into regions:

1. Find edges in the elevation map
2. Find seed points in the elevation map
3. Apply region growing based on smoothness constraint
4. Report the region (e.g. as polygons

Putting everything together

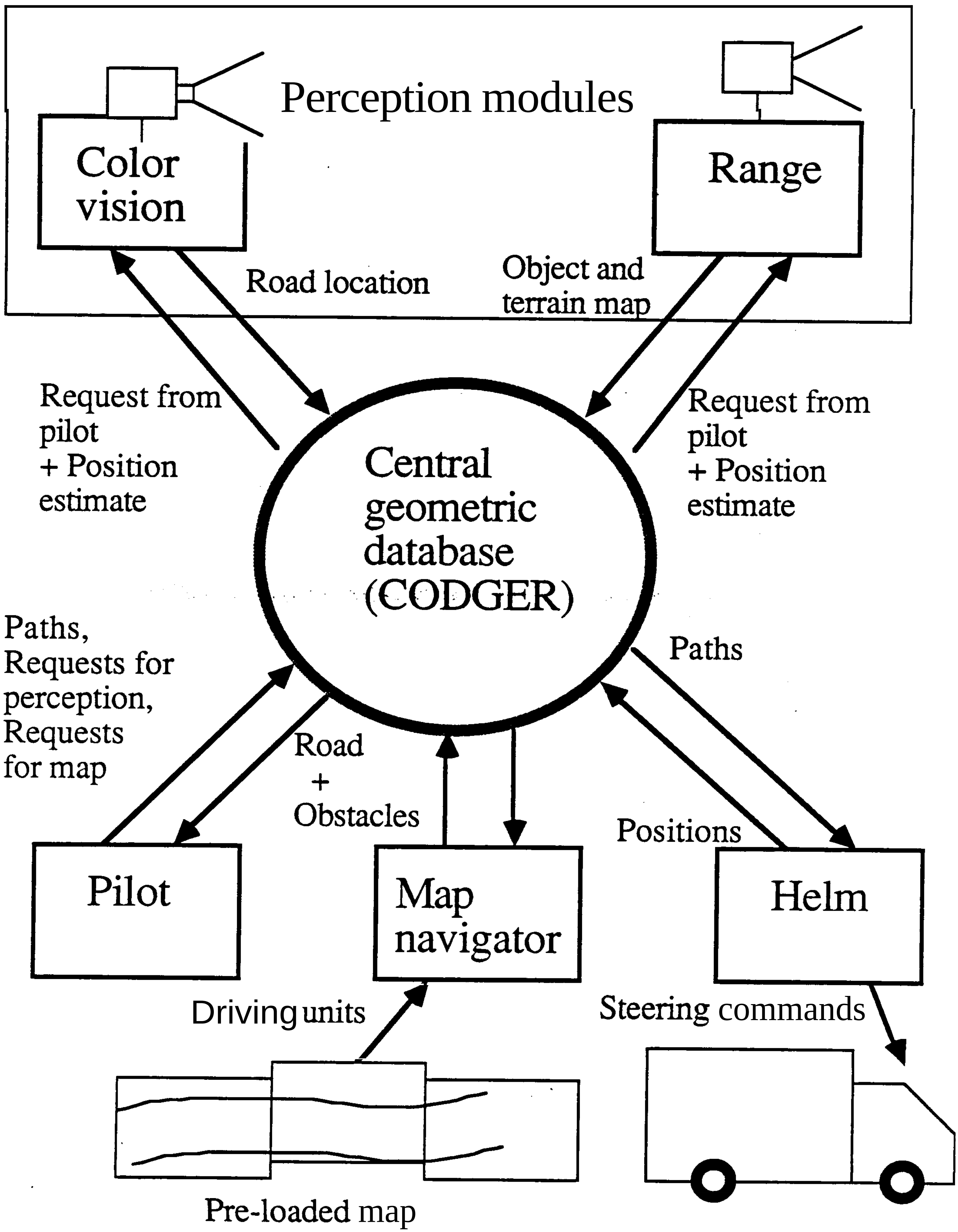

Additions to the current system

- Uncertainty representation for road location, vehicle position, and objects' locations. Updating through filtering
- Better path planner, including off-road capabilities
- Improved vision: two cameras, intersections..
- **Map** revision

Years left	Device	Difficulty
0	**Toys**	cost
1/2 (Brooks, Durrant-White)	Watchdog	reliability
??	Factory transport	planned motion
1 (Crowley) 10(Chatilla)	Industrial cleaning	coverage
73	Wheelchair	planning, liability
1993 (Harmon)	Tank simulator	rough terrain
77	**Mine** sweeper	coverage
5 (Somalvico) 30 (Binford)	Household servant	tough manipulation
10 (Chang)	Street sweeper	traffic
	Mail delivery	manipulation
	Garbage collection	manipulation
77	Tank	weapons
10 (Harmon) (Somalvico)	Construction	force
7 (Graefe)	Chauffeur	psychology

A partial list of research efforts in mobile robotics (from J.L. Crowley, "The State of the Art in Mobile Robotics")

LAAS-CNRS, T. Ave. Colonel Roche, 31077 Toulouse, France. Project Hilare, Principle investigators: George Giralt, Raja Chatila, J-P. Laumond. Perhaps one of the longest running projects. Recent applications include a cleaning robot for the Paris Metro as well as a ware-house robot.

SRI-International, AI Group, 333 Ravenswood Ave., Menlo Park, California, 94025 USA. Principle Investigators: Stan Rosenschein and Leslie Kaibling. Robot hardware: Flakey the robot, designed and built by Stan Reifle.

C-MU Robotics Institute, Schenley Park, Pittsburgh Pa, 15213 USA. Principle investigators: Takeo Kanade, Chuck Thorpe, Hans Moravec, Red Whittaker. At least 5 distinct projects have been performed at C-MU in the last 5 years. Major projects include The ALV NavLab, the Terragator, the Denning surveillance robot, the IMP, and Moravec's Pluto, Neptune and Uranus.

MIT AI Lab: 545 Technology Square, Cambridge MA, 02139, Principle Investigator. Rod Brooks. Robots: Allen, Tom, Jerry, Sydney, Seymour.

INRIA: Domaine de Voluceau, Rocquencourt, BP 105, 78153 Le Chesnay, France. Principal Investigators: Olivier Faugeras, Nicholas Ayache, Francis Lustman. A commercial copy of the INRIA robot is sold by RobotSoft SARL, of Asniers France.

LIFIA: INPG, 46 ave Felix Viallet, 38031 Grenoble, France. Principal Investigator: Jim Crowley. Developing a Surveillance Robot for project EUREKA - Mithra. Currently using a Denning robot named Lurch.

GM Research, Warren Michigan, USA: Principle Investigators: Steve Holland, Bob Tilove

Univ. of Amsterdam, Kruislaan 4090, The Netherlands. Principle Investigator Dr. Willem Duinker.

Stanford University: AI Laboratory, Computer Science Dept, Stanford University, Stanford, Ca, 94305 USA. Principal Investigator: Thomas Binford.

ORNL: P.O. Box X, Oak Ridge Tenn, 37831 USA. Principle Investigator: Charles Weisbin.

FMC Corp. 1205 Coleman Ave., Santa Clara, Ca. 95052. Principle Investigator Andrew Chang Military applications of mobile robots.

NBS: Industrial Systems Division, National Bureau of Standards, Building 220/B 124, Gaithersberg, MD. 20899. Prinicipal Investigator: Marty Herman.

Insitiit der Bundeswehr Mûnchen, Inst. fur Messtechnik, 8014 Neubiberg, W. Germany. Principle Investigator: Volker Graefe. Real time road-following system integrating simple real time vision with control theory.

Jet Propulsion Laboratory, 4800 Oak Grove Drive, Pasadena, Ca. 91109 USA. Principle Investigator: Brian Wilcox.

References

[1] R.C. Arkin, E. Riseman, A. Hanson.
Visual strategies for mobile robot navigation.
In *Proc. Workshop on Computer Vision.* 1987.

[2] N. Ayache, F. Lustman.
Fast and reliable trinocular stereovision.
In *Proc. ICCV'87.* 1987.

[3] A. Bergman, C. K. Cowan.
Noise-Tolerant Range Analysis for Autonomous Navigation.
In IEEE *Conf. on Robotics and Automation.* San Francisco, 1986.

[4] R. Brooks.
Aspects of mobile robot visual map making.
In *Second International Robotics Research Symposium.* MIT press, 1985.

[5] R. Brooks, A.M. Flynn, T. Marill.
Self calibration of motion and stereo vision for mobile robot navigation.
In *Proc. Image Understanding Workshop.* Cambridge, 1988.

[6] M.K. Brown.
Locating object surfaces with an ultrasonic range sensor.
In *Proc.* IEEE *International Conference on Robotics and Automation.* St. Louis, 1985.

[7] S.S. Chen.
Multisensor fusion and navigation of mobile robots.
International Journal Intelligent Systems, Vol. 2 , 1987.

[8] J. Crowley.
Dynamic world modeling for an intelligent mobile robot using a rotating ultrasonic ranging device.
In *Proc.* IEEE *International Conference on Robotics and Automation.* St. Louis, 1985.

[9] M. J. Daily, J. G. Harris, K. Reiser.
Detecting Obstacles in Range Imagery.
In *Image Understanding Workshop.* Los Angeles, 1987.

[10] M.J. Daily, J.G. Harris, K. Reiser.
An operational perception system for cross-country navigation.
In *Proc. Image Understanding Workshop.* Cambridge, 1988.

[11] E.D. Dickmanns, A. Zapp.
A curvature-based scheme for improving road vehicle guidance by computer vision.
In *Proc. SPIE Conference 727 on Mobile Robots.* Cambridge, 1986.

[12] E.D. Dickmanns, A. Zapp.
Autonomous high-speed road vehicle guidance by computer vision.
In *Proc. 10th* IFAC. Munich, 1987.

[13] K.C. Drake, E.S. McVey, R.M. Tingo.
Experimental position and ranging results for mobile robots.
Jownal of Robotics and Automation, Vol. 3 , 1987.

[14] M. Drumheller.
Mobile robot lacalization using sonar.
PAMI-9 , 1987.

[15] R. T. Dunlay, D. G. Morgenthaler.
Obstacle detection and avoidance from range data.
In *Proc. SPIE Mobile Robots Conference.* Cambridge, MA, 1986.

[16] A. Elfes.
Sonar-based real-world mapping and navigation.
Journal of Robotics and Automation, Vol. 3, 1987.

[17] O.D. Faugeras, F. Lustman, G. Toscani.
Motion and structure from motion from point and line matches.
In *Proc. ICCV'87.* 1987.

[18] O.D. Faugeras, N. Ayache, B. Faverjon.
Building visual maps by combining noisy stereo measurements.
In *Proc. IEEE Conf. on Robotics and Automation.* 1986.

[19] G. Giralt, R. Chatila, M. Vaisset.
An integrated navigation and motion control system for autonomous multisensory mobile robots.
In *Proc. 1st International Symposium Robotics Research.* Cambridge, 1984.

[20] K.D. Gremban, C.E. Thorpe, T. Kanade.
Geomemc camera calibration using systems of linear equations.
In *Proc. Image Understanding Workshop.* Cambridge, 1988.

[21] S.Y. Harmon.
The ground surveillance robot (GSR): An autonomous vehicle designed to transit unknown terrain.
Journal of Robotics and Automation, Vol. 3, 1987.

[22] M. Hebert, T. Kanade.
First results on outdoor scene analysis.
In *Proc.* IEEE *Robotics and Automation.* San Francisco, 1985.

[23] M. Hebert T. Kanade.
3-D vision for outdoor navigation by an autonomous vehicle.
In *Proc. Image Understanding Workshop.* Cambridge, 1988.

[24] T. Kanade, C. Thorpe, W. Whittaker.
Autonomous Land Vehicle *at* CMU.
In *Proc.* ACM *Computer Conference.* Cincinnati, February, 1986.

[25] D.J. Knegman, T.O. Binford.
Generic models for robot navigation.
In *Proc. Image Understanding Workshop.* Cambridge, 1988.

[26] D. Knegman, E. Triendl, T.O. Binford.
A mobile robot: sensing, planning and locomotion.
In *Proc.* IEEE *Conf. on Robotics and Automation.* 1987.

[27] D. Kuan, G. Phipps, A.C. Hsueh.
Autonomous land vehicle road following.
In *Proc. ICCV.* 1987.

[28] R. Kuc, M.W. Siegel.
Physically based simulation model for acoustic sensor robot navigation.
PAMI-9, 1987.

[29] S.P. Liou, R.C. Jain.
Road following using vanishing points.
Compufer Vision, Graphics, and Image Processing, 1987.

[30] L. Matthies, S. A. Shafer.
Error Modelling in Stereo Navigation.
Technical Report CMU-RI-TR-86-140, Carnegie-Mellon University, the Robotics Institute, 1986.

[31] L. Matthies, S.A. Shafer.
Error modeling in stereo navigation.
Journal of Robotics and Automation, Vol. 3, 1987.

[32] L. Matthies, R. Szeliski, T. Kanade.
Kalman filter-based algorithms for estimating depth from image sequences.
In *Proc. Image Understanding Workshop.* Cambridge, 1988.

[33] D. Miller.
A spaual representation system for mobile robots.
In *Proc. IEEE International Conference on Robotics and Automation.* St. *Louis,* 1985.

[34] H.P. Moravec, A. Elfes.
High-resolution maps from wide angle sonar.
In *Proc. IEEE International Conference on Robotics and Automation.* St. Louis, 1985.

[35] R.C. Nelson, J. Aloimonos.
Using flow field divergence for obstacle avoidance in visual navigation.
In *Proc. Image Understanding Workshop.* Cambridge, 1988.

[36] K. E. Olin, F. M. Vilnrotter, M. J. Daily, K. Reiser.
Developments in Knowledge-Based Vision for Obstacle Detection and Avoidance.
In *Image Understanding Workshop.* Los Angeles, 1987.

[37] J.L. Olivier, F. Ozguner.
A navigation algorithm for an intelligent vehicle with a laser rangefinder.
In *Proc. IEEE Conf. on Robotics and Automation.* San Francisco, 1986.

[38] S.V. Rao, S.S. Iyengar, C.C. Jorgenson, C.R. Weisbin.
Concurrent algorithms for autonomous robot navigation in an unexplored terrain.
In *Proc. IEEE Conf. on Robotics and Automation.* San Francisco, 1986.

[39] AX. de Saint Vincent.
A 3D perception system for the mobile robot HILARE.
In *Proc. IEEE Conf. on Robotics and Automation.* San Francisco, 1986.

[40] K. Sakurai, H. Zen, H. Ohta, Y. Ushioda, S. Ozawa.
Analysis of a road image as seen from a vehicle.
In *Proc. ICCV.* 1987.

[41] S. A. Shafer, A. Stentz, C. E. Thorpe.
An Architecture for Sensor Fusion in a Mobile Robot.
Technical Report CMU-RI-TR-86-9, Carnegie-Mellon University, the Robotics Institute, 1986.

[42] R.C. Smith, P. Cheeseman.
On the representation and estimation of spatial uncertainty.
International Journal of Robotics Research , 1986.

[43] W.K. Stewart.
A non-deterministic approach to 3-D modeling underwater.
In *Proc. Fifth International Symposium on Unmanned Untethered Submersible.* University of New Hampshire, 1987.

[44] C.E. Thorpe.
The CMU rover and the FIDO vision and navigation system.
PhD *thesis,* Camegie-mellon University, 1984.

[45] C.E. Thorpe, M. Hebert, T. Kanade, S.A. Shafer.
Vision and navigation for the Camegie-Mellon Navlab.
PAMI 10(3), 1988.

[46] D. Y. Tseng, M. J. Daily, K. E. Olin, K. Reiser, F. M. Vilnrotter.
Knowledge-based vision techniques annual technical report.
Technical Report ETL-0431, U.S. Army ETL, Fort Belvoir, VA. 1986.

[47] S. Tsuji. J.Y. Zheng.
Visual path planning for a mobile robot.
In *Proc. IJCAI.* 1987.

[48] R. Wallace, K. Matsuzaki, Y. Goto, Y. Webb, J. Crisman, T. Kanade.
Progress on Robot Road Following.
In *IEEE Conf. on Robotics and Automation.* San Francisco, 1986.

[49] A.M. Waxman, JJ. LeMoigne, L.S. Davis, B. Srinivasan, T.R. Kushner, E. Liang. T. Siddalingaiah.
A visual navigation system for auatonomous land vehicles.
Journal of Robotics and Automation, Vol. 3, 1987.

[50] W.J. Wolfe, N. Marquina, Eds.
Mobile Robots II.
In *Proc. SPIE* 852. Cambridge, MA, 1987.